Advances in coatings on magnesium alloys for cardiovascular stents – A review

Zhao-Qi Zhang [a], Yong-Xin Yang [a], Jing-An Li [a], Rong-Chang Zeng [b], Shao-Kang Guan [a],*

[a] School of Material Science and Engineering & Henan Key Laboratory of Advanced Magnesium Alloy & Key Laboratory of Materials Processing and Mold Technology (Ministry of Education), Zhengzhou University, 100 Science Road, Zhengzhou, 450001, PR China
[b] Corrosion Laboratory for Light Metals, College of Material Science and Engineering, Shandong University of Science and Technology, Qingdao, 266590, China

ARTICLE INFO

ABSTRACT

Magnesium (Mg) and its alloys, as potential biodegradable materials, have drawn wide attention in the cardiovascular stent field because of their appropriate mechanical properties and biocompatibility. Nevertheless, the occurrence of thrombosis, inflammation, and restenosis of implanted Mg alloy stents caused by their poor corrosion resistance and insufficient endothelialization restrains their anticipated clinical applications. Numerous surface treatment tactics have mainly striven to modify the Mg alloy for inhibiting its degradation rate and enduing it with biological functionality. This review focuses on highlighting and summarizing the latest research progress in functionalized coatings on Mg alloys for cardiovascular stents over the last decade, regarding preparation strategies for metal oxide, metal hydroxide, inorganic nonmetallic, polymer, and their composite coatings; and the performance of these strategies in regulating degradation behavior and biofunction. Potential research direction is also concisely discussed to help guide biological functionalized strategies and inspire further innovations. It is hoped that this review can give assistance to the surface modification of cardiovascular Mg-based stents and promote future advancements in this emerging research field.

1. Introduction

Cardiovascular disease (CVD) is one of the principal causes of human death in recent years, and the number of deaths caused by CVD has been increasing yearly in our country [1,2]. Since the invention of the vascular stent in the 1980s [3], it has been one of the most effective medical interventions to deal with coronary and peripheral artery diseases [4]. The most extensively used material for the production of stents is 316 L stainless steel (316 L SS). The characteristics of 316 L SS, such as its low carbon content, corrosion resistance, and easily deformable property, render it a standard material for balloon expandable stents. Other materials like tantalum (Ti), niobium (Ni), cobalt-chromium (Co-Cr), and their alloys are used in stents because of their better radiopacity, higher strength; improved corrosion resistance, better nuclear magnetic resonance imaging (MRI) compatibility, and higher strength, which allow the design of stents with low profile [5–8]. A stent made of inert material, however, is a permanent foreign body because of its non-biodegradability, leading to the inflammation of the blood vessels and the risk of recurrence of atherosclerosis in the body

[9–11].

Recently, degradable polymeric and metallic stents have attracted increasing attention due to their acceptable biodegradability and biocompatibility [12–14]. There are several polymeric stents in development but just a couple merit mention at this stage based on clinical data [15]. The bioresorbable vascular stent (BVS, Abbott Laboratories Inc) is made from poly-L-lactic acid (PLLA) [16], and exciting results of clinical trials have been reported (e.g. Absorb China and Absorb Japan) [17]; however, polymer-based stents remain problematic because of their insufficient mechanical strength and easy elastic shrinkage, longer degradation time (about 3 years), and poor vascular compliance [18]. The toughness and mechanical strength of the polymer stents are inherently lower than those of the metallic stents, which means that stents made of polymers, must have a greater volume to acquire a mechanical performance similar to that of a metallic stent.

The degradable metallic stents mainly include iron (Fe), zinc (Zn), and magnesium (Mg) together with their alloys. Fe, a promising candidate material, has a high elastic modulus and radial support force [19]. Mueller et al. [20] stated that excessive ferrous ions (Fe^{2+}) could hinder the growth of smooth muscle cells (SMCs), thereby combatting

Abbreviations

AH	Alkali-heat
ALD	Atomic layer deposition
BVS	Bioresorbable vascular stent
CS	Chitosan
ECM	Extracellular matrix
EGCG	Epigallocatechin gallate
EPCs	Endothelial progenitor cells
ECs	Endothelial cells
FDA	Food and Drug Administration
GA	Gallic acid
GO	Graphene oxide
HA	Hyaluronic acid
Hep	Heparin
HPM	High purity Mg
HUVECs	Human umbilical vein endothelial cells
HR	Hemolysis ratio
IVU	SIntravascular ultrasound
JDBM	Mg-Nd-Zn-Zr
LDH	Layered double hydroxide
LbL	Layer by layer assembly
LLL	Late lumen loss
MRI	Nuclear magnetic resonance imaging
Mg	Magnesium
MAO	Micro arc oxidation
OCT	Optical coherence tomography
PLA	Polylactic acid
PCL	Polycaprolactone
PLGA	Poly(lactide-*co*-glycolic) acid
PEA	Polymethyl acrylate
PDA	Polydopamine
PCUU	Poly (carbonate urethane) urea
PEUU	Poly (ester urethane) urea
PTX	Paclitaxel
REDV	Arg–Glu–Asp–Val peptide
SF	Silk fibroin
SRL	Sirolimus
SMCs	Smooth muscle cells
VEGF	Vascular endothelial growth factor
ZE21B	Mg-Zn-Y-Nd

restenosis. Although animal experiments have shown that there is no intravascular thrombosis or severe inflammation during the implantation of Fe-based stents (e.g. nitrided Fe-based stents) [21], they lack the support of clinical trial data. Moreover, the degradation period of Fe-based stents is too long [22], and they are extremely susceptible to the influence of magnetic fields, which makes it impossible for patients implanted with Fe-based stents to undergo MRI [23]. Zn, an essential trace element for the human body, has become one of the choices for the production of fully degradable metal stents because of its appropriate flexural strength, better elongation, and suitable degradation rate [24, 25]. Zhu et al. [26] found that Zn ions (Zn^{2+}) produced by the Zn-containing material exerted a two-phase effect on cell proliferation, spreading, and migration. Zn^{2+} at low concentration promoted cell viability, whereas Zn^{2+} at high concentration yielded the opposite effects. Research on zinc-based stents started fairly late, with in vivo tests consisting mainly in the implantation of a pure zinc wire or stent into
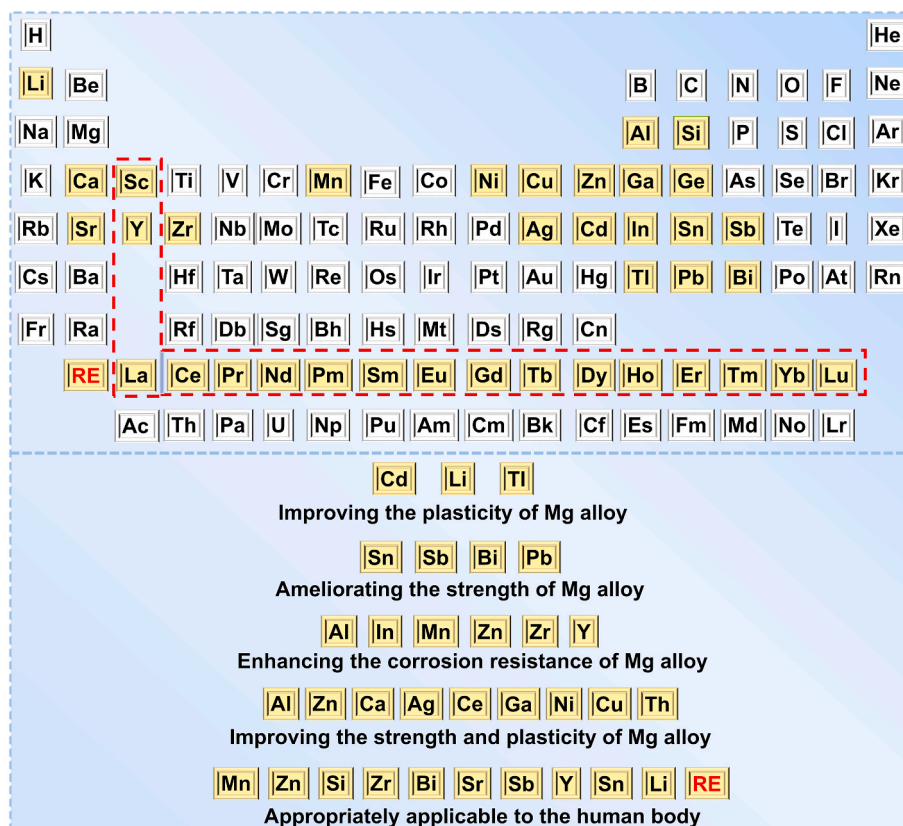

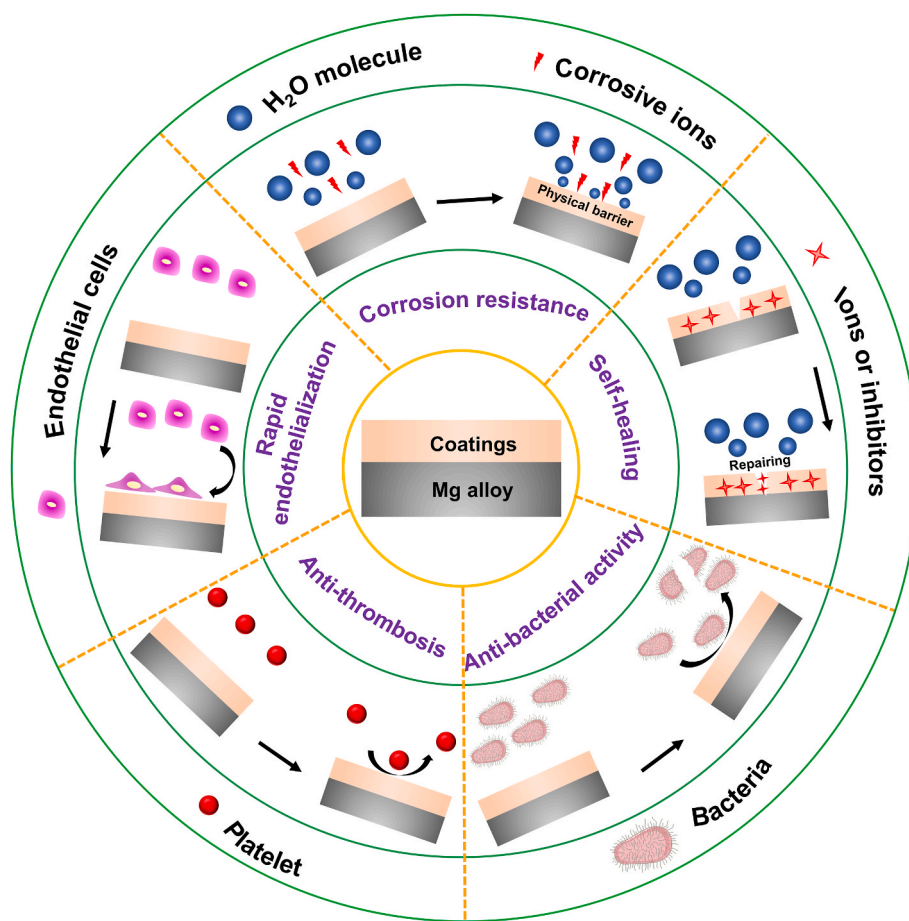**Fig. 1.** Alloying elements for improving the performance of Mg alloys.

Fig. 2. Mg alloys modified by the functionalized coatings.

animal blood vessels to observe their degradation behavior; thus, the biofunctionability of Zn-based stents needs to be studied further [27].

Mg is one of the essential macro-elements for the human body, and the concentration of Mg ions (Mg^{2+}) is about 0.70–1.10 mmol/L in the blood [28]. Mg plays a vital part in inhibiting abnormal nerve excitability, participating in protein synthesis, reducing hypertension, treating acute myocardial infarction, and preventing atherosclerosis [29]. Moreover, the release of Mg^{2+} from the degradable implanted Mg alloy is negligible, and it is not harmful in humans [30]. Currently, Mg and its alloys have been widely used in bone implant materials, and the degradable Mg bone nail developed by Yian Technology Co., Ltd. has been officially certified by Conformite Europeenne (CE). Moreover, Mg alloys are a promising material for cardiovascular stents because of their high elastic modulus, fine mechanical characteristics, and biodegradability [10,31–34]. Mg-based stents have potential advantages over polymeric stents in terms of higher radial strength due to their metallic nature and biocompatibility as a naturally occurring element in the body. Research studies on biodegradable Mg alloy stents are ongoing internationally, and the related animal experiments and clinical trials are described in detail in section 2. Unfortunately, the degradation rates of Mg in body fluids containing chloride ions (Cl^-) are faster because of a lower standard potential (-2.37 V/SCE) [35]. The adverse reactions caused by rapid degradation behaviors after implantation, such as enrichment of Mg^{2+} [36], local alkalization [37], and the by-corrosion products [38], can bring about the early loss of radial support, thus leading to the failure of implantation, mainly in the following three aspects: (a) too fast degradation behavior will lead to the failure of the stent due to the premature loss of radial support; (b) stent fracture and collapse caused by the uneven degradation behavior of Mg alloy can easily result in restenosis; (c) the uncontrollable degradation behavior of

Mg alloy will produce huge amounts of hydrogen within a short time, which is unfavorable for the healing of neovascularization tissues. Therefore, effective control of the degradation behavior of Mg alloys is of great significance in the promotion of the clinical application of Mg-based stents [39,40].

The alloying strategy is usually addressed to deal with the degradation issue of Mg alloys [41]. The alloying design of medical Mg refers to the addition of elements (e.g. Zn [42,43], manganese (Mn) [44,45], calcium (Ca) [44,46], lithium (Li) [47,48], rare earth elements (RE) (e.g. cerium (Ce) [49], neodymium (Nd) [50,51], and yttrium (Y)) [52,53], and zirconium (Zr) [54,55], etc. [56]), to pure Mg, to render the metal (under certain process conditions) become an alloy with expected performance. Moreover, the alloying design has an important effect on the strength, plasticity, and corrosion resistance of Mg (Fig. 1) [37,57,58]. According to application requirements, a large number of Mg alloys with excellent performance that is suitable for vascular stents have been designed, including AE21 alloy [59], WE43 alloy [60,61], AZ91 alloy [62], Mg-Nd-Zn-Zr alloy (JDBM) [63,64], and Mg-Zn-Y-Nd alloy (ZE21B) [65,66]. However, the amount of alloy elements required is larger, and the cost is higher. Moreover, the related in vivo degradation mechanism needs to be further studied and clarified [67].

Surface modification, as another candidate strategy, is an efficacious tactic to ameliorate the property of Mg-based stents [68,69]. At present, a large number of papers have reviewed the advances in the surface treatment of Mg alloy and discussed the scientific issues and cutting-edge development of coatings [70]. However, the reported reviews focused mainly on the surface modification of Mg alloy in industrial (e.g. superhydrophobic coating [71,72]) and orthopedic applications [73], but scarcely on the coatings of Mg-based stents. Hence, it is necessary to review this momentous area of research. This
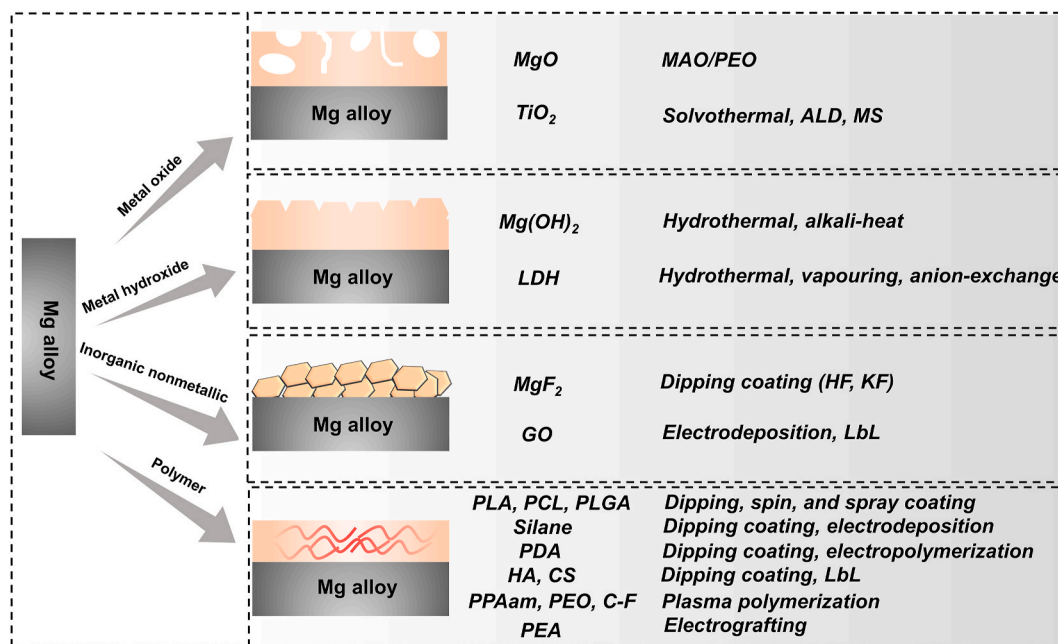
Fig. 3. Strategies for surface treatment of Mg alloy and their preparation methods.
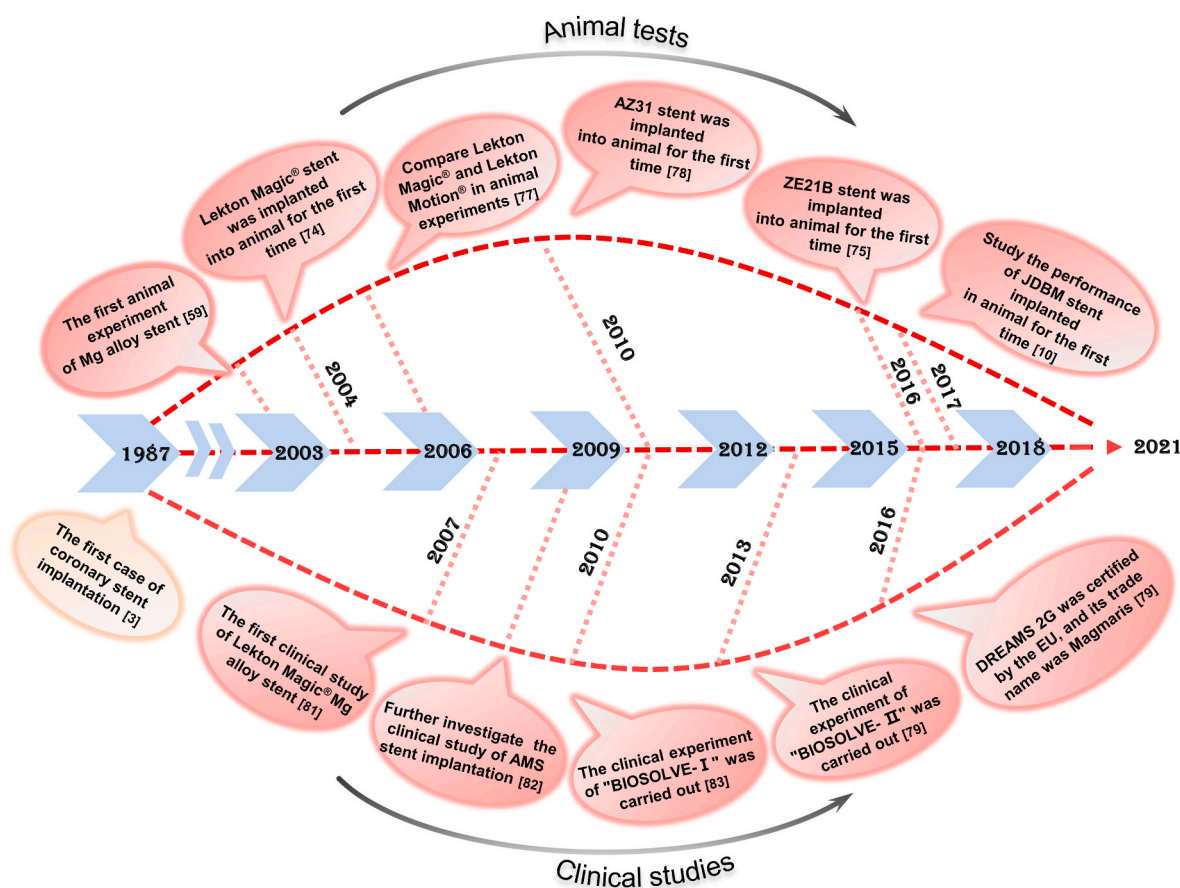

Fig. 4. Timeline of progress in animal and clinical experiments of Mg-based stents, indicating "landmarks" since the first case of coronary stent implantation in 1987.

article summarizes the latest developments of functionalized coatings of Mg and its alloys for vascular stents to fill this gap in knowledge, including corrosion resistance (biodegradability), self-healing, anti-thrombosis and anti-microbial activity, and rapid endothelialization

(Fig. 2). This paper aims to construct a system of surface modification for biodegradable Mg-based stents, including metal oxide coating, metal hydroxide coatings, inorganic nonmetallic coating, organic or polymer coating, and their composite coating, by discussing the preparation

Table 1
Research progress in animal and clinical experiments for Mg alloy stents.

Mat.	Rese.	Deg.	End.	Ani.	Clin.	Res. Ref.
AE21	Heublein et al.	89 d	–	Porcine coronary artery	–	The implanted stent did not cause major problems or show indications of initial fracture in the histologic evaluation. Moreover, no thromboembolic events occurred [59].
WE 43	Mario et al.	98 d	6 d	Porcine coronary artery	–	Inhibitory effect on the smooth muscle cells, rapid endothelialization, a thin layer of neointima covered the stent after 6 d, degradation caused inflammation and intimal hyperplasia [74].
ZE21B	Xi et al.	> 89 d	1 m (Complete)	Porcine coronary artery	–	ZE21B stents could complete the endothelialization process at the end of 1 month, thereby avoiding advanced stent thrombosis [75].
AMS	Maeng et al.	60 d	–	Porcine coronary artery	–	No signs of ongoing inflammation, the lumen area was the smallest at 3 months because of negative vascular remodeling [76].
AMS	Waksman et al.	–	3 d	Porcine coronary artery	–	Compared with stainless stents, AMS stents were safe and formed less new intima, and the lumen area was unchanged [77].
AZ31	Yang et al.	104.5 d	–	Rabbit abdominal aorta	–	AZ31 alloy stents implanted in rabbit abdominal aorta lost their radial force in 2 months and completely degraded at 4 months [78].
JDBM	Yuan et al.	180 d	28 d (Complete)	Rabbit abdominal aorta	–	The implantation of the Mg alloy stent verified good histocompatibility and maintained structural and mechanical integrity in vivo for up to 6 months [10].
AZ91	Yue et al.	7 d	–	Coronary or femoral arteries in dogs	–	2–4 weeks after stent implantation, the intima hyperplasia was mild, but there was no distinct inflammatory reaction and initial thrombosis [62].
AMS	Schranz et al.	–	–	–	Newborn	15 days after implantation, the blood flow velocity was evidently accelerated, the blood perfusion was restored, and the lumen diameter increased from 1.5-1.8 mm to 2–2.8 mm [80].
Mg alloy	Zartner et al.	5 m	–	–	Small children	The lumen diameter increased, and there was no damage to the artery wall during stent degradation [11].
Lekton Magic®	Erbel et al.	4 m	–	–	65 patients	After a continuous intravascular ultrasound examination, only a small amount of the original strut remnants was visible, and they were fully embedded in the intima [81].
AMS	Dalby et al.	–	–	–	63 patients	After 3 months of AMS implantation, there was no difference between the vasomotor function of the reference segment and that observed with PMS. However, compared with PMS, there was demonstrable vasodilation in AMS implanted segments [82].
DREAMS-1G	Haude et al.	9–12 m	–	–	46 patients	Device and procedural success were 100%, and there was no cardiac death or old thrombosis [83].
DREAMS-2G	Haude et al.	12 m	–	–	123 patients	For up to 12 months, the recovery of blood vessel geometry, vasomotion, and signs of bio-resorption was observed [79].

*Rese. = Researcher, Deg. = Degradation period, End. = Endothelialization period, Ani. = Animal experiments, Clin. = Clinical experiment, Res. = Results, Ref. = Reference.

methods, characteristics, challenges, and development directions of various coatings for Mg-based stents. The scheme and preparation methods of these coatings are shown in Fig. 3.

2. Development course of Mg-based stents

Biodegradable Mg-based stents are at the forefront of the development of biodegradable stents because of their high support strength and bioabsorbable characteristics. Researchers have confirmed the feasibility of Mg alloys as cardiovascular stents through animal [10,59,62, 74–78] and clinical [11,79–83] experiments. The representative studies of Mg alloy stents are shown in Fig. 4 and Table 1.

2.1. Animal experiments of Mg-based stents

In 2003, Heublein et al. [59] first implanted 20 prototype coronary stents made of AE 21 Mg alloy into the coronary arteries of 11 domestic pigs. The results of the study revealed that the AE 21 Mg alloy stent was completely covered by the vascular intima in the early stage of implantation, and there was no thrombus and inflammation. Ten to 35 d after implantation, it was found that the diameter of the arterial lumen was reduced by about 40% because of the obvious intimal hyperplasia. Moreover, the study suggested that the degradation rates of AE 21 Mg alloys in the body were faster than expected. Mario et al. [74] implanted WE 43 Mg alloy (i.e. Lekton Magic®) stents into pig coronary arteries. The results showed that the vascular stent underwent endothelialization after implantation (6 d) and that the proliferation of SMCs was significantly inhibited. The histological study demonstrated that the implanted WE 43 Mg alloy stent exhibited an obvious degradation behavior at 35 d after implantation and that the expected complete degradation time was 98 d. JDBM stents were implanted into the abdominal artery of

rabbits by Yuan et al. [10]; the outcomes of this experiment demonstrated that the designed stents had uniform degradation and could provide support for 6 months. Moreover, the inflammatory reaction was modest in peripheral vascular tissues, which was acceptable in the clinic. The ZE21B alloy developed by Zhengzhou University had excellent mechanical and corrosion-resisting features, and its effectiveness and safety as an absorbable stent were confirmed in animal experiments [75].

2.2. Clinical trials of Mg-based stents

In terms of clinical trials of Mg-based stents, Biotronik Company implanted 123 "DREAMS 2G" stents into 123 patients with coronary heart disease to assess the availability and safety of the stents. The clinical results demonstrated that complete degradation of "DREAMS 2G" stents occurred 9 months after implantation. The 12-month follow-up results showed that "DREAMS 2G" stent had good safety and that the late lumen loss (LLL) of the lesion was about 0.39 ± 0.27 mm, implying that "DREAMS 2G" stent owned many advantages such as better radial support, higher vascular compliance, lower acute rebound rate, and no cardiac death or stent thrombosis after implantation [79]. "DREAMS 2G" stents obtained the certification of CE and, in June 2016, became the first biodegradable Mg alloy stent marketed in Europe under the trade name Magmaris [79]. Moreover, Biotronik Company carried out a clinical trial (code-named "BIOSOLVE-III") to further evaluate the efficacy of Magmaris. The follow-up results confirmed that Magmaris was safe and effective [84]. Although the studies mentioned above have fully demonstrated the safety of Mg alloy stents, the problems of excessive degradation rate and insufficient endothelialization need to be further resolved to meet the radial support required for the gradual reconstruction of blood vessels.

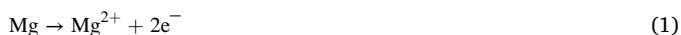# 3. Surface modification of Mg alloy stents

3.1. Metal oxide coatings

Metal oxide coatings, such as titanium dioxide (TiO$_2$) and magnesium oxide (MgO), have good biocompatibility and high stability and are widely used to ameliorate the anti-corrosion property of Mg alloy [68]. Currently, many technologies have been utilized to fabricate metal oxide coatings on Mg alloys, including atomic layer deposition (ALD), solvothermal method, micro-arc oxidation (MAO), or plasma electrolytic oxidation (PEO) [85].

3.1.1. Titanium dioxide (TiO$_2$) coatings

Nanoparticles of TiO$_2$, which is a chemically stable metal oxide, are usually used in oral pharmaceutical preparations, and the pharmaceutical excipients manual regards TiO$_2$ as a non-toxic excipient (which is, of course, dependent on concentration) [86]. The TiO$_2$ film has been extensively exploited to modify vascular stents because of its excellent performance, such as its anti-thrombosis effect, rapid endothelialization, and good blood compatibility [87]. In a representative paper, Huang et al. [88] utilized ion beam-enhanced deposition to synthesize a Ti-O film on cobalt alloy and confirmed that the Ti-O coating was an outstanding blood contact material because of its semi-conductor nature. In addition, as TiO$_2$ has shown good corrosion resistance and biocompatibility on traditional metal-based stents, it can become a positive protective barrier for Mg-based stents. Hou et al. [89] fabricated an anatase TiO$_2$ nanosheet film (thickness, 50 nm) on degradable Mg–Zn alloy stents via a facile solvothermal method at 160 °C. The outcomes revealed that the fabricated coating significantly decreased the degradation rates of Mg–Zn alloys. Nevertheless, the above-mentioned literature lacks a comprehensive evaluation of the application prospects of TiO$_2$-coated absorbable Mg alloy stents. Yang et al. [86] reported the deposition of a TiO$_2$ film on Mg-Zn alloys via the ALD method (an advanced technology that adopts surface sequential reactions to achieve atomic-level film deposition and has the merits of improving the surface coverage and adhesion of the thin film [90]), the TiO$_2$-150 °C nanoscale film protected Mg alloy from corrosion and promoted endothelial cells (ECs) adhesion and proliferation; however, the TiO$_2$-200 °C thin film showed an unsatisfactory result in cell assays because of its unstable surface microstructure and lower than optimal surface energy, which did not match that of key proteins for mediating ECs attachment. Hou et al. [91] successfully prepared a 400 nm-thick TiO$_2$ coating on Mg-Zn Alloy via a facile magnetron sputtering (MS) route at room temperature and evaluated the biocompatibility and corrosion resistance of the resulting material. The outcomes showed that the degradation behavior of Mg alloys was suppressed apparently, and the degradation degree of Mg alloys coated with TiO$_2$ was not serious after 14 d of soaking in simulated body fluid (SBF) solution. Also, the TiO$_2$ coating had a better anti-platelet ability with a lower hemolysis ratio (HR, < 1%) and facilitated the adhesion of ECs. However, the fabricated Ti-O film was very thin (nano-scale) and exhibited weak bonding with the substrate.

3.1.2. Magnesium dioxide (MgO) coatings

MAO refers to a novel technology for in-situ growth of ceramic oxide film on a valve's metal surface (Al, Mg, Ti, and their alloys) [92,93]. Implementing a MAO strategy can effectively ameliorate the anti-corrosive and biocompatible properties of Mg-based materials and significantly enhance the continued adhesion of MAO coating to the substrate [31,94], its formation mechanism is as follows [95]:

$$Mg \rightarrow Mg^{2+} + 2e^- \tag{1}$$

$$4OH^- \rightarrow O_2\uparrow + 2H_2O + 4e^- \tag{2}$$

$$2H_2O \rightarrow 2H_2\uparrow + O_2 \tag{3}$$

$$Mg^{2+} + 2OH^- \rightarrow Mg(OH)_2\downarrow \tag{4}$$

$$Mg(OH)_2 \rightarrow MgO\downarrow + H_2O \tag{5}$$

$$2\,Mg + O_2 \rightarrow 2MgO\downarrow \tag{6}$$

Liehn et al. [96] prepared MAO coatings (mainly MgO) on Mg-RE and Mg-Zn-Ca alloys, followed by the evaluation of the hemocompatibility of the Mg substrate and MAO coating via static and dynamic experiments using human blood. The results revealed that two types of Mg alloy displayed indicators of corrosion and produced corrosion by-products in the static tests, leading to an inaccurate assessment of platelet adhesion. All test methods (static and dynamic experiments) consistently indicated that MAO coating reformed blood compatibility by reducing platelet adhesion compared with uncoated samples. Matykina et al. [97] designed four bioactive MAO coatings on Mg-0.8Ca alloy using a Ca/P-based electrolyte with added silicon (Si) and fluorine (F), to evaluate their biocompatibility. The incorporation of F was critical for ECs, and the MAO coating with a high F content (~9%–11%) and roughness (Ra $\geq$ 3.6 μm) limited the formation of a structured monolayer of ECs. The corrosion resistance and HR of MAO-coated WE 42 alloy were studied by Lu et al. [98]. The electrochemical tests alluded that the corrosion resistance of Mg alloy treated by MAO technology was enhanced. The MAO coating, however, was destroyed badly after 4 weeks of immersion. A hemolysis test indicated that the HR of the WE42 and MAO groups was 50.37% $\pm$ 0.42%, 3.67% $\pm$ 0.47%, respectively, implying a good hemocompatibility of the MAO coating. Echeverry-Rendon et al. [99] investigated the influence of the surface chemistry and topography of MAO-coated pure Mg on the biological response of vascular cells. The results indicated that the MAO coating impacted the survival of vascular cells. Moreover, human umbilical vein endothelial cells (HUVECs) and SMCs were more susceptible to changes in Mg. In vitro evaluation has certain limitations in predicting material properties, and the vulnerability of HUVECs to the components of coated Mg needs to be further studied in vivo. Besides, the typical porous microstructures of MAO coating weaken the protective effect on the Mg alloy. To further extend the degradation period, a subsequent treatment is usually performed to coat the polymer coating, thus sealing the micropores. However, MAO coating, as a rigid coating with high hardness, may not be able to meet the requirements of elastic deformation necessary for the use of an Mg alloy as a vascular stent [100].

3.2. Metal hydroxide coatings

The degradation products of Mg-based materials are primarily composed of Mg(OH)$_2$ with a loose structure. Hence, researchers have attempted to create a uniform and compact Mg-based hydroxide layer on Mg alloy for enhancing its corrosion resistance [101,102]. Currently, the hydroxide films prepared using a hydrothermal method (hydrothermal treatment is a strategy in which the precursor is placed in an autoclave to react under high pressure and temperature [103]), including Mg(OH)$_2$ and layered double hydroxide (LDH), have been highlighted [104,105].

3.2.1. Magnesium hydroxide (Mg(OH)$_2$) coatings

Wang et al. [106] synthesized a film on ZE21B alloy via an alkali-heat method (AH; an essential measure of Mg-based materials for removing oil and other impurities that forms a hydroxide film for better corrosion resistance [68,107]), the specific step of which consisted in immersing the Mg alloy into a 5 M boiled NaOH solution for 3 h. Unfortunately, the results demonstrated that the AH-treated ZE21B exhibited high cytotoxicity, which may have been caused by the large amount of Mg^{2+} released and the over alkali pH value [108]. Moreover, the Cl$^-$ ion in the solution can decompose the Mg(OH)$_2$ film and convert it into soluble magnesium chloride (MgCl$_2$). Therefore, Mg(OH)$_2$ coating as a physical barrier can successfully separate the Mg substrate from an aqueous solution or physiological environment, but is not sufficient to endow Mg alloys with long-term corrosion resistance [109]. Mg(OH)$_2$
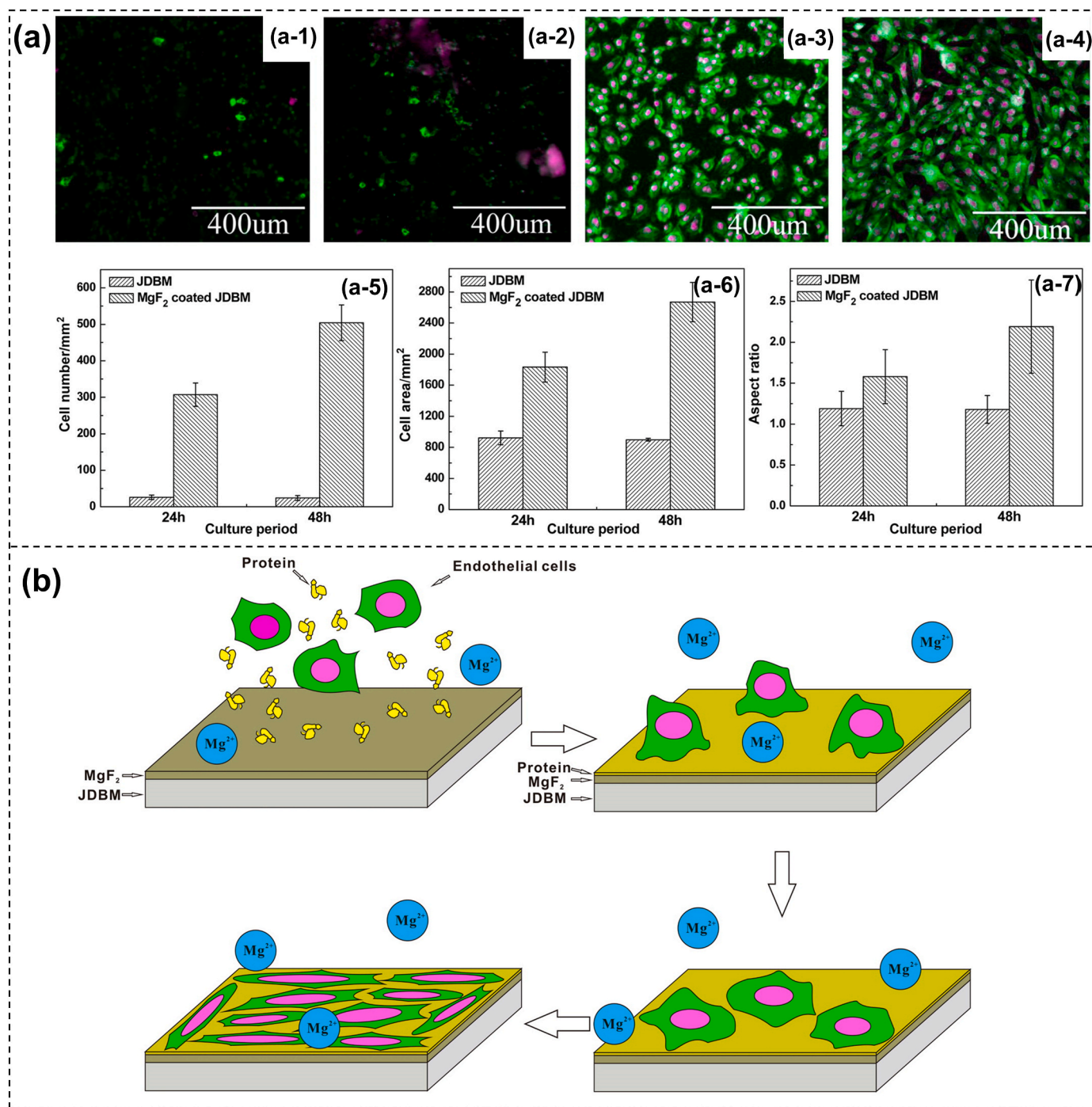
Fig. 5. (a) Cell attachment and elongation on JDBM alloy and MgF$_2$ coating, (b) and the corresponding schematic diagrams of the ECs behaviors on JDBM alloy modified by MgF$_2$ coating [124].

film is often used as an inner layer for augmenting the adhesion between the Mg substrate and the outer layer.

3.2.2. Layered double hydroxide (LDH) coatings

LDH coatings, which are a type of anionic clay with a highly adjustable brucite structure, have interlayer structures that can store anions and are used to resist Cl$^-$ [110,111]. The general formula of LDH can be expressed as $M^{2+}_{1-x}M^{3+}_x(OH)_2A^{n-}_x/n\bullet mH_2O$, where M^{2+} and M^{3+} are divalent and trivalent metal cations; x is the molar ratio of $M^{3+}/(M^{2+} + M^{3+})$ (ranging from 0.2 to 0.33), and A^{n-} represents the interlayer anions, such as NO_3^-, Cl^-, PO_4^{3-}, and CO_3^{2-} [112–114]. Liu et al. [115] successfully introduced the Mg-Al LDH to the JDBM alloy

pretreated with a Mg(OH)$_2$ coating through hydrothermal treatment. Tafel curves and hydrogen evolution tests suggested that the LDH coating had good corrosion-resistant characteristics and significantly promoted the ECs adhesion, migration, and proliferation in vitro. The low HR (<5%) of the LDH coating perfectly satisfied the requirements of clinical application. In vivo upshot found that the coating provided the most durable corrosion protection and caused the slightest inflammation compared with other samples, demonstrating that the LDH coating containing Mg(OH)$_2$ held promise for ameliorating anti-corrosion performance and biocompatibility. That research team further developed an LDH film to plug the micropores of MAO layer-coated AZ31 Mg alloy through hydrothermal treatment [116]. The MAO/LDH hybrid coating
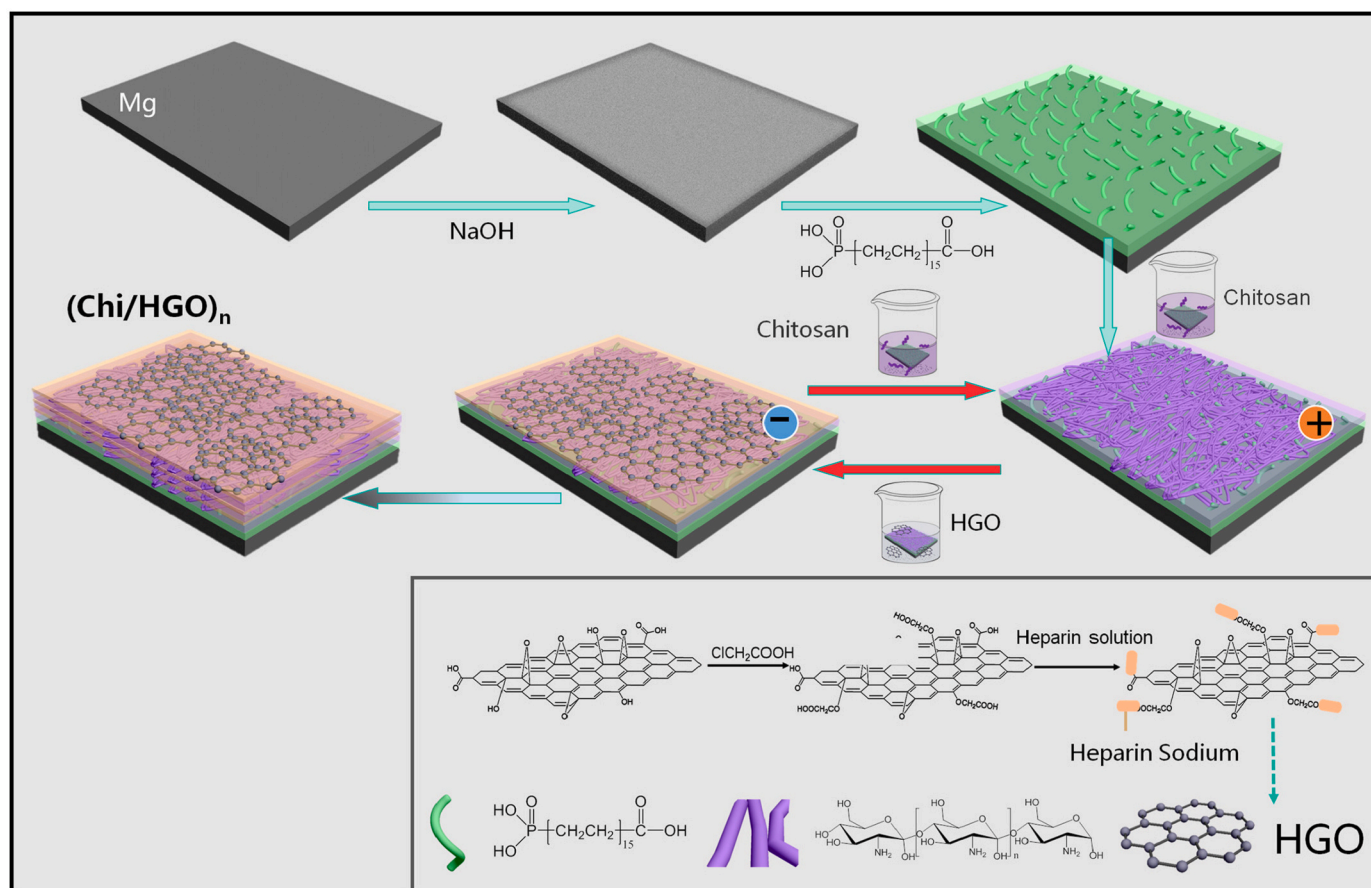
Fig. 6. Diagrammatic sketch of preparing CS/HGO multilayer film on the Mg alloy [136].

afforded a two-layer structure consisting of an inner MAO coating (~5 μm) and an outer LDH coating (~2 μm). The results indicated that the MAO/LDH coating acted as a physical barrier to avert the rapid degradation rates of the Mg alloy. The HR test showed that the HR value of the MAO/LDH coating was 1.10% ± 0.47%, indicating good blood compatibility. However, the nano-microstructure of the LDH coating fell off easily because of its poor abrasion resistance, and the exfoliated microstructures may enter the blood and cause adverse effects on the human body.

3.3. Inorganic nonmetallic coatings

Inorganic nonmetallic coatings are another alternative surface modification, including phosphate [117], magnesium fluoride (MgF_2) [118,119], and graphene oxide (GO) [120] coatings.

3.3.1. Phosphate coatings

In recent years, phosphate coatings have been reported as a feasible alternative to chromate coatings as a biomedical coating because they are insoluble in water and have high chemical stability and are environment-friendly [121]. Song et al. [117] developed a chemical conversion $Mg_3(PO_4)_2$ coating with a lamellar structure of about 1–5 μm width on the JDBM alloy, aiming to enhance its corrosion resistance and biological response. The phosphate coating markedly decreased the degradation rate. In addition, an in vitro cytocompatibility test showed that the coated JDBM alloy had a minimal negative effect on HUVECs viability, growth, and proliferation. Moreover, an in vitro hemocompatibility assay confirmed a reduced hemolysis ratio and the excellent anti-platelet adhesion property of the phosphate-coated JDBM stent. Although phosphate coating exhibited excellent biocompatibility, it may not be suitable as a coating of Mg alloy for vascular stents due to

its high brittleness. Zheng et al. [65] also proposed a similar viewpoint that phosphate surfaces were not appropriate for stent application because they were fragile and broke down easily. Usually, phosphate coatings (e.g. hydroxyapatite) are mainly used in Mg alloy for bone implant materials [68].

3.3.2. Fluoride conversion coatings

Fluorination treatment is a technology to prepare a fluoride conversion film on Mg substrates [122,123], and the corresponding formation mechanism of MgF_2 film is shown in reaction (7) [124]:

$$Mg^{2+} + 2F^- \rightarrow MgF_2\downarrow \tag{7}$$

Fluoride modification has been proverbially reported to reform the corrosion resistance of Mg alloys in industrial [125] and biomedical [126–128] fields. Mao et al. [129] applied hydrofluoric acid (HF) to obtain an MgF_2 conversion coating on the JDBM Mg alloy and studied its degradation and biocompatibility in vitro. Electrochemical tests unveiled that the degradation behavior of the Mg substrate was substantially improved by the formed MgF_2 protective layer. Also, the HR of the MgF_2 coating was lower (10.1%), and the cytotoxicity was decreased tremendously. Moreover, the MgF_2 coating exhibited a good anti-platelet adhesion ability. However, HF treatment is not an environmentally friendly method and may seriously affect the life and health of laboratory personnel. Yuan et al. [124] developed an environmentally friendly and simple technique to fabricate MgF_2 films with nanoscale on JDBM alloy in 5.8 g/L of potassium fluoride solution (KF). Compared with the Mg substrate, the corrosion rate of the MgF_2 sample was decreased by about 20% (0.269 mm/y vs. 0.337 mm/y) in artificial plasma. The team further attested that the prepared MgF_2 coating could facilitate the adhesion, proliferation, and spreading of ECs because the

nanoscale structures (200–300 nm) offered a much more favorable surface (Fig. 5). Furthermore, the JDBM stent exhibited excellent radial strength and compliance performance. The angiography images showed absence of thrombosis or serious in-stent restenosis in the MgF$_2$-coated JDBM stent, implying that the modified stent was safe and efficient in vivo. A follow-up intravascular ultrasound (IVUS) indicated that the coated stent was well-apposed to the vessel wall with no evidence of strut fracture, in-stent restenosis, or thrombosis. Furthermore, histological observation revealed that the MgF$_2$ coating aided in the re-endothelialization process of the JDBM stent into the denuded artery, demonstrating the acceptable mechanical durability and excellent tissue compatibility of the biodegradable stents. Nevertheless, the MgF$_2$ film is thin and can be destroyed easily; therefore, it is often used as a pre-treatment technique followed by organic coatings [130].

3.3.3. Graphene oxide (GO) coatings

GO is a nanomaterial with a single carbon structure that has a large specific surface area, good mechanical properties, and biocompatibility [131]. When GO is deposited onto the Mg surface, the oxygen-containing groups (including the hydroxyl (-OH), carboxyl (-COOH), and epoxy (–CH(O)CH–) groups) on the GO surface can evidently improve the anti-corrosive ability of the Mg alloy [132]. Concomitantly, GO can adsorb extracellular matrix (ECM) proteins via non-covalent combinations, hydrogen bonds, or electrostatic attraction, thereby promoting cell adhesion and proliferation. Moreover, the active groups of GO can be connected with other molecules to enhance their biological activity [133–135]. Pan et al. [136] proposed a chitosan (CS)/heparinized graphene oxide (HGO) coating on an alkali-treated Mg alloy using a layer by layer assembly (LbL) strategy (Fig. 6). The results of electrochemical measure, pH value change, and Mg^{2+} release suggested that the multilayer coating dramatically reformed the corrosion resistance of Mg alloy. Besides, CS/HGO multilayer coating could prominently reduce the platelet adhesion and accelerate the adhesion and proliferation of ECs. The LbL approach mentioned above, which is a novel and simple surface treatment tactic, is based on the fact that the charged substrate is alternately exposed to positively and negatively charged polyelectrolyte solutions using electrostatic interactions between opposite charges [137,138]. Moreover, LbL films with different polyelectrolytes and cycle times can realize multi-functionalization coating (drug release [139], self-healing properties [140], etc.) on the Mg alloy. Currently, the LbL technology is more widely used in the preparation of organic or polymer coatings on Mg-based materials, which will be discussed in detail below [141].

3.4. Polymer coatings

During the service of implanted Mg-based stents, the coating composed of inorganic substances may not be able to play the expected protective role [142]. In contrast, polymer or organic coatings are more prominent than inorganic coatings in the field of implanted stent materials due to their degradation ability, biocompatibility, drug delivery, self-healing, and cellular-response-mediating ability (e.g. adhesion, proliferation, and differentiation) [143]. Polymer or organic coatings mainly include polylactic acid (PLA), polycaprolactone (PCL), poly (lactide-*co*-glycolic) acid (PLGA), silane, polydopamine (PDA), hyaluronic acid (HA), chitosan (CS), and other representative polymer coatings [144]. Many technologies have been proposed for fabricating polymer coatings on Mg alloys, such as dipping coating, spin coating, LbL, and electrochemical technologies (electrodeposition, electrochemical grafting, and electropolymerization).

3.4.1. Polylactic acid (PLA) coatings

PLA, a product of lactide polymerization, is widely studied as a biodegradable polymer material [145]. The deposition of a PLA/PLLA coating on Mg alloy can endow Mg-based stents with the excellent performance regarding biodegradability and biocompatibility [146].

Zhang et al. [147] successfully prepared a homogeneous and smooth PLLA film (15–20 μm) on high-purity Mg (HPM, 99.99%) via the dipping method. The outcomes of the experiment illustrated that the PLLA coating had a smaller i_{corr} (3.565×10^{-5} A/cm^2) in the modified SBF at 37 °C. The bulging of the PLLA coating that occurred during the degradation process was caused by the locally released hydrogen, which likely escaped and pushed away the polymer film, thereby destroying the adhesive strength between the HPM substrate and the polymer coating. A similar phenomenon was reported by Zeng et al. [148]. Moreover, the accumulated Mg(OH)$_2$ could catalyze the degradation of the PLLA coating into acid according to the following equation (8):

$$(-COOR-)_n \xrightarrow{Mg(OH)_2} R_1COOH + R_2OH \qquad (8)$$
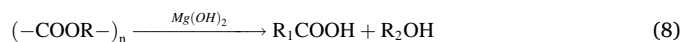
However, the adhesion of the PLLA coating to the Mg substrate is weak. Synthesizing an inorganic inner layer with strong adhesion to the Mg substrate via physical or chemical methods may usefully resolve the problem of weak adhesion of the outer organic coating. Liu et al. [149] fabricated a MAO/PLLA hybrid coating on the biodegradable AZ31 alloy by immersing the MAO coating in a PLLA solution. The bonding strength of the outer PLLA coating was obviously enhanced, as the porous MAO coating provided physical locking sites. These results attested that the MAO/PLLA coating tremendously reduced the i_{corr} of the Mg substrate. Moreover, the MAO/PLLA coating showed a lower HR (0.806% ± 0.771%), revealing good biological safety.

3.4.2. Polycaprolactone (PCL) coatings

PCL, which is commonly referred to as a "biodegradable" polyester because of its susceptibility to hydrolysis [150], has excellent physical and chemical properties, such as biodegradability, biocompatibility, and structural stability [151]. PCL is considered as a potential coating material to regulate the degradation rate and mechanical strength of materials, and has been approved by the US Food and Drug Administration (FDA) for use in extensive research in the field of biomedicine [152]. Virtanen et al. [153] developed biodegradable PCL coatings at different concentrations (2.5, 5.0, and 7.5 wt%) on the pure Mg via spin coating for investigating the degradation behavior of samples. The results indicated that the obtained PCL-7.5 coating availably protected the Mg substrate against corrosion for at least 15 d. However, all coatings expressed a weakly adhesive force to the Mg substrate. Hanas et al. [154] exploited the electrospinning technique to create a PCL nano-fibrous layer on the Mg alloy AZ31 pretreated with HNO$_3$. The tape test indicated that the adhesion of the outer PCL coating was immensely enhanced (4B grade). PCL coating combined with prior acid treatment could tailor degradation rate with enhanced bioactivity of Mg alloys because the combination of the acid treatment with polymer coating resulted in enhanced biomineralization, and then exerted a synergetic effect in controlling degradation rate in vitro. However, a critical evaluation of the biological performance of PCL coatings is necessary. Liu et al. [155] further evaluated the endothelialization of PCL coatings completely covering the Mg substrate. A PCL coating with a thickness of 0.5–2 μm was realized by optimizing the parameters of spin coating. The outcomes of the electrochemical test demonstrated that the coating considerably reduced the degradation rates of the bare Mg substrate, but a low adhesion density of HUVECs on PCL coating was observed, which might be partly because of its crystal surface [156]. Hence, a more accurate study of the biological properties of PCL coated Mg alloys needs to be carried out in an animal experiment in vivo.
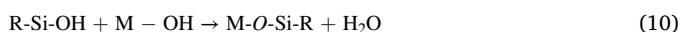
3.4.3. Poly(lactide-co-glycolic) acid (PLGA) coatings

PLGA, as an encouraging candidate, is one of the functional coatings that enhance the corrosion resistance and biocompatibility of Mg-based stents because its hydrolysates (lactic acid and glycolic acid) are endogenous and easily metabolized by the body via the Krebs cycle [157–159]. PLGA has been approved by the European Medicine Agency (EMA) and US FDA for application in various drug delivery systems in

humans [160,161]. Zhang et al. [162] reported a compact and uniform PLGA coating on a medical Mg-Zn alloy via the dip-coating method. The PLGA coating showed good corrosion resistance and a long degradation cycle, which effectively protected the Mg alloy from corrosion and achieved good medical application. Guo et al. [163] designed a drug-release coating composed of MAO coating, PLLA coating, and PLGA coating containing paclitaxel (PTX, an antineoplastic agent, that can inhibit intimal proliferation [164]). SEM images demonstrated that the PLLA coating completely sealed the micro-cracks/holes on the MAO layer. Also, the MAO/PLLA/PLGA (PTX) coating exhibited less platelet adhesion, aggregation, and activation. The drug release rate emphasized that the composite coating kept the PTX in a nearly linear sustained-release state, with no significant burst releases, and prolonged the release time of PTX. Furthermore, the prepared coating had acceptable blood compatibility.

3.4.4. Silane coatings

Silane, as a type of organosilicon compound, contains two groups with different chemical properties [68]. The general formula of the silane molecule is X-R-Si-OR, where X represents a non-hydrolyzable organic group, OR is the hydrolyzable group (methoxy, ethoxy, iso-propyl, etc.), and R stands for the carbon chain, which can be an aromatic hydrocarbon or an alkyl chain [165]. Silane-based coatings have been proved to be efficacious, eco-friendly, and economical and have been applied extensively in safeguarding Mg alloys against corrosion in the industrial field [166–168]. The reaction mechanism of silane coating is described in reactions (9-11):

$$R\text{-}Si\text{-}OR + H_2O \rightarrow R\text{-}Si\text{-}OH + ROH \tag{9}$$

$$R\text{-}Si\text{-}OH + M - OH \rightarrow M\text{-}O\text{-}Si\text{-}R + H_2O \tag{10}$$

$$2R\text{-}Si\text{-}OH \rightarrow R\text{-}Si\text{-}O\text{-}Si\text{-}R + H_2O \tag{11}$$

The hydrolysis of -Si-OR yields silanol groups (-Si-OH) in water, which can combine with hydrated Mg surfaces (Mg-OH) via an Mg-O-Si chemical bond; simultaneously, the silanol groups undergo self-crosslinking by forming siloxane bonds (Si-O-Si), thus creating a cross-linked anti-corrosion barrier [169]. Recently, several reports revealed that silane coating has been employed in the surface treatment of biomedical Mg alloys as a bio-functional coating due to its excellent biocompatibility, favorable cellular adhesion behavior, and proper protein absorption [170]. Gu et al. [171] synthesized poly triethoxy (octyl) silane (PTHOS) coatings on the Mg alloy AZ31B via an electro-deposition method at various cathodic potentials (−1.8, −2, and −2.2 V). The upshot showed that the silane coating (−2.0 V) yielded a slower corrosion rate compared with other silane coatings (−1.8 and −2 V). Moreover, the prepared silane coatings had satisfactory bio-compatibilities, such as increased cell viability (HUVECs), reduced hemolysis, and platelet adhesion. Moreover, the formation of the Mg-O-Si bond in the silane coating can powerfully enhance the interfacial compatibility between inorganic and organic materials [172]. Further-more, the active groups of silane coating can conjugate the functional groups of the bioactive molecules [173]. Liu et al. [174] developed a biofunctionalized anti-corrosive silane coating on the Mg alloy AZ31 via a facile two-step procedure. The first step immobilized a layer of densely crosslinked bistriethoxysilylethane (BTSE) coating with good corrosion resistance on the NaOH-activated Mg; the second step aimed to endow the surface with amine functionality by modifying a 3-amino-propyltri-methoxysilane (γ-APS) coating. In addition, heparin (Hep) molecules were covalently conjugated onto the silane-treated Mg alloy. Tafel and EIS curves illustrated that the hybrid coating exhibited an increased anti-corrosion ability compared with the bare Mg substrate. Moreover, the platelet adhesion of the composite coatings decreased significantly.

3.4.5. Polydopamine (PDA) coatings

Compared with synthetic polymers (e.g. PCL, PLA, and PLGA),

natural polymers exhibit enhanced biocompatibility, largely because of the absence of highly acidic degradation products [175]. Dopamine (DA), a high-adhesion protein inspired by mussel foot, can be used as a polymeric coating in a variety of materials because mussel foot protein-5 can firmly adhere to various substrate surfaces, including anti-adhesion polytetrafluoroethylene (PTFE) materials [176]. Poly-dopamine (PDA) synthesized via molecular self-polymerization can combine with many biological molecules because of its various functional groups (amine and catechol) [177]. Many studies have proved that the PDA layer can effectively enhance the attachment, proliferation, and migration of ECs [178,179]. Virtanen et al. [180] polymerized a PDA layer with a thickness of ~1 μm on pure Mg via a one-step immersion process in Tris buffer and studied the effects of pH value, immersion time, immersion angle, and dopamine concentration. The results of Tafel curves sug-gested that an immersion angle of 0° and a coating time of 2 h provided the best corrosion protection in a 0.1 M NaCl solution. Moreover, opti-mum corrosion resistance was achieved at both pH 10 and 1 mg/mL of DA and pH of 8 and 2 mg/mL of DA. A coating on Mg alloy for vascular stents needs to have both good anti-corrosion performance and other functional properties, including outstanding bioactivity, biocompati-bility, and suitability. Pan et al. [181] applied the self-assembly strategy to prepare a PDA coating on the Mg alloy AZ31B treated by alkali (NaOH) heating treatment. Electrochemical tests revealed that the i_{corr} of the PDA sample was reduced by three orders and that the E_{corr} increased from −1.174 to −0.178 V, suggesting the good corrosion resistance of the PDA coating. Moreover, ECs exhibited an improved proliferative profile compared with those grown on the unmodified Mg alloy, implying that the PDA film-coated Mg alloy had good cyto-compatibility with ECs. These results might be attributed to the fact that the different chemical groups (e.g. amine) introduced by the self-assembly technology can further react with other biomolecules with different functions, to improve biocompatibility. Unfortunately, the preparation of self-polymerizing PDA coatings on Mg alloys using the traditional method is time consuming and yields a large amount of PDA agglomeration. Moreover, Mg alloys can be corroded seriously, causing the cracking and high roughness of PDA coating [182,183]. To address this problem, Guan et al. [184] developed an electropolymerized dopamine (ePDA) coating on the ZE21B alloy through the galvanostatic method in sodium salicylate (SS) aqueous solutions. SEM images revealed that the ePDA coatings were more uniform than were dip-polydopamine (dPDA) coatings. However, as the corrosion resis-tance of ePDA coatings was slightly lower than that of dPDA coatings, it is necessary to further investigate the underlying mechanism and opti-mize the process of ePDA coating on Mg alloys. Recently, many studies stated that PDA can be used as an intermediate layer for additional surface functionalization (to improve adhesion and biocompatibility) [185]; however, the blood compatibility of PDA coatings is very poor because the imino and quinine groups will rapidly adsorb proteins, thus leading to the occurrence of adverse reactions, such as platelet adhesion, aggregation, and coagulation [186,187]. Hence, researchers have attempted to conjugate functional biomolecules (heparin, etc.) to PDA coatings for improved blood compatibility [188].

3.4.6. Hyaluronic acid (HA) coatings

HA, a bio-derived polymer, is one of the major components of the ECM that has the key functions of anti-thrombosis and anti-inflammation [189,190]. HA can hinder bacterial cell adhesion because of its anionic and hydrophilic properties [191]. Also, HA pro-vides a suitable environment for cell growth and can play a role in lubricating implant materials, and HA can promote the transition of SMCs from a synthetic to a contractile phenotype [192]. Lee et al. [193] manufactured a biosynthesized HA coating on absorbable pure Mg, for restraining the corrosion behavior of this material. The outcomes of the electrochemical test revealed that the early corrosion rate was markedly enhanced because of the synthetic HA coating. Nevertheless, the HA-coated pure Mg was peeled off during implantation in rats, which led
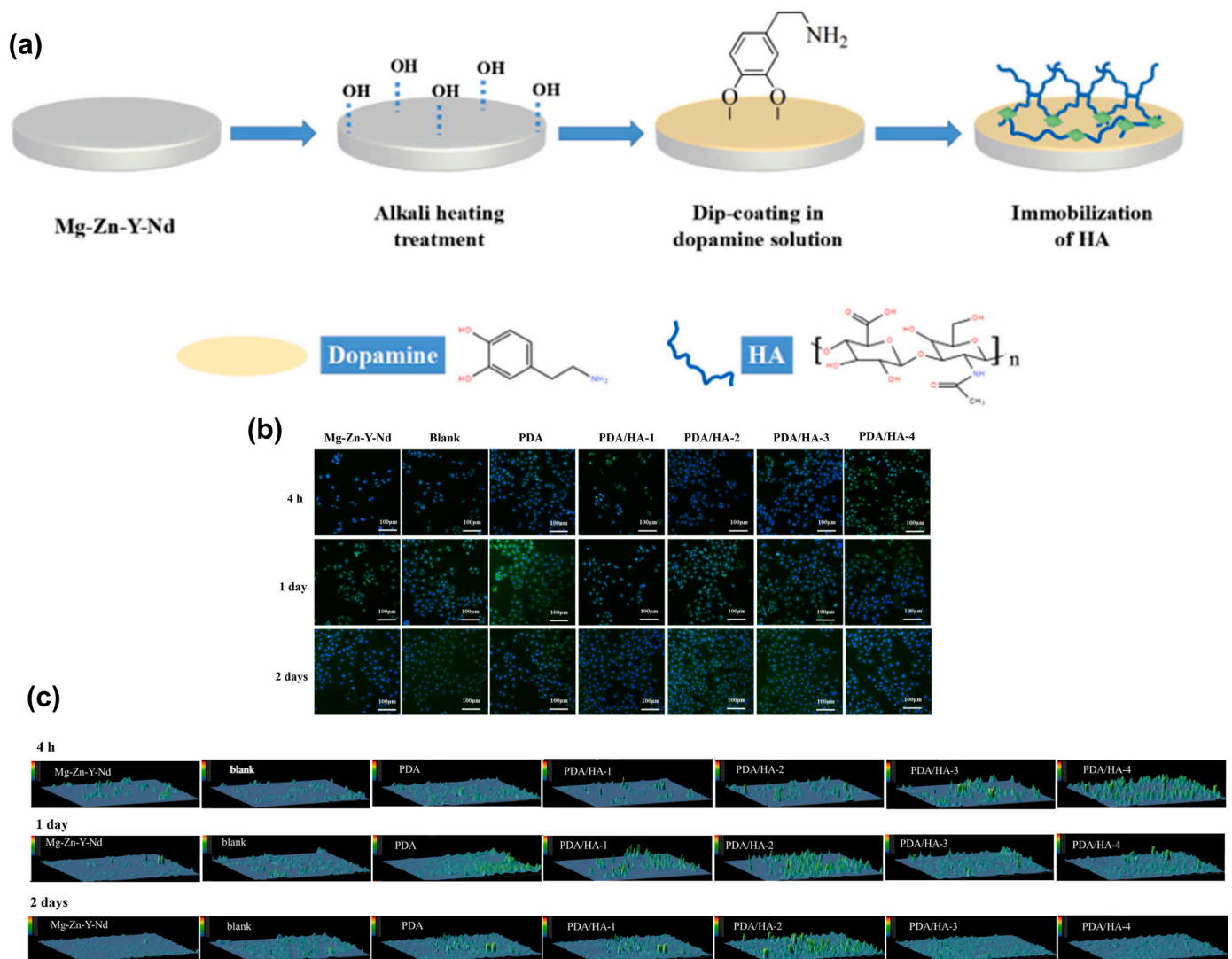
Fig. 7. (a) Preparation process of PDA/HA coating on ZE21B substrate, (b) immunofluorescence staining images of CD 31 antibody and DAPI in all samples, (c) the expression quantity of CD 31 of HUVECs in all samples [194].

to local and persistent corrosion, implying that the adhesion of the coating might be weak. To improve this shortcoming of HA coatings on Mg-based materials, Li et al. [194] prepared HA coatings with different molecular weights (MWs; 4×10^3, 1×10^5, 5×10^5, and 1×10^6 Da) on the ZE21B alloy using PDA coating as the intermediate layer (Fig. 7). The results showed that the PDA/HA coating (1×10^5 Da) improved better corrosion resistance and pro-endothelialization ability. In addition, the PDA/HA coating enhanced blood compatibility and the anti-hyperplasia and anti-inflammation functions of the ZE21B alloy. However, the poor mechanical property, rapid degradation and clearance in vivo of HA limit many of its direct clinical applications [195]. These deficiencies of HA can be addressed by chemical modifying or crosslinking [189].

3.4.7. Chitosan (CS) coatings

CS, which is composed of glucosamine and N-acetylglucosamine units linked by one to four glycosidic bonds, is a kind of naturally derived polysaccharide polymer that has good biodegradability and can promote cell adhesion and proliferation [196]. Moreover, CS shows a good antibacterial property due to the large amount of positive charges on its surface [197]. Xu et al. [198] prepared CS coatings on different Mg alloys (AM 20 and WE 43) using various pre-treatment methods (un-treatment, acid treatment, coupling agent treatment, and

glutaraldehyde treatment) for studying the effect of CS coatings on Mg alloy corrosion. That study demonstrated that the WE 43 alloy containing rare earth was more suitable as a biomaterial. Moreover, CS coating slowed down the corrosion rate, but different treatment methods had different effects. A more in-depth study of the in-situ degradation mechanism is crucial for the realization of controllable degradation of Mg alloys. Nevertheless, the weak interfacial adhesion force between CS coatings and the bare substrate limits their wide application. Cui et al. [199] devised a functionalized coating with corrosion-resistant and antimicrobial properties on the Mg alloy AZ31 via the electrostatic attraction between CS and poly-L-glutamic acid (PGA). Compared with the Mg alloy substrate, the obtained (CS/PGA)$_5$ exhibited a good corrosion resistance when immersed in SBF solution because of the pH-buffering action of the weak-weak polyelectrolyte pair. Moreover, a good antibacterial property was afforded to the Mg alloy using the contact-killing strategy. Pan et al. [200] used the LbL technology to synthesize a bioactive chitosan-functionalized graphene oxide/heparin (GOCS/Hep) multilayer on the AZ31B Mg alloy treated with a combination of surface chemical treatment with in-situ self-assembly of 16-phosphoryl-hexadecanoic acid, for exploring corrosion resistance and biocompatibility. The outcomes of this study indicated that the GOCS/Hep composite coating provided an excellent in vitro corrosion resistance to the Mg alloy. GOCS/Hep coating immensely decreased the
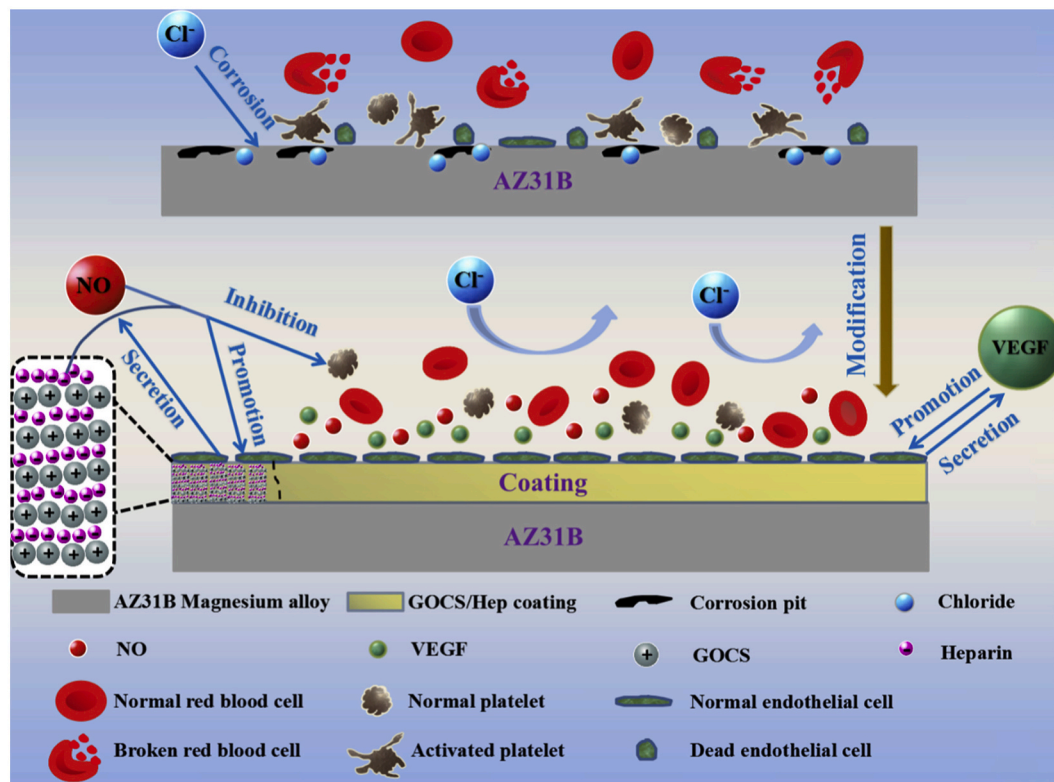
Fig. 8. Mechanism of GOCS/Hep coating on the corrosion resistance and biocompatibility of Mg alloy [200].

HR and platelet adhesion and activation, leading to excellent blood compatibility. Furthermore, the GOCS/Hep coating enhanced the adhesion and proliferation of ECs and promoted the expression of vascular endothelial growth factor (VEGF) and nitric oxide (NO) on the surface of the attached ECs [201]; a schematic diagram is shown in Fig. 8.

3.4.8. Other representative polymer coatings

The above-mentioned classic polymer coatings have been proverbially used to ameliorate the biological functions of Mg alloys. Moreover, other emerging polymer coatings have come to the forefront of research in this field because of their multifunctional characteristics and simple operation.

Liu et al. [202] reported a self-designed biodegradable arginine-leucine-based poly (ester urea urethane)s (Arg-Leu-PEUUs) pseudo-protein material that was used as a protective and bio-functional coating for the ZE21B alloy in cardiovascular stent applications, whereas the PLGA coating was used as the control. The Arg-Leu-PEUU coating exhibited a stronger bonding strength to the Mg substrate compared with PLGA coating; the electrochemical and immersion tests performed in vitro demonstrated the substantially better corrosion resistance of the coating. The results of acute blood contact tests revealed the superior hemocompatibility of the Arg-Leu-PEUU coating. Furthermore, the Arg-Leu-PEUU coating stimulated HUVECs to release a suitably increased amount of nitric oxide (NO), signifying that it possessed the potential to inhibit thrombosis and restenosis. Gu et al. [203] prepared poly (carbonate urethane) urea (PCUU) and poly (ester urethane) urea (PEUU) coatings on Mg alloy AZ31 stents, whereas PLGA coating was employed as the control. Dynamic degradation tests revealed that the PCUU coating evidently restrained the degradation behavior of the Mg alloy compared with the PEUU coating, PLGA coating, and Mg substrate. The PCUU coating effectively reduced platelet adhesion in acute blood contact tests, and the PCUU coating containing paclitaxel successfully inhibited the proliferation of SMCs,

revealing that the PCUU coating might be a promising candidate in the cardiovascular field because of its corrosion retardation, low thrombogenicity, drug loading capacity, and high elasticity.

Wang et al. [204] devised a simple and universal Mg^{2+} incorporated epigallocatechin gallate (EGCG, which is the main component of tea polyphenols in green tea and has a well-known anti-inflammatory and antioxidant capacity) multilayer conversion coating on the Mg alloys AZ31 using the LbL strategy (Fig. 9). Surface morphology indicated that the as-formed EGCG/Mg coating with the incorporation of Mg^{2+} presented a more uniform and dense morphology than did the pure EGCG coating. The results of corrosion-resistance tests revealed that the degradation rate of the EGCG/Mg coating was significantly slower than that of the AZ31 substrate. An in vitro assay suggested that the EGCG/Mg coating owned excellent anti-thrombosis ability and inhibition of cytokine release compared with the EGCG coating and bare AZ31 substrate. In vivo assays demonstrated that EGCG/Mg exhibited better tissue compatibility, re-endothelization, and suppression of the over-proliferation of SMCs, revealing that EGCG/Mg coating might be a good candidate coating on Mg alloys for cardiovascular implants. The use of tea polyphenols to construct bio-layers on Mg alloys has also been reported by Wang et al. [205,206], with results consistent with those reported in the literature cited above.

Silk fibroin (SF), which is produced by silkworms (*Bombyx* mori), is an attractive natural protein for biomedical application because of its controlled biodegradability, good cell adhesion, high tensile strength, and low inflammatory response [207,208]. SF has been used in drug reservoirs (e.g. PTX, Hep, and antibodies), nanospheres, hydrogels, and films [209,210]. Niidome et al. [211] developed an SF coating containing sirolimus (SRL, a drug that prevents intimal hyperplasia) on the Mg alloy AZ31 treated with HF, for evaluating corrosion resistance and biocompatibility. The results of corrosion-resistance tests showed that MgF_2/SF coating prevented the local and deep corrosion of the Mg alloy, although total corrosion remained unaffected. Moreover, uniform corrosion, without local or deep corrosion, was observed, thus extending
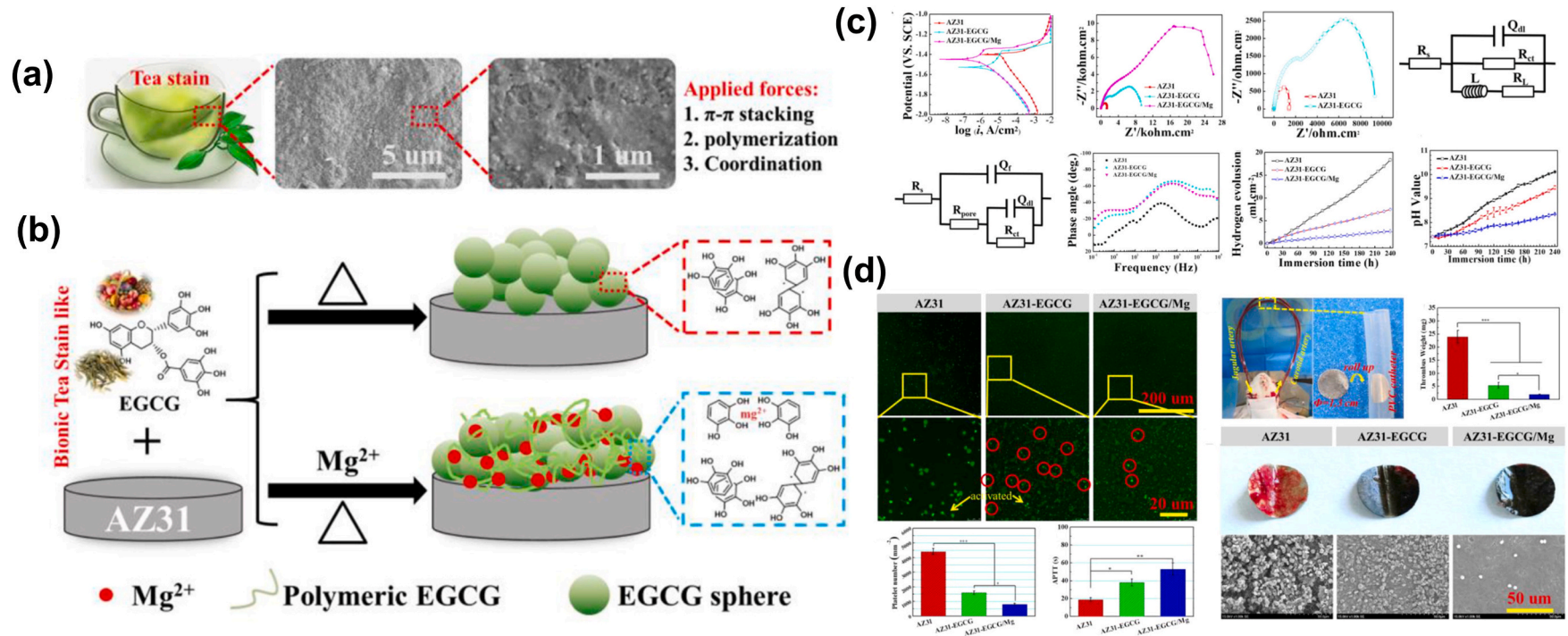
Fig. 9. (a) SEM images of tea stains deposited on cup after using for several weeks, (b) schematic formation process of EGCG/Mg coating on Mg alloy using LbL methods, (c) electrochemical and immersion tests of all samples, and (d) hemocompatibility of sample surfaces [204].
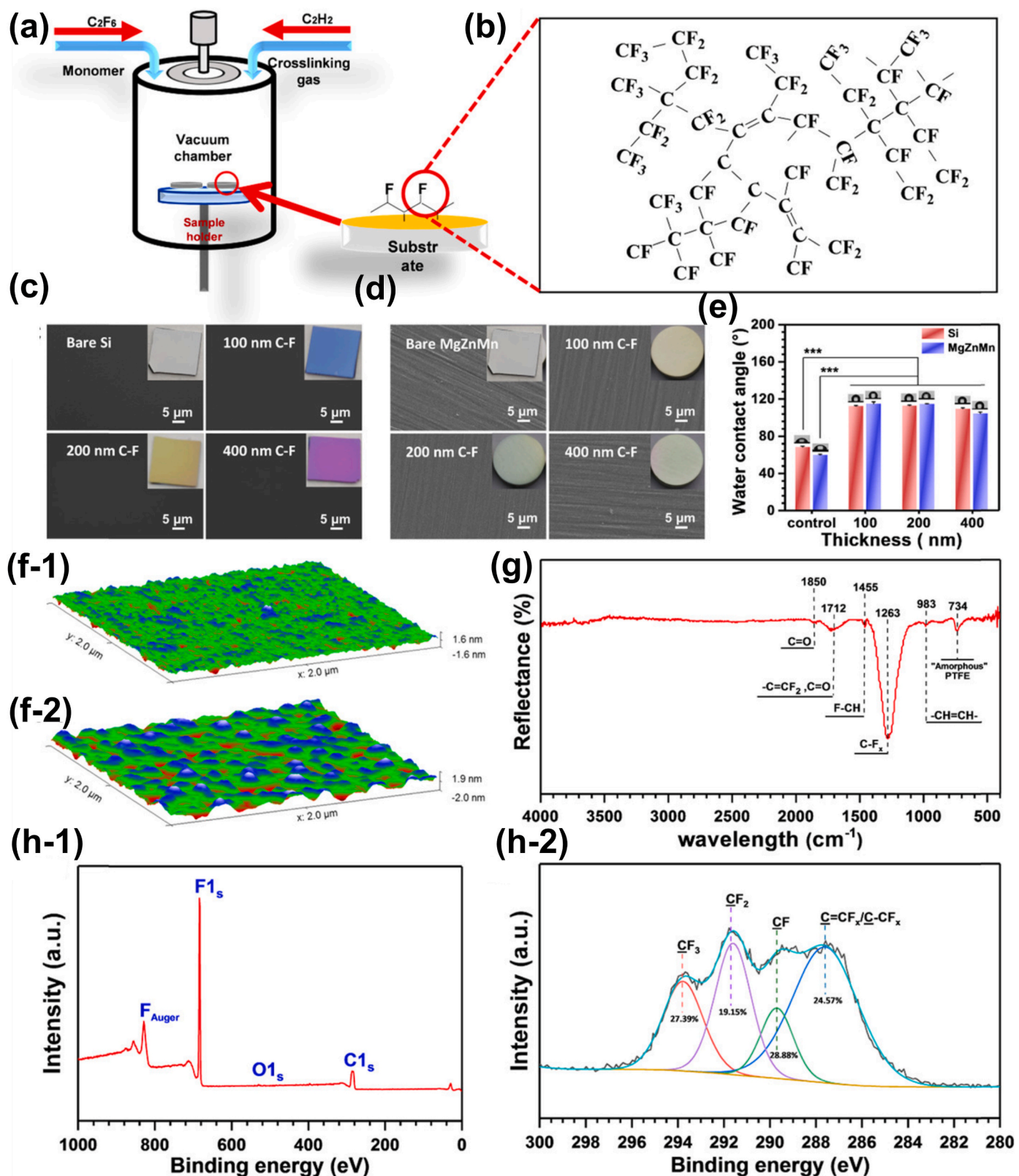
Fig. 10. (a, b) Schematic diagram of the fabrication of the C−F coatings on the Mg alloy, (c–h) the surface characteristics of prepared C−F coating [220].

the radial strength of the stent. The biocompatibility evaluation revealed that the composite coating yielded outstanding HUVEC adhesion and minimal platelet adhesion, implying that SF is a potential coating for stent applications.

Proteins (e.g. SF) are composed of different amino acids, such as

alanine, serine, and proline [212]. Currently, amino acids have been widely used as corrosion inhibitors (a chemical or a mixture of several chemicals that can decrease the corrosion rates of metallic materials in the corrosive medium [213]) in engineering applications because they can produce a protective film via physical adsorption onto, and chemical
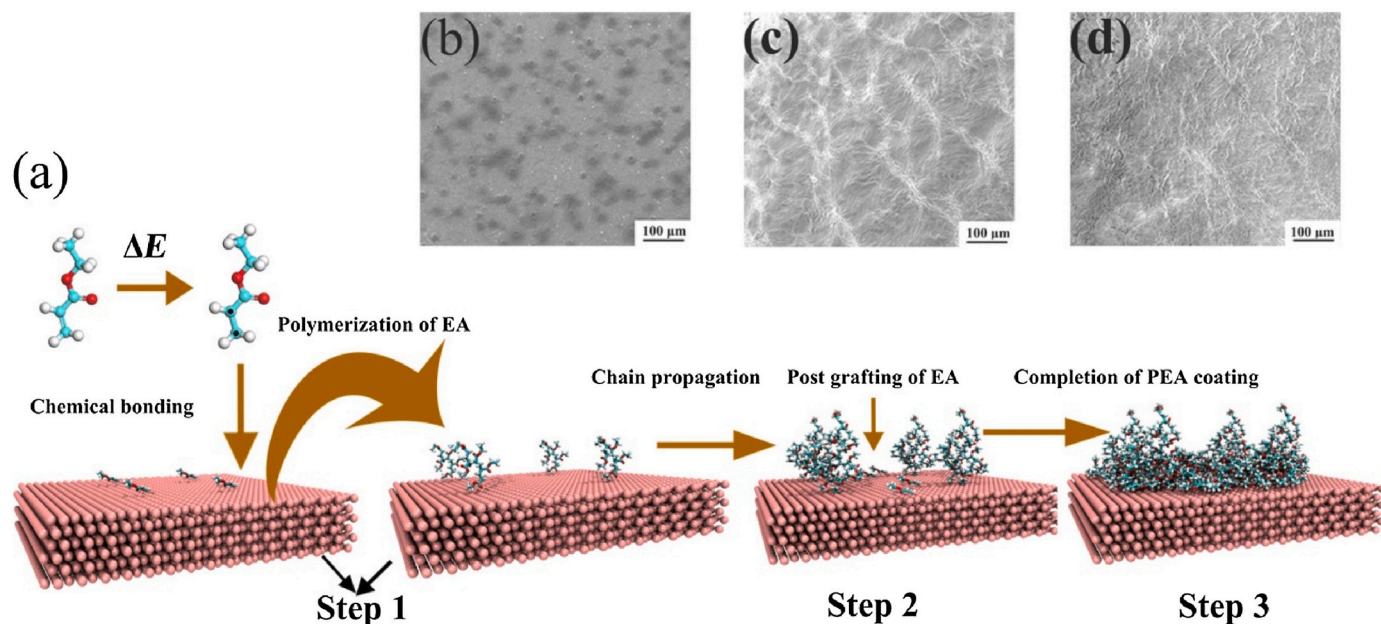
Fig. 11. (a) Schematic of the formation mechanism of PEA coating on Mg alloy, (b) the corresponding SEM images of PEA coating [225].

interaction with a metal surface. Unfortunately, efficient engineering corrosion inhibitors may not be suitable for dominating the degradation rates of Mg alloys in physiological environments. Guan et al. [214] innovatively developed a class of non-toxic Schiff base (SB, which is a compound that contains an azomethine group and serves as a corrosion inhibitor owing to the existence of the C=N bond in the molecule [215]) corrosion inhibitor applicable to Mg alloys in the biomedical application via the reaction between paeonol and amino acids. Furthermore, the effects of different concentrations of inhibitors on HUVECs were evaluated. The results of corrosion-resistance tests revealed that new corrosion inhibitors effectively inhibited the degradation rate of the ZE21B alloy because SB molecules could react with Mg^{2+} to form complete and stable corrosion products, thus achieving a self-healing effect. Cell-based experiments suggested that the relative survival rate of HUVECs was increased significantly by reducing the concentration of the SB medium. As a huge concentration difference between the cell wall and the environment outside the cell wall led to cell dehydration and death, the relative survival rate of ECs decreased with the increase in the concentration of the inhibitor in the medium. However, the reported study was limited regarding the saline solution containing the corrosion inhibitor and was not introduced into the coating; therefore, further experiments combining SB corrosion inhibitors with coating need to be carried out.

Plasma polymerization, a method that uses plasma to polymerize gas molecules, can produce ultra-thin, pinhole-free polymer-like layers and convert monomer functional groups (especially amine and carboxyl groups) onto a polymerized molecule backbone that serves as an anchoring point or improves cellular adhesive interactions [216]. Plasma polymerized allylamine coatings are being extensively used to introduce amine groups onto various biomaterials because they can enhance the adhesion of proteins and cells, inhibit inflammatory reactions, and influence the differentiation of mesenchymal stem cells [100,217,218]. Qi et al. [219] constructed a multifunctional plasma polymeric allylamine (PPAam) coating with a thickness of ~250 nm on a biodegradable MgZnMn alloy stent. Electrochemical and immersion evaluations confirmed that PPAam coatings ameliorated the corrosion resistance properties of MgZnMn alloys. The results of endothelial cytocompatibility tests suggested that the PPAam coating had good ECs adhesion, spreading, and proliferation properties. Interestingly, the protective coating remained smooth, without cracks or webbing, before

and after balloon expansion tests. Huang et al. [220] further used acetylene (C_2H_2) as the crosslinking agent to obtain a thin, uniform, pinhole-free, polymer-free, and hydrophobic C−F coating on MgZnMn alloys using the plasma polymerization technology, as shown in Fig. 10, followed by the deposition of a hydrophilic PPAam layer on the C-F coating. Electrochemical and in vitro immersion tests demonstrated that the C-F coating dramatically decreased the corrosion rate of MgZnMn alloys in phosphate-buffered saline (PBS) solution at 37 °C. Moreover, the C-F-PPAam composite usefully facilitated HUVEC adhesion and viability.

Electrochemical grafting is a type of electrochemical polymerization technology that can form a covalent bond between organic molecules and conductors or semi-conductors or their oxides, and can be divided into anodic and cathodic electrochemical grafting according to the different graft monomers [221,222]. Ascencio et al. [223] synthesized polypyrrole (PPy) coatings on the WE 43 alloy via an anodic electropolymerized method (using cyclic voltammetry at a scan rate of 20 mV s^{-1} over 20 cycles), and the results of which showed that the PPy coating effectively reduced the degradation rate of the WE 43 alloy. However, organic coatings prepared on the Mg alloy by anodic electrochemical grafting usually lead to the oxidation of the substrate, resulting in the dissolution of Mg^{2+}, and then participate in the formation of the organic coating [224]. The mechanisms underlying the formation of this coating may lead to the decline of the mechanical support performance of Mg alloy stents, to a certain extent, because of the smaller wall thickness of Mg alloy stents.

The cathodic electrochemical grafting technology can avoid the dissolution of metal ions and form chemical bonds through the charge transfer between the metal and the organic molecules, thereby strengthening the bond between the organic coating and the metal substrate. Yang et al. [225] developed a polymethyl acrylate (PEA) coating on the ZE21B alloy via cathodic electrochemical grafting for stent application (Fig. 11). The SEM images revealed that the PEA coating afforded a network structure on the Mg alloy. Time-of-flight secondary ion mass spectrometry (ToF-SIMS) confirmed that a covalent bond was established during the grafting process, implying a strong adhesion. Tafel curves indicated that the PEA coating with an intact and compact structure markedly decreased the degradation rate of the ZE21B substrate. The results of the immersion test suggested that the complete morphologies of PEA coatings were maintained after soaking

Table 2
Single-layer coatings used for Mg and its alloys.

Mat.	Coa.	Th. (μm)	Sol.	E_{corr} (V/SCE)		i_{corr} (μA/cm²)		Cor.(mm/a)		Im. (d)	Res. Ref.
				Sub.	Coa.	Sub.	Coa.	Sub.	Coa.		
Mg–Zn	TiO₂	0.05	SBF	–	–	789.5	24.4	18.04	0.557	–	Ameliorative corrosion resistance was offered by the TiO₂ coating, and drugs were expected to be loaded on the TiO₂ film by physical adsorption [89].
Mg–Zn	TiO₂	0.400	SBF	−1.70	−1.65	1050	49.0	23.99	1.119	14	TiO₂ film had a low HR (1%) and inhibited platelet adhesion and promoted ECs attachment [91].
AZ31B	Mg(OH)₂ MgF₂	–	SBF	−1.57	−1.174 −1.128	37.26	2.052 0.6821	0.851	0.046 0.015	7	MgF₂ coating had relatively better corrosion resistance than Mg(OH)₂ coating, however, Mg (OH)₂ coating showed better anti-thrombosis and cytocompatibility to ECs than MgF₂ coating [109].
JDBM	Mg₃(PO₄)₂	3.5	Artificial plasma	−1.74	−1.63	1.59	1.08	0.036	0.024	–	The prepared phosphate coating improved the corrosion resistance and biological response. Also, the Mg₃(PO₄)₂ coating showed excellent biocompatibility and anti-platelet adhesion property [117].
JDBM	MgF₂	1.5	Artificial plasma	−1.69	−1.59	1.41	1.05	0.032	0.023	10	MgF₂ film effectively improved the corrosion resistance and showed good anti-platelet adhesion. Moreover, the cytotoxicity of MgF₂ film satisfied the requirement of a cellular application [129].
Pure Mg	PCL PLA	15–20	SBF	–	– –	207.3	12.93 35.65	4.736	0.295 0.814	10	PCL and PLA coating improved corrosion resistance of pure Mg, but the interaction between Mg and polymer coating might destroy its corrosion resistance in the physiological environment [147].
AZ31B	Pho PAPTMS PDA	–	DMEM	−1.556	−1.151 −1.229 −1.419	168.7	0.00135 0.6279 0.956	3.854	0.00003 0.014 0.022	7	Mg-Pho showed the best corrosion resistance due to the phosphating effect. Three coatings enhanced the blood compatibility to varying degrees, and further improved the cytocompatibility of ECs [181].
AZ31B	THOS	–	Hank's	–	–	32.93	0.68–0.88	0.752	0.015–0.02	29	Silane coating exhibited a superior corrosion resistance, cyto- and hemocompatibility [171].
ZE21B	PDA	–	SBF	−1.755	−1.748	370.0	285.1	8.454	6.514	7	PDA coating prepared by electropolymerization as a single coating had no significant corrosion protection effect on Mg alloys, and secondary modification was still needed to increase the anti-corrosive ability [184].
ZE21B	PEA	–	SBF	−1.79	−1.56	577	8.17	13.184	0.186	7	PEA coatings markedly decreased the degradation rates of Mg substrates, and the PEA coating was safe and own favorable hemocompatibility (HR, 1.31 ± 0.11%) [225].
AZ31	ECGG/Mg	0.415	SBF	−1.39	−1.45	16.2	0.104	0.370	0.002	10	EGCG/Mg coating showed durable corrosion protection, inhibition of the release of cytokines, and anti-thrombosis ability. Also, the EGCG/Mg coating exhibited better tissue compatibility, antithrombosis formation, re-endothelization, and suppression of the over-proliferation of SMCs in vitro and in vivo assays [204].

*T = Thickness, Sol. = Solution, Sub. = Substrate, Coa. = Coating, Im. = Immersion time, Cor. = Corrosion rate (the corrosion rate of samples is calculated by the following relationship: Cor. = 22.85i_{corr} [36]), SBF = Simulated body fluid, DMEM = Dulbecco's minimum essential medium, PCL = Polycaprolactone, PLA= Polylactic acid, Pho = 3-Phosphonopropionic acid, PAPTMS = Poly (3-aminopropyltrimethoxysilane), PDA = Polydopamine, PTHOS = Poly triethoxy(octyl)silane, PEA = Polyethylacrylate, ECGG = Epigallocatechin gallate.

in SBF (7 d). Moreover, the PEA coating had acceptable hemocompatibility and safety and reduced the risk of thrombosis after implantation. However, further assessment of the biocompatibility of PEA coatings on Mg-based stents should be conducted. Various single-layer coatings on Mg and its alloys are listed in Table 2.

3.5. Composite coatings

Using a single layer, it is difficult to simultaneously meet the actual application requirements of Mg-based stents, which require strong bonding strength and excellent functional characteristics. Considering the exceedingly complicated biological environment, multilayer coatings composed of a single-layer coating with different properties may be an effective way to resolve this issue; these coatings include inorganic layer/inorganic layer, inorganic layer/organic layer, and organic layer/functional biomolecular coatings. Various composite coatings on Mg-based materials are listed in Table 3.

3.5.1. Inorganic layer/inorganic layer

Li et al. [226] reported a nanosheet-structured Mg-Al LDH coating with a thickness of 3.8 μm on the MAO-coated Mg alloy AZ31, which was obtained using a water bath with a higher pH (13.76) at a lower temperature (60 °C). The results demonstrated that the i_{corr} of the MAO-LDH coating was decreased by four orders of magnitude compared with the Mg substrate, implying that the hybrid coating possessed excellent corrosion resistance. Furthermore, the MAO-LDH coating possessed a certain degree of self-healing ability because of the appearance of a wide passivation region in the anodic polarization branch. Unfortunately, that

Table 3
Multi-layer composite coatings used for Mg and its alloys.

Mat.	Coa.	Th. (μm)	Sol.	E_{corr} (V/SCE)		i_{corr} (μA/cm²)		Cor.(mm/a)		Im. (d)	Res. Ref.
				Sub.	Coa.	Sub.	Coa.	Sub.	Coa.		
AZ31	MAO/LDH	3.8	Hank's	−1.43	−1.49	12.80	0.0068	0.292	0.0066	6.5	MAO/LDH coating remained intact without cracking during the immersion process, implying good corrosion resistance [226].
AZ31	MAO/LDH	7.0	PBS	−1.45	−1.20	16.60	3.92	0.379	0.089	–	The anti-corrosion property of the Mg substrate was remarkably enhanced due to the coated MAO/LDH coating. Also, the MAO/LDH coating showed that the HR value was 1.10 ± 0.47%, implying good blood compatibility [116].
ZK60	MAO/MgF₂	10	Hank's	−1.49	−1.53	16.82	2.52	0.384	0.057	10.5	HF treatment sealed the micropores/cracks of the MAO coating, thereby improving corrosion resistance. Also, MAO/MgF₂ coating showed no hemolytic potential [230].
Mg−Zn−Sr	MAO/Ag	3.7 ± 0.7	SBF	–	−1.137	–	0.006532	–	0.00015	21	MAO/Ag coatings had a good corrosion resistance, and the addition of Ag led to obvious antibacterial properties [227].
Mg−4Li−1Ca	MAO/CS	11	Hank's	−1.557	−1.932	24.84	6.714	0.567	0.153	7	The preparation of MAO/CS coating significantly enhanced the corrosion resistance of Mg alloy. And MAO/CS coating possessed a good effect in reducing bacteria growth due to the contact-killing strategy [236].
WE 42	MAO/PLLA	–	Hank's	–	–	–	–	–	–	28	MAO/PLLA coating was changed little after soaking for 4 weeks, and it had a good hemocompatibility (HR, 1.79% ± 0.67%) [98].
AZ31	MAO/PLLA	–	SBF	−1.663	−1.317	290.2	–	6.631	–	14	MAO/PLLA coating protected AZ31 from fast degradation in the physiological environment. Besides, the coating could be used as a blood-contacting protective layer on AZ31 alloy due to a low HR (0.806% ± 0.771%) [149].
AZ31	MAO/PLLA/PDA/Hep	–	SBF	−1.623	−1.483	69.51	0.5581	1.588	0.0127	–	The composite coating improved the surface hemocompatibility enhanced the HUVECs proliferation and simultaneously inhibited the SMCs proliferation [94].
AZ31B	Mg(OH)₂/PDA/HA	–	SBF	−1.682	−1.399	14.40	7.37	0.329	0.168	8	Mg(OH)₂/PDA/HA coating showed a distinct amelioration in corrosion resistance, anti-thrombotic properties, and biocompatibility [237].
JDBM	LDH/Mg(OH)₂	2.6	PBS	−1.7749	−1.5277	15.62	0.3626	0.356	0.0083	30	LDH/Mg(OH)₂ exhibited favorable corrosion resistance and cell adhesion, migration, and proliferation in vitro. The coating with a low HR (<5%) offered the greatest long-lasting protection from corrosion and triggered the mildest inflammation in vivo [115].
AZ31	LDH/PDA/Hep	–	PBS	−1.603	−1.378	27.40	10.60	0.626	0.242	–	LDH/PDA/Hep film protected Mg alloy from corrosion and improved HUVECs migration rate and inhibited platelet adhesion and had a low hemolysis rate [241].
ZE21B	MgF₂/PDA	0.1	DMEM +40 g/L BSA	−1.64	−1.45	21.75	0.16	0.496	0.0036	14	MgF₂/PDA coating demonstrated the enhancement of dramatic corrosion resistance in vitro and exhibited great performance of cell adhesion and proliferation, which was preferable for re-endothelialization [119].
ZE21B	MgF₂/TA	1.71 ± 0.08	DMEM	–	–	–	0.24 ± 0.02	–	0.0054 ± 0.0004	14	MgF₂/TA coating endowed the Mg surface with excellent antioxidant and platelet-repellent capabilities and supported ECs growth and proliferation. Besides, no significant inflammatory response was observed for the MgF₂/TA coating [232].
AZ31	AT/PCL	–	SBF	–	–	–	–	–	–	5	HNO₃ treatment boosted adhesion of the PCL coating, and the AT/PCL coating was effective in impeding degradation rates and enhancing bioactivity [154].
AZ31B	CS/HGO	0.755	SBF	−1.801	−1.376	88.63	0.7483	2.025	0.017	14	CS/HGO films improved corrosion resistance of Mg alloy, and it reduced the platelets adhesion and promoted the proliferation of ECs [136].

Table 3 (*continued*)

Mat.	Coa.	Th. (μm)	Sol.	E_{corr} (V/SCE)		i_{corr} (μA/cm^2)		Cor.(mm/a)		Im. (d)	Res. Ref.
				Sub.	Coa.	Sub.	Coa.	Sub.	Coa.		
AZ31B	GOCS/ Hep	7.24	SBF	−1.755	−1.385	88.41	1.359	2.020	0.031	7	GOCS/Hep coating enhanced corrosion resistance of Mg alloy and simultaneously improved the hemocompatibility and HUVECs proliferation [200].
Pure Mg	PDA/PCL	–	HBSS	−1.55	−1.55	5.90	0.10	0.134	0.0022	10	PDA layer improved the bonding force of PCL coating, and PDA/PCL coating enhanced the early corrosion resistance of Mg substrate in HBSS [185].
AZ31	(CS/ PGA)$_5$	–	SBF	−1.47	−1.67	6.85	0.40	0.156	0.009	–	(CS/PGA)$_5$ coating owned good corrosion resistance, and the excellent anti-bacterial property was obtained due to the contact-killing strategy [199].
ZK60	PLGA/ GA/PLGA	2.1 ± 0.3	SBF	−1.59	−0.24	20.51	0.01	0.468	0.0002	–	The corrosion rate of the coating was ~2000 times lower than that of the bare substrate. The released GA molecules selectively promoted the proliferation of ECs, and inhibit SMCs growth [238].
AZ60	APTES/ PCL	–	SBF	−1.41	−0.365	70.5	0.293	1.610	0.0069	7	The corrosion rates of Mg alloys were extremely improved due to the preparation of the APTES/PCL coating [168].
Mg−Zn−Ca	APTES/ SF	7	SBF	−1.56	−0.80	–	–	–	–	7	APTES/SF coatings were an effective protective coating for Mg substrates and delayed the degradation period of Mg alloys. Also, the coating showed excellent biocompatibility [170].
ZE21B	BTSE-APTES-PLGA	6.4 ± 0.4	Hank's	−1.396	−0.405	31.91	7.148	0.729	0.163	30	BTSE-APTES-PLGA coating exhibited both improved anti-corrosion ability and biocompatibility for cardiovascular stent implants [172].
ZE21B	PDA/HA	–	SBF	−1.6491	−1.5715	103.4	1.303	2.362	0.029	15	PDA/HA displayed better hemocompatibility, pro-endothelialization, anti-hyperplasia, and anti-inflammation functions in vitro, PDA/HA coating had preferable corrosion resistance and biocompatibility in vivo [194].
MgZnMn	CA/PELI/ Hep	3.69	PBS	−1.59	−1.37	64.56	0.0457	1.475	0.001	8.3	CA/PELI coating effectively inhibited the degradation rate of Mg alloy. CA/PELI/Hep coating showed significant improvement in hemocompatibility and HUVECs proliferation, while apparent suppression in SMCs proliferation [205].
MgZnMn	C−F/ PPAam	0.415	PBS	−1.63	−1.15	6.30	0.07	0.143	0.0016	28	The inner C-F coating endued the Mg substrate with markedly elevated corrosion resistance. The outer PPAam coating promoted cell adhesion and viability [220].
ZE21B	Arg-Leu-PEUU		Hank's	−1.72	−1.22	186.4	3.25	4.259	0.074	30	Arg-Leu-PEUU coating showed better corrosion resistance, hemocompatibility, and cytocompatibility. Moreover, it stimulated HUVECs to release a reasonably increased amount of NO [202].

*PBS = Phosphate buffer saline, BSA = Bovine serum albumin, MAO = Micro-arc oxidation, LDH = Layered double hydroxide, TA = Tannic acid, AT = Acid treatment, Hep = Heparin, CS = Chitosan, HGO = Heparinized graphene oxide, GOCS = Chitosan-functionalized graphene oxide, PGA = Poly-L-glutamic acid, GA = Gallic acid, BTSE = Bistriethoxysilylethane. CA = Catechol, PELI = Polyethyleneimine, PPAam = Plasma polymeric allylamine, PEUU = Poly (ester urea urethane).

paper used bone-implant cells alone to evaluate the cytocompatibility of Mg alloys; therefore, further evaluation of the blood compatibility and ECs compatibility is necessary. Chen et al. [227] developed MAO coating sealed by Ag_2O and Ag_2CO_3 phases on the Mg–3Zn–0.5Sr alloy via the addition of different concentrations of silver acetate (CH_3COOAg; 0, 1, 2, and 3 g/L) in the electrolyte. The results of these experiments revealed that the MAO-Ag coating evidently ameliorated the corrosion resistance ability of the Mg alloy because of the decrease in the rate of micro-pores/cracks on its surface. The MAO-Ag coating afforded an evident antibacterial property because Ag_2O nanoparticles possessed the strongest bactericidal effect, and the Ag^+ released by the phase containing Ag also killed bacteria by attaching to and penetrating their cell membrane [228,229]. An MAO/MgF_2 coating was synthesized on the Mg alloy ZK60 by combining MAO and fluorination treatment technology for the first time [230]. The experimental results demonstrated that post-treatment with HF sealed the porous MAO coating, and that MgF_2

became the dominant component of the coating. A hemolytic test illustrated that the HRs of MAO (0.34% ± 0.22%) and the MAO/MgF_2 coating (0.20% ± 0.08%) were substantially reduced according to the ISO 10993–4 standard, showing that the MAO/MgF_2 coating had no hemolytic potential. Although inorganic composite coatings have good performance corrosion resistance, the elastic deformation required for Mg alloy stents needs to be improved.

3.5.2. Inorganic layer/organic layer

To resolve the problem that the degradation rate of Mg-based stents treated with an inorganic coating (i.e. MgF_2 coating) is accelerated by small fragments and cracks on the surface caused by balloon catheter expansion, Niidome et al. [231] proposed a method that uses PLLA to coat MgF_2 coating on AZ31-based stents. As a result, the high corrosion resistance of the MgF_2/PLLA coating was maintained after its expansion, and the MgF_2 coated with a PLLA coating exhibited better cell adhesion
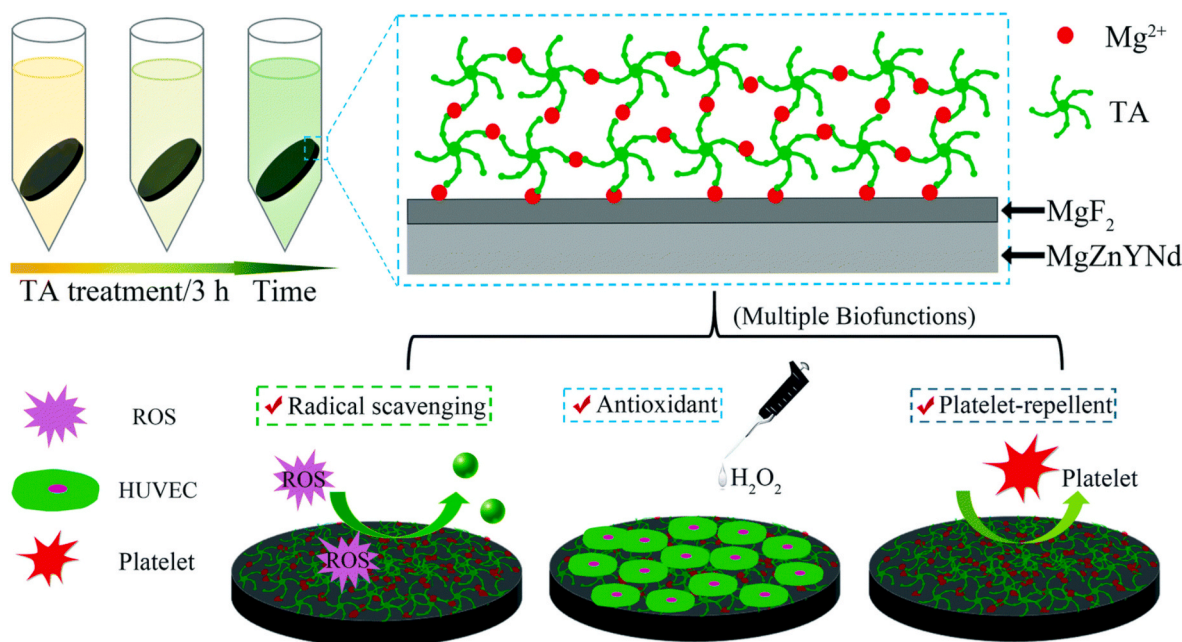
Fig. 12. Schematic diagram of fabricating the MgF₂/TA coating on Mg alloy, and the biological function of the created coating [232].

on the surface, signifying that the MgF$_2$/PLLA hybrid coating was preferable for HUVECs adhesion. Furthermore, Wang et al. [232] prepared a composite coating composed of an inner inorganic coating and an outer organic coating on the ZE21B alloy, namely magnesium fluoride/tannic acid (MgF$_2$/TA) coating. TA, which is a natural polyphenol, contains five catechol and five pyrogallol groups. And TA has a variety of biological effects, including anti-inflammatory, antioxidant, and antibacterial properties [233–235]. The outcomes of this experiment suggested that the MgF$_2$/TA coating endowed the Mg alloy substrate with excellent antioxidant and platelet-repellent capabilities. Besides, the composite coating supported the growth and proliferation of ECs. The rat subcutaneous implantation tests revealed that no obvious inflammatory response was observed for the MgF$_2$/TA coating (Fig. 12).

The regulation of the degradation behavior and moderate pH microenvironment of biodegradable Mg alloys will be confronted with a huge challenge. Yu et al. [236] developed a self-degradable MAO/CS composite coating on an Mg-4Li-1Ca alloy using dip-coating and MAO technology. The results of the electrochemical test demonstrated a distinct amelioration in the anti-corrosive ability of the MAO/CS coating in Hank's solution. In addition, the MAO/CS coating exhibited good effectiveness in inhibiting bacterial growth via the contact-killing strategy. Moreover, with the prolongation of soaking time, the degradation of the MAO/CS coating gave rise to a decrease in pH, and kept the solution pH at a moderate level ($\leq$8.25). Interestingly, the hydrogen evolution rates of the MAO/CS coated Mg substrate increased rapidly after immersion in Hank's solution after 100 h, which was attributed to the fact that the MAO/CS coating was cathodic relative to the Mg substrate.

3.5.3. Organic layer/organic layer

Choi et al. [185] reported a PDA/PCL composite coating obtained by a simple dip-coating method, to study whether the adhesive force between the Mg substrate and the created coating affected corrosion resistance. The results of the Tafel curve showed that the PDA/PCL coating effectively enhanced the corrosion resistance of the Mg substrate. Moreover, the PDA pretreatment substantially improved the adhesion of the outer PCL layer, thereby revealing the possibility of preventing the corrosion of the Mg substrate. Zhang et al. [237] further adopted a facile and highly efficient strategy of alkali treatment to obtain a bottom hydroxyl (–OH) layer with a negative charge, and

combined this approach with the LbL method to successively immobilize PDA and HA (1 or 2 g/L) on the Mg alloy AZ31B. Electrochemical results revealed that the Mg-OH/PDA/HA coating endowed the Mg substrate with good corrosion resistance. Utilizing the anti-thrombosis ability of HA and the biocompatibility of PDA, a balance between anti-thrombogenicity and biocompatibility could be achieved by regulating the content of HA molecules on the PDA surface. Moreover, a multifunctional Mg-OH-PDA-HA (1 g/L) coating markedly boosted HUVECs proliferation because of the exposure of more active sites on the PDA layer; interestingly, the intrinsic anti-thrombotic function of the HA layer was also retained. For providing the degradation rate required to match the vascular reform speed, Yeh et al. [238] designed a layer of sandwich-like coating with a gallic acid layer (GA, which is a type of phenolic acid with biological activity that has anti-inflammatory effects, promotes the proliferation of ECs and inhibits the growth of SMCs [239, 240]) enclosed between the PLGA layers on the ZK60 alloy. An electrochemical analysis attested that the corrosion rate of the PLGA/-GA/PLGA coating with a close-packed sandwiched layer was ~2000 times lower than that of the bare Mg substrate, demonstrating a better corrosion resistance. Moreover, PLGA/GA/PLGA coating could selectively inhibit SMCs growth and advance the proliferation of ECs, which was attributed to the GA released from the sandwich coating. The sandwich-layer structure may be a promising treatment strategy for curing atherosclerosis and preventing late-stent restenosis.

3.5.4. Organic layer/functional biomolecular

The introduction of varying bioactive molecules on the surface of Mg alloys to synergistically enhance their biocompatibility, thereby regulating their electrochemical behavior, blood compatibility, and ECs growth behavior, is an important approach to solve the clinical problems of these alloys. Liu et al. [241] immobilized Hep molecules on an LDH/PDA composite coating of the Mg alloy AZ31 via covalent bonding. Electrochemical tests confirmed that the LDH/PDA coating contributed greatly to improving the corrosion resistance of the Mg alloy in vitro. LDH/PDA coating significantly improved the adherence behavior and proliferation rate of HUVECs. Compared with the LDH/PDA coating, the corrosion resistance and long-term proliferation of HUVECs were slightly reduced after Hep immobilization, but were still greatly improved compared with AZ31, LDH coating, and PDA coating (Fig. 13). It is noteworthy that LDH/PDA/Hep hybrid coating substantially
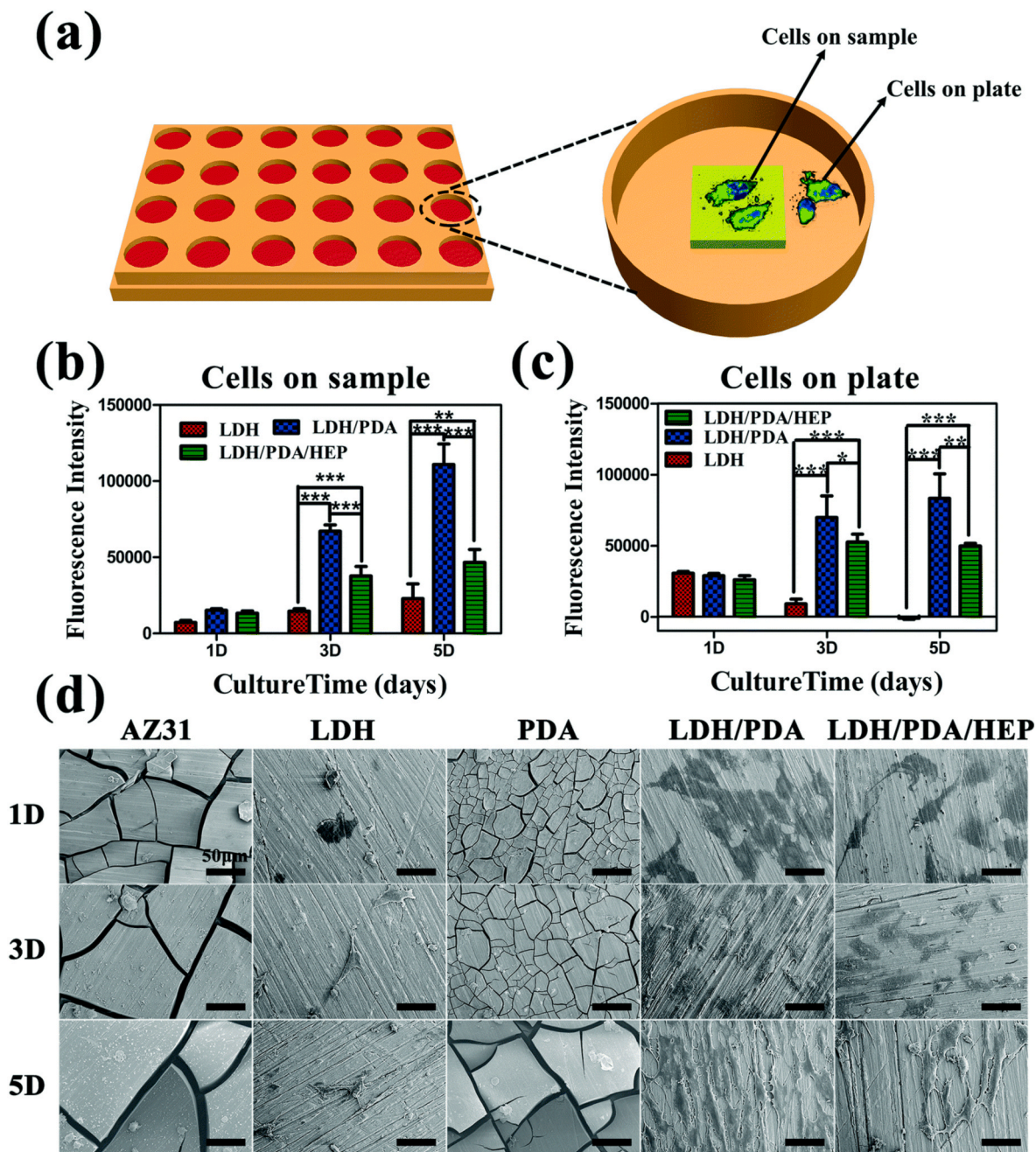
Fig. 13. (a) Description of cells cultured on sample and plate, (b, c) the proliferation rate of cells and plate on various samples, (d) morphologies of cells cultured on all samples [241].

enhanced HUVECs migration rate and inhibited platelet adhesion compared with LDH/PDA coating. Furthermore, HR tests revealed that LDH/PDA/Hep coating had a low HR (0.65%) in vitro, implying that heparinization was a promising strategy to enhance the hemocompatibility of samples. Li et al. [242] conjugated the Hep molecule, the Arg–Glu–Asp–Val peptide (REDV, which is a tetrapeptide derived from fibronectin that can be specifically recognized by $\alpha 4\beta 1$ integrin on the surface of ECs [243]), and an anti-CD 34 antibody (CD 34 is a highly glycosylated type I transmembrane glycoprotein that interacts with anti-CD 34 antibodies and is an important way to promote EPC-targeted adhesion/capture [244,245]) on a silane-treated ZE21B alloy, for improving surface endothelialization. A blood compatibility test suggested that multi-functional coating effectively restrained platelet adhesion/activation and reduced the HR (<5%). Cell culture tests

confirmed that Hep/REDV/anti-CD34 coating promoted endothelialization by improving ECs adhesion and endothelial progenitor cells (EPCs) capture, and inhibiting macrophage attachment. Xi et al. [246] immobilized SF containing Hep molecules and the Gly-Arg-Glu-Asp-Val-Tyrpeptide (GREDVY, which contains glycine and tyrosine in the head and tail of the sequence and can be obtained from REDV) on the ZE21B alloy treated with DA and HF for obtaining functional coatings. Electrochemical and immersion tests indicated that the functionalized coating exhibited preferable anti-corrosion abilities compared with the bare ZE21B alloy. Reduced platelet adhesion, HR, and prolonged blood coagulation time of coating were obtained, signifying an outstanding hemocompatibility. Furthermore, the multi-function afforded better biocompatibility with selectively proliferated HUVECs in systematic in vitro experiments (Fig. 14).
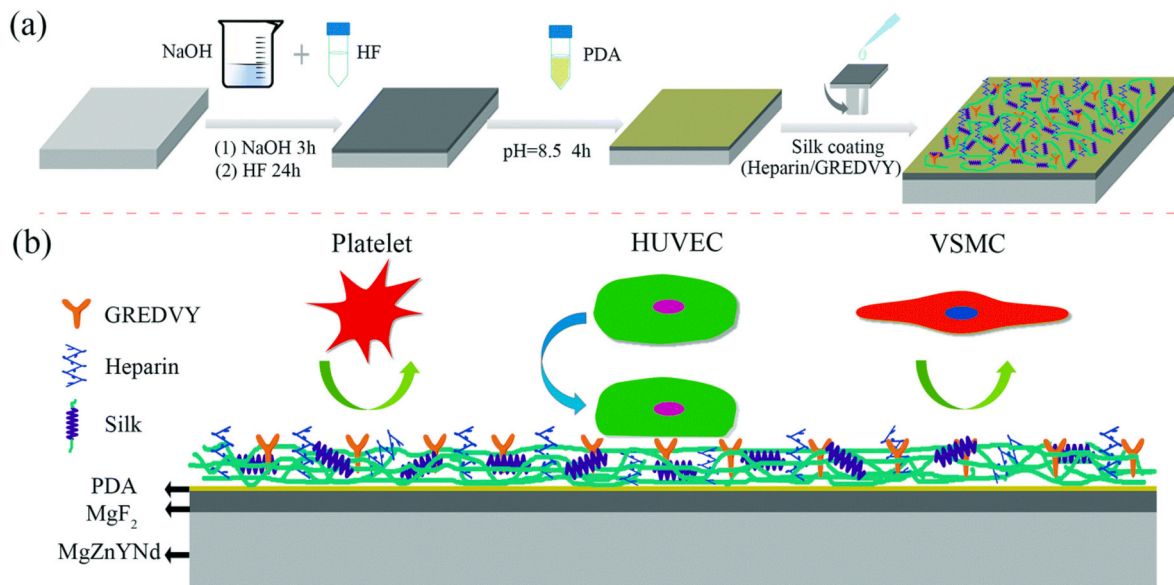
Fig. 14. (a) Scheme of preparing the multi-functional coating on the ZE21B alloy, (b) schematic illustration to show the influence of the multifunctional coating on selective adhesion of HUVECs over SMCs and preventing blood coagulation and platelet adhesion [246].

4. Comparison and challenge in functionalized coatings on Mg alloy stents

Mg alloys appear to be promising candidates as a temporary structural biomaterial for cardiovascular stent applications because of the intriguing combination properties of biocompatibility, biodegradability, and mechanical performance. Mg-based materials are expected to be completely degraded in a physiological environment, and the degradation products should not pose a threat to surrounding tissues [247]. However, the rapid degradation rate of Mg alloys under physiological conditions remains the main obstacle impeding the wide use of Mg alloy implants. Alloying design is an important manner of improving the mechanical properties, degradation behavior, and biocompatibility of Mg alloys. For example, the novel Mg-6 wt.% Zn (Mg-6Zn) alloy developed by Zhang et al. exhibited good biocompatibility, moderate degradation rate, and good mechanical properties [43]. However, the alloying design can slow the degradation rate by an order of magnitude or more, which may still not be sufficient for many applications. There are reports in the literature that micro-alloying and amorphous Mg-based glasses can further inhibit the degradation rate of Mg-based materials [248–250]. Regarding Mg-based metallic glasses, their single-phase structure and chemical homogeneity can minimize the galvanic corrosion effect [65]. The reported Mg-Zn-Ca metallic glasses showed a slower degradation rate and more uniform degradation modes with small and shallow pits that were well distributed on the surface compared with the crystalline pure Mg [251]. Moreover, the addition of RE elements in the design of alloy composition will most likely improve the strength of materials, but their biocompatibility remains uncertain [252]. Alloying elements may introduce a new toxicity risk. Another limitation of alloying is that regulatory approval is usually granted for a fixed composition. Any change to the alloy composition for a different patient population or application would require further regulatory approval [41].

Surface modification, as a very attractive method, can endow Mg-based materials with new surface properties on the premise of maintaining the original properties of materials. Preparing a suitable coating on the surface, followed by the regulation of the composition of the fabricated coating, may effectively dominate the degradation behavior and enhance the biofunctionability of Mg-based implants. Various surface treatment strategies of Mg alloys for vascular stents are summarized in Tables 2–4, demonstrating that the preparation of the functional

coating can endow Mg and its alloys with satisfactory characteristics, including corrosion resistance, self-healing, antimicrobial activity, and rapid endothelialization. Table 2 provides an overview of the experimental results of single-layer coatings applied onto Mg alloys. Electrochemical tests revealed that the fabricated coating can efficaciously reduce the i_{corr} of the Mg substrate (usually by 1–3 orders of magnitude), revealing that Mg alloys are protected from corrosion. The results of the immersion test are consistent and show that the coated samples remain intact or are slightly corroded after long-term immersion. However, the single-layer coating may not satisfy the demand for comprehensive performance with both corrosion resistance and multiple functions.

Constructing a multifunctional composite coating can further ameliorate the corrosion resistance ability and adhesion of one single coating and endue the Mg alloy with a better biological activity. As shown in Table 3, researchers have designed a variety of multifunctional coatings by combining different single-layer coatings (e.g. inorganic coatings, organic coatings, and bioactive molecules) and technologies (e.g. dipping coating, spin coating, MAO, and LbL). Liu et al. [84] developed a functional hybrid coating by modifying an MAO/PLLA pretreated Mg alloy with a heparinized PDA coating. MAO coating with porous structure augmented the adhesion of the PLLA coating due to physical locking. These results declared that the MAO/PLLA/PDA/Hep coating effactually decreased the degradation rates of Mg alloys. Moreover, the introduction of the PDA and Hep molecules substantially hindered platelet adhesion and afforded a low HR, thus leading to a good hemocompatibility of the hybrid coating. Moreover, the hybrid coating became more suitable for HUVECs growth and simultaneously inhibited SMCs growth in an in vitro cell test. However, various studies listed in Table 3 are based solely on Mg alloy sheets, rather than Mg alloy stents.

Table 4 summarizes the coatings that have been directly applied to the Mg-based stents. Yuan et al. [247] prepared an SRL-containing PLLA coating on HF-treated JDBM stents for restraining adverse incidents such as intimal hyperplasia and thrombosis. The results of the electrochemical and hydrogen evolution tests suggested that the polymeric coating afforded considerable in vitro protection against Mg substrate degradation during the immersion period. After implantation in the porcine coronary artery, the angiographic images (immediately) indicated that the coated JDBM stent was completely expanded and well-apposed to the vessel wall with no evidence of acute thrombosis and recoil; the follow-up angiographic images (up to 3 months) demonstrated that a good vascular patency was observed, without any

Table 4
Functional coatings directly used for Mg alloy stents.

Mat.	Coa.	Th. (μm)	Sol.	E_{corr} (V/SCE) Sub.	Coa.	i_{corr} (μA/cm²) Sub.	Coa.	Cor.(mm/a) Sub.	Coa.	Im. (d)	Res. Ref.
MgZnMn	PEO	0.15	PBS	−1.457	−1.342	12.979	2.039	0.296	0.046	10	PEO had an excellent anti-corrosion effect, and there was no cracking or peeling after balloon dilatation [100].
JDBM	MgF₂	0.8	Artificial plasma	−1.70	−1.66	1.91	1.58	0.043	0.036	–	MgF₂ film with a nanoscale reduced the degradation rates of JDBM substrate. MgF₂ offered a much more favorable surface for ECs adhesion, proliferation, and alignment. JDBM stent coated with MgF₂ film confirmed excellent tissue compatibility of the well re-endothelialized stent with no sign of thrombogenesis and restenosis in the stent-supported vessel in vivo implantation test [124].
MgZnMn	PPAam	0.25	PBS	−1.60	−1.30	51.28	8.3176	1.24	0.190	–	PPAam coating not only provided an endothelium-friendly microenvironment (enhancing the ECs attachment, spreading, and proliferation) but also exhibited good corrosion resistance [219].
AZ31	MgF₂/PLLA	–	E-MEM	–	–	–	–	–	–	14	The Mg stents coated by polymer coating maintained the high corrosion resistance after balloon expansion; moreover, it dramatically accelerated ECs adhesion compared with stents [231].
AZ31	PCUU/PTX	–	DMEM	–	–	–	–	–	–	28	PCUU/PTX coating slowed Mg alloy corrosion and reduced platelet adhesion, and the release of PTX from PCUU coatings effectively impeded SMCs proliferation [203].
WE43	PEI/PLGA/SRL	0.85	Artificial plasma	−1.612	−1.542	62.24	3.00	1.422	0.068	14	By introducing the PEI coating, the coating showed super adhesion force to the WE43 stent and greatly improved corrosion resistance after stent expansion. Interestingly, only SMCs were directly influenced by SRL because of the asymmetric geometry of PLGA/PEI double coating, which had a satisfactory anti-proliferation effect [159].
ZE21B	APTES/PLGA/SRL	9.60	Hank's	−1.626	−0.401	3.223	0.141	0.073	0.0016	30	APTES/PLGA/SRL coating improved anti-corrosion ability and biocompatibility in vitro experiments. Furthermore, ZE21B stents treated with coating were implanted in the porcine coronary artery of minipigs, confirming superb tissue compatibility and re-endothelialization capacity without a severe sign of injury, thrombosis, or restenosis of the vascular wall for as long as 6 months [75].
AZ31	MgF₂/SF/SRL	–	PBS	–	–	–	–	–	–	14	The outer SF coating restrained local and deep corrosion of HF-treated Mg stents. MgF₂/SF/SRL composite coating allowed outstanding HUVECs adhesion and minimal platelet adhesion on its surface [211].
JDBM	MgF₂/PLLA/SRL	6.0	–	–	–	–	0.039	–	0.0009	30	MgF₂/PLLA/SRL coated Mg-based stent showed favorable safety compared with non-degradable commercial DESs, with no signs of in-stent thrombus and restenosis [247].

*E-MEM = Eagle's minimum essential medium, PEO = Polyethylene oxide, PEI = Poly (ether imide), PTX = Paclitaxel, SRL = Sirolimus or Rapamycin, DESs = Drug-eluting stents.

signs of elastic recoil, stent malposition, or restenosis, confirming the safety and efficacy of the stent. IVUS and optical coherence tomography (OCT) detection indicated a low degradation rate and a long radial supporting duration of the SRL-eluting JDBM stent. Overall, these coatings reported in Table 4 may be an available surface treatment for a commercialized stent platform for enhancing corrosion resistance and preventing late-stent restenosis. Those coatings, however, basically contain SRL, PTX, or other anti-tumor drugs, which not only inhibit the proliferation of the vascular intima but also restrain HUVECs growth, proliferation, and migration [253]. To tackle this problem, Jiang et al. [159] prepared an asymmetric PLGA/PEI/SRL coating via spray coating that could provide Mg-based stents with a better corrosion resistance, vascular compatibility, and sustained drug-delivery capability (Fig. 15a). These results proved that the degradation rate of the WE 43 stents was greatly enhanced, even after balloon dilation. SMCs alone were directly affected by SRL because of the asymmetric geometry of PLGA/PEI double coating, thereby inhibiting restenosis in the stent; however, it did not achieve the effect of rapid endothelialization (Fig. 15b–e). Although research in this field has come a long way, many

challenges and questions remain to be addressed.

Designing a functionalized coating suitable for Mg-based stents is critical for realizing hemocompatibility for anti-thrombosis and regulating cell fate for rapid re-endothelialization. The preparation method, interfacial bonding, and biological function of the coating are important factors that need to be considered when developing a multifunctional coating for short and long-term clinical applications:

(1) The preparation method is suitable for the Mg alloy sheets, is it feasible to prepare a controllable and uniform coating on the Mg-based stent with complex structures? Spinning coating, MAO, dipping coating, etc. may not be efficacious preparation strategies for Mg-based stents. Polymer coating (e.g. PCL layer) prepared by spinning coating may not be suitable to obtain a uniform coating on the Mg-based stent; the high voltage in the MAO process can destroy the microstructure of the Mg alloy stent.

(2) Interfacial bonding with the Mg-based stent is a significant factor affecting the quality and stability of the prepared coating, regarding whether the functional coating can remain smooth
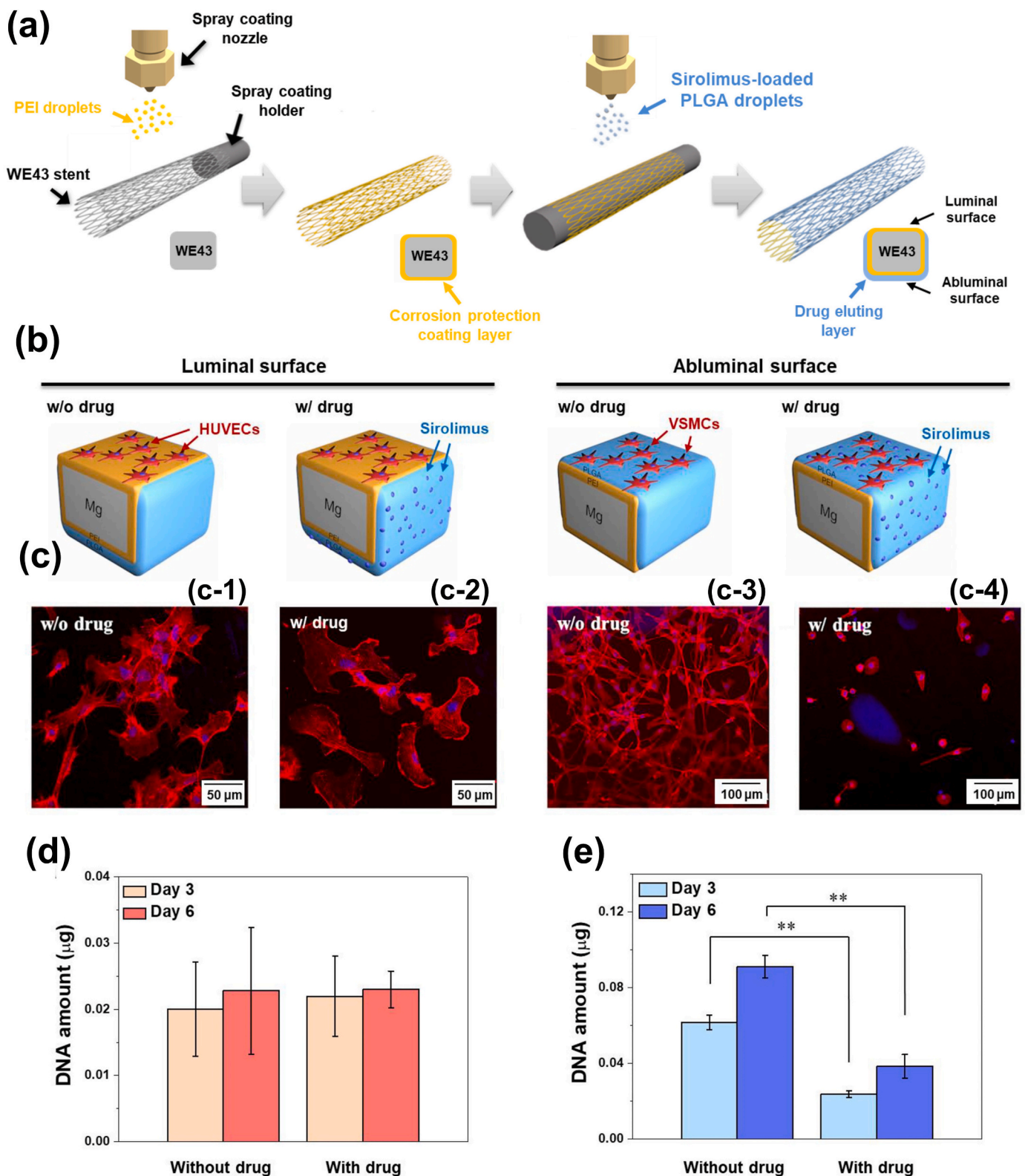
Fig. 15. (a) Schematic diagram of the sequential spray coatings for fabricating an asymmetric surface coating with PEI and PLGA/PEI layers on the WE 43 stent, (b) schematic images of asymmetrically coated WE 43 samples with and without SRL loading used for in vitro cellular experiments, (c) representative CLSM micrographs of (c-1, 2) HUVECs and (c-3, 4) SMCs adhered on the PEI- and PLGA/PEI-coated WE 43 stent, and the proliferation of (d) HUVECs and (e) SMCs on all samples [159].

without cracks or peeling before and after balloon expansion. The rough inorganic surfaces obtained by the alkali-heat, MAO, chemical conversion, and electrodeposition methods are not appropriate for stent application, whereas biopolymer coatings

can meet the required mechanical and biological performance of the bare Mg-based stent, especially at the initial implantation stage.

(3) After implantation in animals or the human body, it remains to be determined whether the coating owns satisfactory functional characteristics. The challenges in this setting include the regulation of the degradation rate and the achievement of rapid in-situ endothelialization to ensure long-term effectiveness, thereby resolving the adverse reactions such as thrombosis, inflammation, and restenosis after implantation.

5. Conclusions and outlook

Mg and its alloy are promising, yet challenging materials and are expected to be used as biodegradable implants in cardiovascular stent applications. The disadvantages of Mg alloy stents include their fast dissolution and insufficient endothelialization after implantation. Promoting the rapid endothelialization of cardiovascular Mg-based stents is changing into an encouraging therapeutic approach to avoid thrombosis and intimal hyperplasia. Considerable efforts have been dedicated to safeguarding Mg and its alloy with various coatings and yield miscellaneous functional properties, including self-healing, anti-thrombosis, antimicrobial activity, and rapid endothelialization. This article emphasizes the classification, preparation methods, and functional characteristics of the reported strategies for Mg alloy stents, and the main conclusions are listed as follows:

(1) Inorganic coatings include conversion coatings (e.g. MAO, LDH, and MgF_2 coatings) and deposited coatings (e.g. TiO_2 and GO coatings). Conversion coatings are strongly bonded to Mg substrates because of their in-situ growth mechanism, and they are usually used as the inner layer. Deposited inorganic coatings are generally fabricated by physical adsorption and are classified as ex-situ coatings, revealing a weak interfacial adhesion to Mg substrates. They can act as an outer layer to endue Mg alloy stents with certain functionality. Inorganic coatings are materials with a high hardness and simple preparation; however, they are fragile. After balloon catheter expansion, the produced small fragments may block the blood vessels

(2) Polymer coatings also belong to deposited coatings, and the interface combination between the polymer coating and the Mg substrate is generally achieved by utilizing physical (e.g. electrostatic attraction) or chemical (e.g. covalent bonding) strategies. The flexibility, degradability, and abundant functional groups of polymer coatings provide the possibility of promoting the clinical application of Mg-based stents. The polymer coatings can be divided into synthetic (e.g. PLLA, PCL, and PLGA) and natural (e.g. HA, CS, and SF) coatings. The synthetic polymer coatings show better corrosion resistance and drug delivery ability on Mg alloys for vascular stents, but their bonding strength is relatively weak. In comparison with the synthetic polymer coatings, the natural polymer coatings exhibit more biocompatible and other biological functions (e.g. anti-thrombotic and antibacterial properties).

(3) Composite coatings can combine the advantageous properties of every single-layer coating to dispose of the poor adhesion and deficient bioactivity of Mg-based stents. Furthermore, the conjugation of biomolecules with the hybrid coatings promises a new route for boosting the rapid endothelialization and for tailoring the degradation behaviors of Mg alloy stents. However, the degradation behaviors of the composite coatings are complex, and a systematic long-term evaluation needs to be carried out in future investigations.

The incorporation of alloying design and surface treatment may be an inevitable method for moderating degradation, enhancing rapid endothelialization, and suppressing hyperplasia of blood vessels in Mg-based stent. A coating might inhibit the degradation rate and promote cell growth or attachment in the early stages after implantation.

However, obviously, any coating must provide only a temporary level of protection, since if the coating is a permanent barrier, then ultimate biodegradation cannot occur, thus defeating the purpose of using resorbable implants. In terms of the alloying design of Mg alloy, micro-alloying or plainification can reduce the use of precious, rare, or toxic elements and ameliorate the material performance, which may provide important prospects for the development of medical Mg alloys.

From the perspective of surface modification, the electrochemical grafting technology may be able to fabricate a uniform, firm, and stable polymer coating on Mg-based stents, thereby effectively avoiding physical barriers caused by coating cracks after the stent is crimped or expanded. Moreover, the design and development of targeted biomolecules with good biocompatibility based on the bionics of blood vessels and their microenvironments may be an efficacious method to promote rapid endothelialization and suppress hyperplasia of blood vessels in Mg-based stents. Gene engineering is becoming a serviceable approach to facilitate the endothelialization and vascular regeneration of coronary stents. It can achieve long-term sustained expression of cytokines that affect the behavior of ECs. Gene transfer to target cells usually needs highly efficient gene carriers. Specific DNA and/or micro-RNAs are used to transfect vascular cells for the promotion of ECs migration/proliferation and/or the regulation of SMCs phenotype/ growth. We believe that the introduction of targeted biomolecules onto Mg-based stents modified by multifunctional coating to construct a biomolecule delivery surface is an anticipating tactic for regulating degradation rates, rapid endothelialization, and anti-hyperplasia. Moreover, long-term studies using animal models and the human body are needed to evaluate the performance, stability, and bioactivity of Mg alloy stents directly coated with the designed coatings. We hope that our comprehensive review of the surface modification of cardiovascular Mg-based stents will motivate further advances and clinical applications.

Declaration of competing interest

The authors declare that they have no known competing financial interests or personal relationships that could have appeared to influence the work reported in this paper.

Acknowledgments

References

[1] Y. He, Y. Li, X. Yang, E.C. Hemler, Y. Fang, L. Zhao, J. Zhang, Z. Yang, Z. Wang, L. He, J. Sun, D.D. Wang, J. Wang, J. Piao, X. Liang, G. Ding, F.B. Hu, The dietary transition and its association with cardiometabolic mortality among Chinese adults, 1982–2012: a cross-sectional population-based study, Lancet Diabet. Endocrinol 7 (2019) 540–548.

[2] J. Lv, C. Yu, Y. Guo, Z. Bian, L. Yang, Y. Chen, X. Tang, W. Zhang, Y. Qian, Y. Huang, X. Wang, J. Chen, Z. Chen, L. Qi, L. Li, G. China Kadoorie Biobank Collaborative, Adherence to healthy lifestyle and cardiovascular diseases in the Chinese population, J. Am. Coll. Cardiol. 69 (2017) 1116–1125.

[3] U. Sigwart, J. Puel, V. Mirkovitch, F. Joffre, L. Kappenberger, Intravascular stents to prevent occlusion and Re-stenosis after transluminal angioplasty, N. Engl. J. Med. 361 (1987) 701–706.

[4] P. Qi, Y. Yang, F.M. Maitz, N. Huang, Current status of research and application in vascular stents, Chin. Sci. Bull. 58 (2013) 4362–4370.

[5] A. Bekmurzayeva, W.J. Duncanson, H.S. Azevedo, D. Kanayeva, Surface modification of stainless steel for biomedical applications: revisiting a century-old material, Mater. Sci. Eng. C 93 (2018) 1073–1089.

[6] J. Fu, Y. Su, Y.X. Qin, Y. Zheng, Y. Wang, D. Zhu, Evolution of metallic cardiovascular stent materials: a comparative study among stainless steel, magnesium and zinc, Biomaterials 230 (2020), 119641.

[7] C.S. Nes, A. Enkelhardt, L. Bogdan, N. Faur, Fatigue life assessment of self-expandable NiTi stent, Key Eng. Mater. 627 (2014) 45–48.

[8] D. Kereiakes, G. Stone, P. Teirstein, I. Meredith, G. Levy, F. Schiele, T. Downes, D. Dudek, M. Foster, M. Buchbinder, H. Lui, D. Allocco, K. Dawkins, Four-Year

results of the platinum randomized trial: can stent metal alloy composition and design affect late clinical outcomes? J. Am. Coll. Cardiol. 63 (2014) A1705.

[9] P.W. Serruys, H.M. Garcia-Garcia, Y. Onuma, From metallic cages to transient bioresorbable scaffolds: change in paradigm of coronary revascularization in the upcoming decade? Eur. Heart J. 33 (2012) 16–25.

[10] L. Mao, L. Shen, J. Chen, X. Zhang, M. Kwak, Y. Wu, R. Fan, L. Zhang, J. Pei, G. Yuan, C. Song, J. Ge, W. Ding, A promising biodegradable magnesium alloy suitable for clinical vascular stent application, Sci. Rep. 7 (2017), 46343.

[11] P. Zartner, M. Buettner, H. Singer, M. Sigler, First biodegradable metal stent in a child with congenital heart disease: evaluation of macro and histopathology, Cathet. Cardiovasc. Interv. 69 (2007) 443–446.

[12] J. Shi, X. Miao, H. Fu, A. Jiang, Y. Liu, X. Shi, D. Zhang, Z. Wang, In vivo biological safety evaluation of an iron-based bioresorbable drug-eluting stent, Biometals 33 (2020) 217–228.

[13] C. Zhou, H.F. Li, Y.X. Yin, Z.Z. Shi, T. Li, X.Y. Feng, J.W. Zhang, C.X. Song, X. S. Cui, K.L. Xu, Y.W. Zhao, W.B. Hou, S.T. Lu, G. Liu, M.Q. Li, J.Y. Ma, E. Toft, A. A. Volinsky, M. Wan, X.J. Yao, C.B. Wang, K. Yao, S.K. Xu, H. Lu, S.F. Chang, J. B. Ge, L.N. Wang, H.J. Zhang, Long-term in vivo study of biodegradable Zn-Cu stent: a 2-year implantation evaluation in porcine coronary artery, Acta Biomater. 97 (2019) 657–670.

[14] P.K. Bowen, R.J. Guillory 2nd, E.R. Shearier, J.M. Seitz, J. Drelich, M. Bocks, F. Zhao, J. Goldman, Metallic zinc exhibits optimal biocompatibility for bioabsorbable endovascular stents, Mater. Sci. Eng. C 56 (2015) 467–472.

[15] A. Strohbach, R. Busch, Polymers for cardiovascular stent coatings, Int. J. Polymer Sci. 2015 (2015) 1–11.

[16] J. Iqbal, Y. Onuma, J. Ormiston, A. Abizaid, R. Waksman, P. Serruys, Bioresorbable scaffolds: rationale, current status, challenges, and future, Eur. Heart J. 35 (2014) 765–776.

[17] R. Gao, Y. Yang, Y. Han, Y. Huo, J. Chen, B. Yu, X. Su, L. Li, H.C. Kuo, S.W. Ying, W.F. Cheong, Y. Zhang, X. Su, B. Xu, J.J. Popma, G.W. Stone, Bioresorbable vascular scaffolds versus metallic stents in patients with coronary artery disease: ABSORB China trial, JACC (J. Am. Coll. Cardiol.) 66 (2015) 2298–2309.

[18] X.N. Zhang, M.C. Zuo, S.X. Zhang, H.L. Wu, W.H. Wang, W.Z. Chen, J.H. Ni, Advances in clinical research of biodegradable stents, Acta Metall. Sin. 53 (2017) 1215–1226.

[19] W.J. Lin, D.Y. Zhang, G. Zhang, H.T. Sun, H.P. Qi, L.P. Chen, Z.Q. Liu, R.L. Gao, W. Zheng, Design and characterization of a novel biocorrodible iron-based drug-eluting coronary scaffold, Mater. Des. 91 (2016) 72–79.

[20] P.P. Mueller, T. May, A. Perz, H. Hauser, M. Peuster, Control of smooth muscle cell proliferation by ferrous iron, Biomaterials 27 (2006) 2193–2200.

[21] W. Lin, H. Zhang, W. Zhang, H. Qi, G. Zhang, J. Qian, X. Li, L. Qin, H. Li, X. Wang, H. Qiu, X. Shi, W. Zheng, D. Zhang, R. Gao, J. Ding, In vivo degradation and endothelialization of an iron bioresorbable scaffold, Bioact. Mater. 6 (2021) 1028–1039.

[22] M. Peuster, C. Hesse, T. Schloo, C. Fink, P. Beerbaum, C. von Schnakenburg, Long-term biocompatibility of a corrodible peripheral iron stent in the porcine descending aorta, Biomaterials 27 (2006) 4955–4962.

[23] L.D. Hou, Z. Li, Y. Pan, M. Sabir, Y.F. Zheng, L. Li, A review on biodegradable materials for cardiovascular stent application, Front. Mater. Sci. 10 (2016) 238–259.

[24] P.K. Bowen, J. Drelich, J. Goldman, Zinc exhibits ideal physiological corrosion behavior for bioabsorbable stents, Adv. Mater. 25 (2013) 2577–2582.

[25] C. Wang, H.T. Yang, X. Li, Y.F. Zheng, In vitro evaluation of the feasibility of commercial Zn alloys as biodegradable metals, J. Mater. Sci. Technol. 32 (2016) 909–918.

[26] J. Ma, N. Zhao, D. Zhu, Endothelial cellular responses to biodegradable metal zinc, ACS Biomater. Sci. Eng. 1 (2015) 1174–1182.

[27] Y. Zheng, H. Yang, Research progress in biodegradable metals for stent application, Acta Metall. Sin. 53 (2017) 1227–1237.

[28] E.S. Ford, A.H. Mokdad, Dietary magnesium intake in a national sample of U.S. Adults, J. Nutr. 133 (2003) 2879–2882.

[29] Y. Zhang, J. Xu, Y.C. Ruan, M.K. Yu, M. O'Laughlin, H. Wise, D. Chen, L. Tian, D. Shi, J. Wang, S. Chen, J.Q. Feng, D.H. Chow, X. Xie, L. Zheng, L. Huang, S. Huang, K. Leung, N. Lu, L. Zhao, H. Li, D. Zhao, X. Guo, K. Chan, F. Witte, H. C. Chan, Y. Zheng, L. Qin, Implant-derived magnesium induces local neuronal production of CGRP to improve bone-fracture healing in rats, Nat. Med. 22 (2016) 1160–1169.

[30] P. Erne, M. Schier, T.J. Resink, The road to bioabsorbable stents: reaching clinical reality? Cardiovasc. Intervent. Radiol. 29 (2006) 11–16.

[31] Z.Q. Zhang, L. Wang, M.Q. Zeng, R.C. Zeng, M.B. Kannan, C.G. Lin, Y.F. Zheng, Biodegradation behavior of micro-arc oxidation coating on magnesium alloy-from a protein perspective, Bioact. Mater. 5 (2020) 398–409.

[32] Z.Q. Zhang, R.C. Zeng, W. Yan, C.G. Lin, L. Wang, Z.L. Wang, D.C. Chen, Corrosion resistance of one-step superhydrophobic polypropylene coating on magnesium hydroxide-pretreated magnesium alloy AZ31, J. Alloys Compd. 821 (2020), 153515.

[33] W. Yan, Y.J. Lian, Z.Y. Zhang, M.Q. Zeng, Z.Q. Zhang, Z.Z. Yin, L.Y. Cui, R. C. Zeng, In vitro degradation of pure magnesium-the synergetic influences of glucose and albumin, Bioact. Mater. 5 (2020) 318–333.

[34] Y. Zhu, H. Zhang, Y. Zhang, H. Wu, L. Wei, G. Zhou, Y. Zhang, L. Deng, Y. Cheng, M. Li, H.A. Santos, W. Cui, Endovascular metal devices for the treatment of cerebrovascular diseases, Adv. Mater. 31 (2019), e1805452.

[35] Z.Y. Ding, L.Y. Cui, R.C. Zeng, Y.B. Zhao, S.K. Guan, D.K. Xu, C.G. Lin, Exfoliation corrosion of extruded Mg-Li-Ca alloy, J. Mater. Sci. Technol. 34 (2018) 1550–1557.

[36] Z. Shi, A. Atrens, An innovative specimen configuration for the study of Mg corrosion, Corrosion Sci. 53 (2011) 226–246.

[37] G. Song, Control of biodegradation of biocompatable magnesium alloys, Corrosion Sci. 49 (2007) 1696–1701.

[38] M. Esmaily, J.E. Svensson, S. Fajardo, N. Birbilis, G.S. Frankel, S. Virtanen, R. Arrabal, S. Thomas, L.G. Johansson, Fundamentals and advances in magnesium alloy corrosion, Prog. Mater. Sci. 89 (2017) 92–193.

[39] C. Pan, Y. Zhao, Y. Yang, M. Yang, Q. Hong, Z. Yang, Q. Zhang, Immobilization of bioactive complex on the surface of magnesium alloy stent material to simultaneously improve anticorrosion, hemocompatibility and antibacterial activities, Colloids Surf., B 199 (2020), 111541.

[40] J. Song, J. She, D. Chen, F. Pan, Latest research advances on magnesium and magnesium alloys worldwide, J. Magnesium Alloys 8 (2020) 1–41.

[41] R. Karunakaran, S. Ortgies, A. Tamayol, F. Bobaru, M.P. Sealy, Additive manufacturing of magnesium alloys, Bioact. Mater. 5 (2020) 44–54.

[42] H.X. Wang, S.K. Guan, X. Wang, C.X. Ren, L.G. Wang, In vitro degradation and mechanical integrity of Mg-Zn-Ca alloy coated with Ca-deficient hydroxyapatite by the pulse electrodeposition process, Acta Biomater. 6 (2010) 1743–1748.

[43] S. Zhang, X. Zhang, C. Zhao, J. Li, Y. Song, C. Xie, H. Tao, Y. Zhang, Y. He, Y. Jiang, Y. Bian, Research on an Mg-Zn alloy as a degradable biomaterial, Acta Biomater. 6 (2010) 626–640.

[44] Z.M. Hua, B.Y. Wang, C. Wang, C.Y. Ma, P.K. Ma, Z.P. Guan, Y.J. Li, J.S. Li, H. Y. Wang, Development of low-alloyed Mg–Zn–Ca–Sn–Mn alloy with high strength-ductility synergy by sub-rapid solidification and hot rolling, J. Alloys Compd. 855 (2021), 157317.

[45] S.M. Baek, S.Y. Lee, J.C. Kim, J. Kwon, H. Jung, S. Lee, K.S. Lee, S.S. Park, Role of trace additions of Mn and Y in improving the corrosion resistance of Mg–3Al–1Zn alloy, Corrosion Sci. 178 (2021), 108998.

[46] Z.M.B. Teo, G. Parande, V. Manakari, M. Gupta, Using low-temperature sinterless powder method to develop exceptionally high amount of zinc containing MgeZneCa alloy and MgeZneCa/SiO2 nanocomposite, J. Alloys Compd. 853 (2021), 156957.

[47] H. Yang, L. Wu, B. Jiang, W. Liu, J. Song, G. Huang, D. Zhang, F. Pan, Clarifying the roles of grain boundary and grain orientation on the corrosion and discharge processes of α-Mg based Mg-Li alloys for primary Mg-air batteries, J. Mater. Sci. Technol. 62 (2021) 128–138.

[48] S.L. Zhou, W. Liu, S.C. Fu, Constitutive modelling of LZ91 magnesium-lithium alloy sheet by uniaxial tension loading tests, Mater. Today:. Proc. 33 (2020) 1787–1791.

[49] Y. Zhang, Z. Li, W. Zhang, W. Bu, Y. Qi, S. Guo, Structure and electrochemical hydrogen storage properties of as-milled Mg–Ce–Ni–Al-based alloys, Acta Metall. Sin. 33 (2020) 630–642.

[50] E.A. Sterling Lee, C.W. Sinclair, The effect of precipitation on recrystallization in a Mg-Nd alloy, Materialia 10 (2020), 100643.

[51] Y. Zhang, Y. Huang, F. Feyerabend, C. Blawert, W. Gan, E. Maawad, S. You, S. Gavras, N. Scharnagl, J. Bode, C. Vogt, D. Zander, R. Willumeit-Römer, K. U. Kainer, N. Hort, Influence of the amount of intermetallics on the degradation of Mg-Nd alloys under physiological conditions, Acta Biomater. 121 (2021) 695–712.

[52] K. Yaddanapudi, B. Leu, M.A. Kumar, X. Wang, J.M. Schoenung, E.J. Lavernia, T. J. Rupert, I.J. Beyerlein, S. Mahajan, Accommodation and formation of {1‾012} twins in Mg-Y alloys, Acta Mater. 204 (2021), 116514.

[53] Y. Zhang, P. Wang, Z. Hou, Z. Yuan, Y. Qi, S. Guo, Structure and hydrogen storage characteristics of as-spun Mg-Y-Ni-Cu alloys, J. Mater. Sci. Technol. 35 (2019) 1727–1734.

[54] C.F. Barros, B. Muzeau, V. L'Hostis, R. François, Impact of fluoride concentration on general corrosion of Mg-Zr alloy in a Na-geopolymer and alkaline solutions, Corrosion Sci. 176 (2020), 109009.

[55] X. Wan, J. Zhang, X. Mo, Y. Luo, Effects of pre-strain on twinning behaviors in an extruded Mg-Zr alloy, Mater. Sci. Eng. A 766 (2019), 138335.

[56] G. Wu, C. Wang, M. Sun, W. Ding, Recent developments and applications on high-performance cast magnesium rare-earth alloys, J. Magnesium Alloys 9 (2021) 1–20.

[57] R. Zeng, L. Cui, W. Ke, Biomedical magnesium alloys: composition, microstructure and corrosion, Acta Metall. Sin. 54 (2018) 1215–1235.

[58] Y. Chen, Z. Xu, C. Smith, J. Sankar, Recent advances on the development of magnesium alloys for biodegradable implants, Acta Biomater. 10 (2014) 4561–4573.

[59] B. Heublein, Biocorrosion of magnesium alloys: a new principle in cardiovascular implant technology? Heart 89 (2003) 651–656.

[60] M. Ascencio, M. Pekguleryuz, S. Omanovic, An investigation of the corrosion mechanisms of WE43 Mg alloy in a modified simulated body fluid solution: the influence of immersion time, Corrosion Sci. 87 (2014) 489–503.

[61] D. Bian, X. Zhou, J. Liu, W. Li, D. Shen, Y. Zheng, W. Gu, J. Jiang, M. Li, X. Chu, L. Ma, X. Wang, Y. Zhang, S. Leeflang, J. Zhou, Degradation behaviors and in-vivo biocompatibility of a rare earth- and aluminum-free magnesium-based stent, Acta Biomater. 124 (2021) 382–397.

[62] Y. Yue, L. Wang, N. Yang, J. Huang, L. Lei, H. Ye, L. Ren, S. Yang, Effectiveness of biodegradable magnesium alloy stents in coronary artery and femoral artery, J. Intervent. Cardiol. 28 (2015) 358–364.

[63] J. Zhang, H. Li, W. Wang, H. Huang, J. Pei, H. Qu, G. Yuan, Y. Li, The degradation and transport mechanism of a Mg-Nd-Zn-Zr stent in rabbit common carotid artery: a 20-month study, Acta Biomater. 69 (2018) 372–384.

[64] L. Mao, H. Zhou, L. Chen, J. Niu, L. Zhang, G. Yuan, C. Song, Enhanced biocompatibility and long-term durability in vivo of Mg-Nd-Zn-Zr alloy for vascular stent application, J. Alloys Compd. 720 (2017) 245–253.

[65] Y.F. Zheng, X.N. Gu, F. Witte, Biodegradable metals, Mater. Sci. Eng. R 77 (2014) 1–34.

[66] Y. Feng, S. Zhu, L. Wang, L. Chang, Y. Hou, S. Guan, Fabrication and characterization of biodegradable Mg-Zn-Y-Nd-Ag alloy: microstructure, mechanical properties, corrosion behavior and antibacterial activities, Bioact. Mater. 3 (2018) 225–235.

[67] A.C. Hanzi, I. Gerber, M. Schinhammer, J.F. Loffler, P.J. Uggowitzer, On the in vitro and in vivo degradation performance and biological response of new biodegradable Mg-Y-Zn alloys, Acta Biomater. 6 (2010) 1824–1833.

[68] Z.Z. Yin, W.C. Qi, R.C. Zeng, X.B. Chen, C.D. Gu, S.K. Guan, Y.F. Zheng, Advances in coatings on biodegradable magnesium alloys, J. Magnesium Alloys 8 (2020) 42–65.

[69] F. Pan, X. Yang, D. Zhang, Chemical nature of phytic acid conversion coating on AZ61 magnesium alloy, Appl. Surf. Sci. 255 (2009) 8363–8371.

[70] V.S. Saji, Review of rare-earth-based conversion coatings for magnesium and its alloys, J. Mater. Res. Technol. 8 (2019) 5012–5035.

[71] E. Vazirinasab, R. Jafari, G. Momen, Application of superhydrophobic coatings as a corrosion barrier: a review, Surf. Coating. Technol. 341 (2018) 40–56.

[72] W. Yao, W. Liang, G. Huang, B. Jiang, A. Atrens, F. Pan, Superhydrophobic coatings for corrosion protection of magnesium alloys, J. Mater. Sci. Technol. 52 (2020) 100–118.

[73] Y. Shao, R.C. Zeng, S.Q. Li, L.Y. Cui, Y.H. Zou, S.K. Guan, Y.F. Zheng, Advance in antibacterial magnesium alloys and surface coatings on magnesium alloys: a review, Acta Metall. Sin. 33 (2020) 615–629.

[74] C.D. Mario, H. Griffiths, O. Goktekin, N. Peeters, J. Verbist, M. Bosiers, K. Deloose, B. Heublein, R. Rohde, V. Kasese, C. Ilsley, R. Erbel, Drug-eluting bioabsorbable magnesium stent, J. Intervent. Cardiol. 17 (2004) 391–395.

[75] J. Liu, B. Zheng, P. Wang, X. Wang, B. Zhang, Q. Shi, T. Xi, M. Chen, S. Guan, Enhanced in vitro and in vivo performance of Mg-Zn-Y-Nd alloy achieved with APTES pretreatment for drug-eluting vascular stent application, ACS Appl. Mater. Interfaces 8 (2016) 17842–17858.

[76] M. Maeng, L.O. Jensen, E. Falk, H.R. Andersen, L. Thuesen, Negative vascular remodelling after implantation of bioabsorbable magnesium alloy stents in porcine coronary arteries: a randomised comparison with bare-metal and sirolimus-eluting stents, Heart 95 (2009) 241–246.

[77] R. Waksman, R. Pakala, P.K. Kuchulakanti, R. Baffour, D. Hellinga, R. Seabron, F. O. Tio, E. Wittchow, S. Hartwig, C. Harder, R. Rohde, B. Heublein, A. Andreae, K. H. Waldmann, A. Haverich, Safety and efficacy of bioabsorbable magnesium alloy stents in porcine coronary arteries, Catheter, Cardiovasc. Interv. 68 (2006) 607–617. ; discussion 618-619.

[78] H. Li, K. Xu, K. Yang, J. Liu, B.C. Zhang, X.Y. H, F. Zheng, H.B. Han, L.L. Tan, D. Hong, T.T. Yan, The degradation performance of AZ31 bioabsorbable magnesium alloy stent implanted in the abdominal aorta of rabbits, J. Interv. Radiol. 19 (2010) 315–317.

[79] H.M. Garcia-Garcia, M. Haude, K. Kuku, A. Hideo-Kajita, H. Ince, A. Abizaid, R. Tolg, P.A. Lemos, C. von Birgelen, E.H. Christiansen, W. Wijns, J. Escaned, J. Dijkstra, R. Waksman, In vivo serial invasive imaging of the second-generation drug-eluting bioabsorbable metal scaffold (Magmaris - DREAMS 2G) in de novo coronary lesions: insights from the BIOSOLVE-II First-In-Man Trial, Int. J. Cardiol. 255 (2018) 22–28.

[80] D. Schranz, P. Zartner, I. Michel-Behnke, H. Akinturk, Bioabsorbable metal stents for percutaneous treatment of critical recoarctation of the aorta in a newborn, Catheter, Cardiovasc. Interv. 67 (2006) 671–673.

[81] R. Erbel, C. Di Mario, J. Bartunek, J. Bonnier, B. de Bruyne, F.R. Eberli, P. Erne, M. Haude, B. Heublein, M. Horrigan, C. Ilsley, D. Böse, J. Koolen, T.F. Lüscher, N. Weissman, R. Waksman, Temporary scaffolding of coronary arteries with bioabsorbable magnesium stents: a prospective, non-randomised multicentre trial, Lancet 369 (2007) 1869–1875.

[82] G. Ghimire, J. Spiro, R. Kharbanda, M. Roughton, P. Barlis, M. Mason, C. Ilsley, C. Di Mario, R. Erbel, R. Waksman, M. Dalby, Initial evidence for the return of coronary vasoreactivity following the absorption of bioabsorbable magnesium alloy coronary stents, EuroIntervention 4 (2009) 481–484.

[83] M. Haude, R. Erbel, P. Erne, S. Verheye, H. Degen, D. Böse, P. Vermeersch, I. Wijnbergen, N. Weissman, F. Prati, R. Waksman, J. Koolen, Safety and performance of the drug-eluting absorbable metal scaffold (DREAMS) in patients with de-novo coronary lesions: 12 month results of the prospective, multicentre, first-in-man BIOSOLVE-I trial, Lancet 381 (2013) 836–844.

[84] M. Haude, H. Ince, S. Kische, A. Abizaid, R. Tolg, P. Alves Lemos, N.M. Van Mieghem, S. Verheye, C. von Birgelen, E.H. Christiansen, E. Barbato, H.M. Garcia-Garcia, R. Waksman, Biosolve II, I.I.I. investigators, Safety and clinical performance of a drug eluting absorbable metal scaffold in the treatment of subjects with de novo lesions in native coronary arteries: pooled 12-month outcomes of BIOSOLVE-II and BIOSOLVE-III, Cathet. Cardiovasc. Interv. 92 (2018) E502–E511.

[85] X. Cui, X. Lin, C. Liu, R. Yang, X. Zheng, M. Gong, Fabrication and corrosion resistance of a hydrophobic micro-arc oxidation coating on AZ31 Mg alloy, Corrosion Sci. 90 (2015) 402–412.

[86] F. Yang, R. Chang, T.J. Webster, Atomic layer deposition coating of TiO2 nano-thin films on magnesium-zinc alloys to enhance cytocompatibility for bioresorbable vascular stents, Int. J. Nanomed. 14 (2019) 9955–9970.

[87] L. Mikhalovska, N. Chorna, O. Lazarenko, P. Haworth, A. Sudre, S. Mikhalovsky, Inorganic coatings for cardiovascular stents: in vitro and in vivo studies, J. Biomed. Mater. Res. Part B 96 (2011) 333–341.

[88] N. Huang, P. Yang, X. Cheng, Y. Leng, X. Zheng, G. Cai, Z. Zhen, F. Zhang, Y. Chen, X. Liu, T. Xi, Blood compatibility of amorphous titanium oxide films synthesized by ion beam enhanced deposition, Biomaterials (1998) 771–776.

[89] S. Hou, Solvothermal fabrication of TiO2nanosheet films on degradable Mg–Zn alloys, Surf. Eng. 32 (2016) 745–749.

[90] C.Y. Li, C. Yu, R.C. Zeng, B.C. Zhang, L.Y. Cui, J. Wan, Y. Xia, In vitro corrosion resistance of a Ta2O5 nanofilm on MAO coated magnesium alloy AZ31 by atomic layer deposition, Bioact. Mater. 5 (2020) 34–43.

[91] S. Hou, W. Yu, Z. Yang, Y. Li, L. Yang, S. Lang, Properties of titanium oxide coating on MgZn alloy by magnetron sputtering for stent application, Coatings 10 (2020) 999.

[92] A.G. Rakoch, E.P. Monakhova, Z.V. Khabibullina, M. Serdechnova, C. Blawert, M. L. Zheludkevich, A.A. Gladkova, Plasma electrolytic oxidation of AZ31 and AZ91 magnesium alloys: comparison of coatings formation mechanism, J. Magnesium Alloys 8 (2020) 587–600.

[93] H. Han, R. Wang, Y. Wu, X. Zhang, D. Wang, Z. Yang, Y. Su, D. Shen, P. Nash, An investigation of plasma electrolytic oxidation coatings on crevice surface of AZ31 magnesium alloy, J. Alloys Compd. 811 (2019), 152010.

[94] Z. Wei, P. Tian, X. Liu, B. Zhou, Hemocompatibility and selective cell fate of polydopamine-assisted heparinized PEO/PLLA composite coating on biodegradable AZ31 alloy, Colloids Surf., B 121 (2014) 451–460.

[95] T.S.N. Sankara Narayanan, I.S. Park, M.H. Lee, Strategies to improve the corrosion resistance of microarc oxidation (MAO) coated magnesium alloys for degradable implants: prospects and challenges, Prog. Mater. Sci. 60 (2014) 1–71.

[96] N. Kroger, A. Kopp, M. Staudt, M. Rusu, A. Schuh, E.A. Liehn, Hemocompatibility of plasma electrolytic oxidation (PEO) coated Mg-RE and Mg-Zn-Ca alloys for vascular scaffold applications, Mater. Sci. Eng. C 92 (2018) 819–826.

[97] A. Santos Coquillat, M. Esteban Lucia, E. Martinez Campos, M. Mohedano, R. Arrabal, C. Blawert, M.L. Zheludkevich, E. Matykina, PEO coatings design for Mg-Ca alloy for cardiovascular stent and bone regeneration applications, Mater. Sci. Eng. C 105 (2019), 110026.

[98] P. Lu, L. Cao, Y. Liu, X. Xu, X. Wu, Evaluation of magnesium ions release, biocorrosion, and hemocompatibility of MAO/PLLA-modified magnesium alloy WE42, J. Biomed. Mater. Res. Part B 96 (2011) 101–109.

[99] M. Echeverry-Rendon, F. Echeverria, M.C. Harmsen, Interaction of different cell types with magnesium modified by plasma electrolytic oxidation, Colloids Surf., B 193 (2020), 111153.

[100] D. Yu, K. Xiong, N. Huang, Plasma polymerized poly(ethylene oxide) -like coating for enhancing corrosion resistance of magnesium alloy cardiovascular stents, Mater. Reports 34 (2020) 6166–6171.

[101] Y.X. Zhu, G.L. Song, P.P. Wu, J.F. Huang, D.J. Zheng, A protective superhydrophobic Mg–Zn–Al LDH film on Surface-Alloyed Magnesium, J. Alloys Compd. 855 (2021), 157550.

[102] Z.M. Qiu, R.C. Zeng, F. Zhang, L. Song, S.Q. Li, Corrosion resistance of Mg–Al LDH/Mg(OH)2/silane−Ce hybrid coating on magnesium alloy AZ31, Trans. Nonferrous Metals Soc. China 30 (2020) 2967–2979.

[103] J. Tedim, A. Kuznetsova, A.N. Salak, F. Montemor, D. Snihirova, M. Pilz, M. L. Zheludkevich, M.G.S. Ferreira, Zn–Al layered double hydroxides as chloride nanotraps in active protective coatings, Corrosion Sci. 55 (2012) 1–4.

[104] R. Xu, Y. Shen, J. Zheng, Q. Wen, Z. Li, X. Yang, P.K. Chu, Effects of one-step hydrothermal treatment on the surface morphology and corrosion resistance of ZK60 magnesium alloy, Surf. Coating. Technol. 309 (2017) 490–496.

[105] X. Wang, C. Jing, Y. Chen, X. Wang, G. Zhao, X. Zhang, L. Wu, X. Liu, B. Dong, Y. Zhang, Active corrosion protection of super-hydrophobic corrosion inhibitor intercalated Mg–Al layered double hydroxide coating on AZ31 magnesium alloy, J. Magnesium Alloys 8 (2020) 291–300.

[106] P. Wang, J. Liu, S. Shen, Q. Li, X. Luo, P. Xiong, S. Gao, J. Yan, Y. Cheng, T. Xi, In vitro and in vivo studies on two-step alkali-fluoride-treated Mg-Zn-Y-Nd alloy for vascular stent application: enhancement in corrosion resistance and biocompatibility, ACS Biomater. Sci. Eng. 5 (2019) 3279–3292.

[107] S. Jiang, S. Cai, Y. Lin, X. Bao, R. Ling, D. Xie, J. Sun, J. Wei, G. Xu, Effect of alkali/acid pretreatment on the topography and corrosion resistance of as-deposited CaP coating on magnesium alloys, J. Alloys Compd. 793 (2019) 202–211.

[108] H.M. Wong, Y. Zhao, F.K.L. Leung, T. Xi, Z. Zhang, Y. Zheng, S. Wu, K.D.K. Luk, K. M.C. Cheung, P.K. Chu, K.W.K. Yeung, Functionalized polymeric membrane with enhanced mechanical and biological properties to control the degradation of magnesium alloy, Adv. Healthcare Mater. 6 (2017), 1601269.

[109] C.J. Pan, L.Q. Pang, Y. Hou, Y.B. Lin, T. Gong, T. Liu, W. Ye, H.Y. Ding, Improving corrosion resistance and biocompatibility of magnesium alloy by sodium hydroxide and hydrofluoric acid treatments, Appl. Sci. 7 (2016) 33.

[110] N. Kamiyama, G. Panomsuwan, E. Yamamoto, T. Sudare, N. Saito, T. Ishizaki, Effect of treatment time in the Mg(OH)2/Mg–Al LDH composite film formed on Mg alloy AZ31 by steam coating on the corrosion resistance, Surf. Coating. Technol. 286 (2016) 172–177.

[111] X. Zhang, F. Zhong, X. Li, B. Liu, C. Zhang, B. Buhe, T. Zhang, G. Meng, F. Wang, The effect of hot extrusion on the microstructure and anti-corrosion performance of LDHs conversion coating on AZ91D magnesium alloy, J. Alloys Compd. 788 (2019) 756–767.

[112] M. Zhao, Q. Zhang, J.Q. Huang, F. We, Hierarchical nanocomposites derived from nanocarbons and layered double hydroxides - properties, synthesis, and applications, Adv. Funct. Mater. 22 (2012) 675–694.

[113] X. Bi, H. Zhang, L. Dou, Layered double hydroxide-based nanocarriers for drug delivery, Pharmaceutics 6 (2014) 298–332.

[114] L. Guo, W. Wu, Y. Zhou, F. Zhang, R. Zeng, J. Zeng, Layered double hydroxide coatings on magnesium alloys: a review, J. Mater. Sci. Technol. 34 (2018) 1455–1466.

[115] F. Peng, H. Li, D. Wang, P. Tian, Y. Tian, G. Yuan, D. Xu, X. Liu, Enhanced corrosion resistance and biocompatibility of magnesium alloy by Mg-Al-layered double hydroxide, ACS Appl. Mater. Interfaces 8 (2016) 35033–35044.

[116] F. Peng, D. Wang, Y. Tian, H. Cao, Y. Qiao, X. Liu, Sealing the pores of PEO coating with Mg-Al layered double hydroxide: enhanced corrosion resistance, cytocompatibility and drug delivery ability, Sci. Rep. 7 (2017) 8167.

[117] L. Mao, H. Zhu, L. Chen, H. Zhou, G. Yuan, C. Song, Enhancement of corrosion resistance and biocompatibility of Mg-Nd-Zn-Zr alloy achieved with phosphate coating for vascular stent application, J. Mater. Res. Technol. 9 (2020) 6409–6419.

[118] X.Y. Ye, M.F. Chen, C. You, D.B. Liu, The influence of HF treatment on corrosion resistance and in vitro biocompatibility of Mg-Zn-Zr alloy, Front. Mater. Sci. China 4 (2010) 132–138.

[119] X. Liu, Z. Zhen, J. Liu, T. Xi, Y. Zheng, S. Guan, Y. Zheng, Y. Cheng, Multifunctional MgF2/polydopamine coating on Mg alloy for vascular stent application, J. Mater. Sci. Technol. 31 (2015) 733–743.

[120] F. Gao, C. Xu, H. Hu, Q. Wang, Y. Gao, H. Chen, Q. Guo, D. Chen, D. Eder, Biomimetic synthesis and characterization of hydroxyapatite/graphene oxide hybrid coating on Mg alloy with enhanced corrosion resistance, Mater. Lett. 138 (2015) 25–28.

[121] Y. Ren, P. Sikder, B. Lin, S.B. Bhaduri, Microwave assisted coating of bioactive amorphous magnesium phosphate (AMP) on polyetheretherketone (PEEK), Mater. Sci. Eng. C 85 (2018) 107–113.

[122] N. Li, Y.D. Li, Y.B. Wang, M. Li, Y. Cheng, Y.H. Wu, Y.F. Zheng, Corrosion resistance and cytotoxicity of a MgF$_2$ coating on biomedical Mg-1Ca alloy via vacuum evaporation deposition method, Surf. Interface Anal. 45 (2013) 1217–1222.

[123] Z. Li, S. Shizhao, M. Chen, B.D. Fahlman, L. Debao, H. Bi, In vitro and in vivo corrosion, mechanical properties and biocompatibility evaluation of MgF2-coated Mg-Zn-Zr alloy as cancellous screws, Mater. Sci. Eng. C 75 (2017) 1268–1280.

[124] L. Mao, L. Shen, J. Chen, Y. Wu, M. Kwak, Y. Lu, Q. Xue, J. Pei, L. Zhang, G. Yuan, R. Fan, J. Ge, W. Ding, Enhanced bioactivity of Mg-Nd-Zn-Zr alloy achieved with nanoscale MgF2 surface for vascular stent application, ACS Appl. Mater. Interfaces 7 (2015) 5320–5330.

[125] S. Verdier, N. van der Laak, S. Delalande, J. Metson, F. Dalard, The surface reactivity of a magnesium–aluminium alloy in acidic fluoride solutions studied by electrochemical techniques and XPS, Appl. Surf. Sci. 235 (2004) 513–524.

[126] F. Witte, J. Fischer, J. Nellesen, C. Vogt, J. Vogt, T. Donath, F. Beckmann, In vivo corrosion and corrosion protection of magnesium alloy LAE442, Acta Biomater. 6 (2010) 1792–1799.

[127] Y. Feng, S. Zhu, L. Wang, L. Chang, B. Yan, X. Song, S. Guan, Characterization and corrosion property of nano-rod-like HA on fluoride coating supported on Mg-Zn-Ca alloy, Bioact. Mater. 2 (2017) 63–70.

[128] D. Dvorsky, J. Kubasek, E. Jablonska, J. Kaufmanova, D. Vojtech, Mechanical, corrosion and biological properties of advanced biodegradable Mg–MgF2 and WE43-MgF2 composite materials prepared by spark plasma sintering, J. Alloys Compd. 825 (2020).

[129] L. Mao, G. Yuan, J. Niu, Y. Zong, W. Ding, In vitro degradation behavior and biocompatibility of Mg-Nd-Zn-Zr alloy by hydrofluoric acid treatment, Mater. Sci. Eng. C 33 (2013) 242–250.

[130] A. Zomorodian, F. Brusciotti, A. Fernandes, M.J. Carmezim, T. Moura e Silva, J.C. S. Fernandes, M.F. Montemor, Anti-corrosion performance of a new silane coating for corrosion protection of AZ31 magnesium alloy in Hank's solution, Surf. Coating. Technol. 206 (2012) 4368–4375.

[131] G. Liu, H. Shen, J. Mao, L. Zhang, Z. Jiang, T. Sun, Q. Lan, Z. Zhang, Transferrin modified graphene oxide for glioma-targeted drug delivery: in vitro and in vivo evaluations, ACS Appl. Mater. Interfaces 5 (2013) 6909–6914.

[132] H.R. Bakhsheshi-Rad, E. Hamzah, M. Kasiri-Asgarani, S.N. Saud, F. Yaghoubidoust, E. Akbari, Structure, corrosion behavior, and antibacterial properties of nano-silica/graphene oxide coating on biodegradable magnesium alloy for biomedical applications, Vacuum 131 (2016) 106–110.

[133] Y. Luo, H. Shen, Y. Fang, Y. Cao, J. Huang, M. Zhang, J. Dai, X. Shi, Z. Zhang, Enhanced proliferation and osteogenic differentiation of mesenchymal stem cells on graphene oxide-incorporated electrospun poly(lactic-co-glycolic acid) nanofibrous mats, ACS Appl. Mater. Interfaces 7 (2015) 6331–6339.

[134] E. Nishida, H. Miyaji, A. Kato, H. Takita, T. Iwanaga, T. Momose, K. Ogawa, S. Murakami, T. Sugaya, M. Kawanami, Graphene oxide scaffold accelerates cellular proliferative response and alveolar bone healing of tooth extraction socket, Int. J. Nanomed. 11 (2016) 2265–2277.

[135] W. Shang, F. Wu, Y. Wang, A. Rabiei Baboukani, Y. Wen, J. Jiang, Corrosion resistance of micro-arc oxidation/graphene oxide composite coatings on magnesium alloys, ACS Omega 5 (2020) 7262–7270.

[136] F. Gao, Y. Hu, Z. Gong, T. Liu, T. Gong, S. Liu, C. Zhang, L. Quan, B. Kaveendran, C. Pan, Fabrication of chitosan/heparinized graphene oxide multilayer coating to improve corrosion resistance and biocompatibility of magnesium alloys, Mater. Sci. Eng. C 104 (2019), 109947.

[137] X.J. Ji, L. Gao, J.C. Liu, J. Wang, Q. Cheng, J.P. Li, S.Q. Li, K.Q. Zhi, R.C. Zeng, Z. L. Wang, Corrosion resistance and antibacterial properties of hydroxyapatite coating induced by gentamicin-loaded polymeric multilayers on magnesium alloys, Colloids Surf., B 179 (2019) 429–436.

[138] Z.Y. Tang, Y. Wang, P. Podsiadlo, N.A. Kotov, Biomedical applications of layer-by-layer assembly: from biomimetics to tissue engineering, Adv. Mater. 18 (2006) 3203–3224.

[139] L.Y. Cui, R.C. Zeng, X.X. Zhu, T.T. Pang, S.Q. Li, F. Zhang, Corrosion resistance of biodegradable polymeric layer-by-layer coatings on magnesium alloy AZ31, Front. Mater. Sci. 10 (2016) 134–146.

[140] Y. Zhao, L. Shi, X. Ji, J. Li, Z. Han, S. Li, R. Zeng, F. Zhang, Z. Wang, Corrosion resistance and antibacterial properties of polysiloxane modified layer-by-layer assembled self-healing coating on magnesium alloy, J. Colloid Interface Sci. 526 (2018) 43–50.

[141] L.Y. Cui, L. Gao, J.C. Zhang, Z. Tang, X.L. Fan, J.C. Liu, D.C. Chen, R.C. Zeng, S. Q. Li, K.Q. Zhi, In vitro corrosion resistance, antibacterial activity and cytocompatibility of a layer-by-layer assembled DNA coating on magnesium alloy, J. Magnesium Alloys 9 (2021) 266–280.

[142] L.Y. Li, L.Y. Cui, R.C. Zeng, S.Q. Li, X.B. Chen, Y. Zheng, M.B. Kannan, Advances in functionalized polymer coatings on biodegradable magnesium alloys - a review, Acta Biomater. 79 (2018) 23–36.

[143] J. Sun, Y. Zhu, L. Meng, P. Chen, T. Shi, X. Liu, Y. Zheng, Electrophoretic deposition of colloidal particles on Mg with cytocompatibility, antibacterial performance, and corrosion resistance, Acta Biomater. 45 (2016) 387–398.

[144] J. Wang, Y. He, M.F. Maitz, B. Collins, K. Xiong, L. Guo, Y. Yun, G. Wan, N. Huang, A surface-eroding poly(1,3-trimethylene carbonate) coating for fully biodegradable magnesium-based stent applications: toward better biofunction, biodegradation and biocompatibility, Acta Biomater. 9 (2013) 8678–8689.

[145] R.P. Brannigan, A.P. Dove, Synthesis, properties and biomedical applications of hydrolytically degradable materials based on aliphatic polyesters and polycarbonates, Biomater. Sci. 5 (2016) 9–21.

[146] H. Zhou, J.G. Lawrence, S.B. Bhaduri, Fabrication aspects of PLA-CaP/PLGA-CaP composites for orthopedic applications: a review, Acta Biomater. 8 (2012) 1999–2016.

[147] Y. Chen, Y. Song, S. Zhang, J. Li, C. Zhao, X. Zhang, Interaction between a high purity magnesium surface and PCL and PLA coatings during dynamic degradation, Biomed. Mater. 6 (2011), 025005.

[148] R.C. Zeng, L.Y. Cui, K. Jiang, R. Liu, B.D. Zhao, Y.F. Zheng, In vitro corrosion and cytocompatibility of a microarc oxidation coating and poly(L-lactic acid) composite coating on Mg-1Li-1Ca alloy for orthopedic implants, ACS Appl. Mater. Interfaces 8 (2016) 10014–10028.

[149] Z. Wei, P. Tian, X. Liu, B. Zhou, In vitro degradation, hemolysis, and cytocompatibility of PEO/PLLA composite coating on biodegradable AZ31 alloy, J. Biomed. Mater. Res. Part B 103 (2015) 342–354.

[150] M. Yazdimamaghani, M. Razavi, D. Vashaee, L. Tayebi, Surface modification of biodegradable porous Mg bone scaffold using polycaprolactone/bioactive glass composite, Mater. Sci. Eng. C 49 (2015) 436–444.

[151] M. Vandrovcova, T.E.L. Douglas, W. Mróz, O. Musial, D. Schaubroeck, B. Budner, R. Syroka, P. Dubruel, L. Bacakova, Pulsed laser deposition of magnesium-doped calcium phosphate coatings on porous polycaprolactone scaffolds produced by rapid prototyping, Mater. Lett. 148 (2015) 178–183.

[152] H. Kweon, M.K. Yoo, I.K. Park, T.H. Kim, H.C. Lee, H.-S. Lee, J.-S. Oh, T. Akaike, C.-S. Cho, A novel degradable polycaprolactone networks for tissue engineering, Biomaterials 24 (2003) 801–808.

[153] J. Degner, F. Singer, L. Cordero, A.R. Boccaccini, S. Virtanen, Electrochemical investigations of magnesium in DMEM with biodegradable polycaprolactone coating as corrosion barrier, Appl. Surf. Sci. 282 (2013) 264–270.

[154] T. Hanas, T.S. Sampath Kumar, G. Perumal, M. Doble, Tailoring degradation of AZ31 alloy by surface pre-treatment and electrospun PCL fibrous coating, Mater. Sci. Eng. C 65 (2016) 43–50.

[155] W. Jiang, Q. Tian, T. Vuong, M. Shashaty, C. Gopez, T. Sanders, H. Liu, Comparison study on four biodegradable polymer coatings for controlling magnesium degradation and human endothelial cell adhesion and spreading, ACS Biomater. Sci. Eng. 3 (2017) 936–950.

[156] N.R. Washburn, K.M. Yamada, C.G. Simon Jr., S.B. Kennedy, E.J. Amis, High-throughput investigation of osteoblast response to polymer crystallinity: influence of nanometer-scale roughness on proliferation, Biomaterials 25 (2004) 1215–1224.

[157] F. Danhier, E. Ansorena, J.M. Silva, R. Coco, A. Le Breton, V. Preat, PLGA-based nanoparticles: an overview of biomedical applications, J. Contr. Release 161 (2012) 505–522.

[158] A. Kumari, S.K. Yadav, S.C. Yadav, Biodegradable polymeric nanoparticles based drug delivery systems, Colloids Surf., B 75 (2010) 1–18.

[159] M.H. Kang, K.H. Cheon, K.I. Jo, J.H. Ahn, H.E. Kim, H.D. Jung, T.S. Jang, An asymmetric surface coating strategy for improved corrosion resistance and vascular compatibility of magnesium alloy stents, Mater. Des. 196 (2020), 109182.

[160] R. di Toro, V. Betti, S. Spampinato, Biocompatibility and integrin-mediated adhesion of human osteoblasts to poly(DL-lactide-co-glycolide) copolymers, Eur. J. Pharmaceut. Sci. 21 (2004) 161–169.

[161] L. Liu, B. Huang, X. Liu, W. Yuan, Y. Zheng, Z. Li, K.W.K. Yeung, S. Zhu, Y. Liang, Z. Cui, S. Wu, Photo-controlled degradation of PLGA/Ti3C2 hybrid coating on Mg-Sr alloy using near infrared light, Bioact. Mater. 6 (2021) 568–578.

[162] C. Zhao, S. Zhang, C. He, J. Li, B. Zhang, X. Zhang, Study of PLGA coating on bio-absorbable Mg alloy, J. Funct. Mater. 39 (2008) 987–989, 993.

[163] P. Lu, H. Fan, Y. Liu, L. Cao, X. Wu, X. Xu, Controllable biodegradability, drug release behavior and hemocompatibility of PTX-eluting magnesium stents, Colloids Surf., B 83 (2011) 23–28.

[164] Z. Wang, Q. Zheng, S. Guan, Z. Sun, S. Liu, B. Zhang, T. Duan, K. Xu, In vitro and in vivo assessment of the biocompatibility of an paclitaxel-eluting poly-l-lactide-coated Mg-Zn-Y-Nd alloy stent in the intestine, Mater. Sci. Eng. C 105 (2019), 110087.

[165] D. Kregiel, Advances in biofilm control for food and beverage industry using organo-silane technology: a review, Food Contr. 40 (2014) 32–40.

[166] F. Zucchi, A. Frignani, V. Grassi, A. Balbo, G. Trabanelli, Organo-silane coatings for AZ31 magnesium alloy corrosion protection, Mater. Chem. Phys. 110 (2008) 263–268.

[167] D. Wang, G.P. Bierwagen, Sol–gel coatings on metals for corrosion protection, Prog. Org. Coating 64 (2009) 327–338.

[168] J. Niu, H. Liu, X. Ping, X. Xun, G. Li, Silane coupling agent (SCA) pretreatment and polycaprolactone (PCL) coating for enhanced corrosion resistance for magnesium, J. Coating Technol. Res. 16 (2018) 125–133.

[169] W. Van Ooij, D. Zhu, G. Prasad, S. Jayaseelan, Y. Fu, N. Teredesai, Silane based chromate replacements for corrosion control, paint adhesion, and rubber bonding, Surf. Eng. 16 (2000) 386–396.

[170] C. Wang, H. Fang, C. Hang, Y. Sun, Z. Peng, W. Wei, Y. Wang, Fabrication and characterization of silk fibroin coating on APTES pretreated Mg-Zn-Ca alloy, Mater. Sci. Eng. C 110 (2020), 110742.

[171] X.N. Gu, H.M. Guo, F. Wang, Y. Lu, W.T. Lin, J. Li, Y.F. Zheng, Y.B. Fan, Degradation, hemolysis, and cytotoxicity of silane coatings on biodegradable magnesium alloy, Mater. Lett. 193 (2017) 266–269.

[172] J. Liu, T. Xi, Enhanced anti-corrosion ability and biocompatibility of PLGA coatings on MgZnYNd alloy by BTSE-APTES pre-treatment for cardiovascular stent, J. Mater. Sci. Technol. 32 (2016) 845–857.

[173] R. Muller, J. Abke, E. Schnell, F. Macionczyk, U. Gbureck, R. Mehrl, Z. Ruszczak, R. Kujat, C. Englert, M. Nerlich, P. Angele, Surface engineering of stainless steel materials by covalent collagen immobilization to improve implant biocompatibility, Biomaterials 26 (2005) 6962–6972.

[174] X. Liu, Z. Yue, T. Romeo, J. Weber, T. Scheuermann, S. Moulton, G. Wallace, Biofunctionalized anti-corrosive silane coatings for magnesium alloys, Acta Biomater. 9 (2013) 8671–8677.

[175] S. Kunjukunju, A. Roy, M. Ramanathan, B. Lee, J.E. Candiello, P.N. Kumta, A layer-by-layer approach to natural polymer-derived bioactive coatings on magnesium alloys, Acta Biomater. 9 (2013) 8690–8703.

[176] H. Lee, S.M. Dellatore, W.M. Miller, P.B. Messersmith, Mussel-inspired surface chemistry for multifunctional coatings, Science 318 (2007) 426–430.

[177] C. Shao, M. Wang, L. Meng, H. Chang, B. Wang, F. Xu, J. Yang, P. Wan, Mussel-inspired cellulose nanocomposite tough hydrogels with synergistic self-healing, adhesive, and strain-sensitive properties, Chem. Mater. 30 (2018) 3110–3121.

[178] T. Liu, Y. Liu, Y. Chen, S. Liu, M.F. Maitz, X. Wang, K. Zhang, J. Wang, Y. Wang, J. Chen, N. Huang, Immobilization of heparin/poly-(L)-lysine nanoparticles on dopamine-coated surface to create a heparin density gradient for selective direction of platelet and vascular cells behavior, Acta Biomater. 10 (2014) 1940–1954.

[179] Z. Yang, Q. Tu, Y. Zhu, R. Luo, X. Li, Y. Xie, M.F. Maitz, J. Wang, N. Huang, Mussel-inspired coating of polydopamine directs endothelial and smooth muscle cell fate for re-endothelialization of vascular devices, Adv. Healthcare Mater. 1 (2012) 548–559.

[180] F. Singer, M. Schlesak, C. Mebert, S. Hohn, S. Virtanen, Corrosion properties of polydopamine coatings formed in one-step immersion process on magnesium, ACS Appl. Mater. Interfaces 7 (2015) 26758–26766.

[181] C.J. Pan, Y. Hou, Y.N. Wang, F. Gao, T. Liu, Y.H. Hou, Y.F. Zhu, W. Ye, L.R. Wang, Effects of self-assembly of 3-phosphonopropionic acid, 3-aminopropyltrimethoxysilane and dopamine on the corrosion behaviors and biocompatibility of a magnesium alloy, Mater. Sci. Eng. C 67 (2016) 132–143.

[182] J.L. Wang, B.C. Li, Z.J. Li, K.F. Ren, L.J. Jin, S.M. Zhang, H. Chang, Y.X. Sun, J. Ji, Electropolymerization of dopamine for surface modification of complex-shaped cardiovascular stents, Biomaterials 35 (2014) 7679–7689.

[183] V. Ball, D. Del Frari, V. Toniazzo, D. Ruch, Kinetics of polydopamine film deposition as a function of pH and dopamine concentration: insights in the polydopamine deposition mechanism, J. Colloid Interface Sci. 386 (2012) 366–372.

[184] C. Song, Y. Yang, Y. Zhou, L. Wang, S. Zhu, J. Wang, R. Zeng, Y. Zheng, S. Guan, Electrochemical polymerization of dopamine with/without subsequent PLLA coating on Mg-Zn-Y-Nd alloy, Mater. Lett. 252 (2019) 202–206.

[185] J.B. Choi, Y.S. Jang, S. Mi Byeon, J. Hwa Jang, Y.K. Kim, T.S. Bae, M.H. Lee, Effect of composite coating with poly-dopamine/PCL on the corrosion resistance of magnesium, Int. J. Polym. Mater. Polym. Biomat. 68 (2018) 328–337.

[186] L. Ma, H. Qin, C. Cheng, Y. Xia, C. He, C. Nie, L. Wang, C. Zhao, Mussel-inspired self-coating at macro-interface with improved biocompatibility and bioactivity via dopamine grafted heparin-like polymers and heparin, J. Mater. Chem. B 2 (2013) 363–375.

[187] Q. Wei, B. Li, N. Yi, B. Su, Z. Yin, F. Zhang, J. Li, C. Zhao, Improving the blood compatibility of material surfaces via biomolecule-immobilized mussel-inspired coatings, J. Biomed. Mater. Res. 96 (2011) 38–45.

[188] H.D. Zhang, A.Y. Chen, B. Gan, H. Jiang, L.J. Gu, Corrosion protection investigations of carbon dots and polydopamine composite coating on magnesium alloy, J. Magnes. Alloys (2021), https://doi.org/10.1016/j.jma.2020.11.021.

[189] T. Segura, B.C. Anderson, P.H. Chung, R.E. Webber, K.R. Shull, L.D. Shea, Crosslinked hyaluronic acid hydrogels: a strategy to functionalize and pattern, Biomaterials 26 (2005) 359–371.

[190] J. Li, K. Zhang, H. Chen, T. Liu, P. Yang, Y. Zhao, N. Huang, A novel coating of type IV collagen and hyaluronic acid on stent material-titanium for promoting smooth muscle cell contractile phenotype, Mater. Sci. Eng. C 38 (2014) 235–243.

[191] P.H. Chua, K.G. Neoh, E.T. Kang, W. Wang, Surface functionalization of titanium with hyaluronic acid/chitosan polyelectrolyte multilayers and RGD for promoting osteoblast functions and inhibiting bacterial adhesion, Biomaterials 29 (2008) 1412–1421.

[192] J. Li, K. Zhang, N. Huang, Engineering cardiovascular implant surfaces to create a vascular endothelial growth microenvironment, Biotechnol. J. 12 (2017), 1600401.

[193] Y.K. Kim, Y.S. Jang, S.Y. Kim, M.H. Lee, Functions achieved by the hyaluronic acid derivatives coating and hydroxide film on bio-absorbed Mg, Appl. Surf. Sci. 473 (2019) 31–39.

[194] J.A. Li, L. Chen, X.Q. Zhang, S.K. Guan, Enhancing biocompatibility and corrosion resistance of biodegradable Mg-Zn-Y-Nd alloy by preparing PDA/HA coating for potential application of cardiovascular biomaterials, Mater. Sci. Eng. C 109 (2020), 110607.

[195] Y. Luo, K.R. Kirker, G.D. Prestwich, Cross-linked hyaluronic acid hydrogel films: new biomaterials for drug delivery, J. Contr. Release 69 (2000) 169–184.

[196] U. Adhikari, N.P. Rijal, S. Khanal, D. Pai, J. Sankar, N. Bhattarai, Magnesium incorporated chitosan based scaffolds for tissue engineering applications, Bioact. Mater. 1 (2016) 132–139.

[197] H. Xu, Y.W. Ge, J.W. Lu, Q.F. Ke, Z.Q. Liu, Z.A. Zhu, Y.P. Guo, Icariin loaded-hollow bioglass/chitosan therapeutic scaffolds promote osteogenic differentiation and bone regeneration, Chem. Eng. J. 354 (2018) 285–294.

[198] X. Xu, J. Cheng, C. Zhang, X. Yan, T. Zhu, K. Yao, L. Cao, Y. Liu, Bio-corrosion and polymer coating modification of magnesium alloys for medicine, Rare Met. Mater. Eng. 37 (2008) 1225–1228.

[199] L.Y. Cui, J. Xu, N. Lu, R.C. Zeng, Y.H. Zou, S.Q. Li, F. Zhang, In vitro corrosion resistance and antibacterial properties of layer-by-layer assembled chitosan/poly-L-glutamic acid coating on AZ31 magnesium alloys, Trans. Nonferrous Metals Soc. China 27 (2017) 1081–1086.

[200] F. Gao, Y. Hu, G. Li, S. Liu, L. Quan, Z. Yang, Y. Wei, C. Pan, Layer-by-layer deposition of bioactive layers on magnesium alloy stent materials to improve corrosion resistance and biocompatibility, Bioact. Mater. 5 (2020) 611–623.

[201] Y. Zhang, J. Wang, J. Xiao, T. Fang, N. Hu, M. Li, L. Deng, Y. Cheng, Y. Zhu, W. Cui, An electrospun fiber-covered stent with programmable dual drug release for endothelialization acceleration and lumen stenosis prevention, Acta Biomater. 94 (2019) 295–305.

[202] J. Liu, P. Wang, C.C. Chu, T. Xi, Arginine-leucine based poly (ester urea urethane) coating for Mg-Zn-Y-Nd alloy in cardiovascular stent applications, Colloids Surf., B 159 (2017) 78–88.

[203] X. Gu, C. Mao, S.H. Ye, Y. Koo, Y. Yun, T.R. Tiasha, V. Shanov, W.R. Wagner, Biodegradable, elastomeric coatings with controlled anti-proliferative agent release for magnesium-based cardiovascular stents, Colloids Surf., B 144 (2016) 170–179.

[204] B. Zhang, R. Yao, L. Li, Y. Wang, R. Luo, L. Yang, Y. Wang, Green tea polyphenol induced Mg(2+)-rich multilayer conversion coating: toward enhanced corrosion resistance and promoted in situ endothelialization of AZ31 for potential cardiovascular applications, ACS Appl. Mater. Interfaces 11 (2019) 41165–41177.

[205] H. Zhang, L. Xie, X. Shen, T. Shang, R. Luo, X. Li, T. You, J. Wang, N. Huang, Y. Wang, Catechol/polyethyleneimine conversion coating with enhanced corrosion protection of magnesium alloys: potential applications for vascular implants, J. Mater. Chem. B 6 (2018) 6936–6949.

[206] H. Zhang, R. Luo, W. Li, J. Wang, M.F. Maitz, J. Wang, G. Wan, Y. Chen, H. Sun, C. Jiang, R. Shen, N. Huang, Epigallocatechin gallate (EGCG) induced chemical conversion coatings for corrosion protection of biomedical MgZnMn alloys, Corrosion Sci. 94 (2015) 305–315.

[207] A.S. Gobin, V.E. Froude, A.B. Mathur, Structural and mechanical characteristics of silk fibroin and chitosan blend scaffolds for tissue regeneration, J. Biomed. Mater. Res. 74 (2005) 465–473.

[208] C.B. Borkner, M.B. Elsner, T. Scheibel, Coatings and films made of silk proteins, ACS Appl. Mater. Interfaces 6 (2014) 15611–15625.

[209] X. Wang, X. Zhang, J. Castellot, I. Herman, M. Iafrati, D.L. Kaplan, Controlled release from multilayer silk biomaterial coatings to modulate vascular cell responses, Biomaterials 29 (2008) 894–903.

[210] N. Guziewicz, A. Best, B. Perez-Ramirez, D.L. Kaplan, Lyophilized silk fibroin hydrogels for the sustained local delivery of therapeutic monoclonal antibodies, Biomaterials 32 (2011) 2642–2650.

[211] W. Xu, K. Yagoshi, T. Asakura, M. Sasaki, T. Niidome, Silk fibroin as a coating polymer for sirolimus-eluting magnesium alloy stents, ACS Appl. Bio Mater. 3 (2019) 531–538.

[212] C. Tanaka, T. Asakura, Synthesis and characterization of cell-adhesive silk-like proteins constructed from the sequences of anaphe silk fibroin and fibronectin, Biomacromolecules 10 (2009) 923–928.

[213] Y. Zhu, M.L. Free, R. Woollam, W. Durnie, A review of surfactants as corrosion inhibitors and associated modeling, Prog. Mater. Sci. 90 (2017) 159–223.

[214] L. Ma, W. Li, S. Zhu, L. Wang, S. Guan, Corrosion inhibition of Schiff bases for Mg-Zn-Y-Nd alloy in normal saline: experimental and theoretical investigations, Corrosion Sci. (2021), 109268.

[215] H. Ashassi-Sorkhabi, B. Shaabani, D. Seifzadeh, Corrosion inhibition of mild steel by some schiff base compounds in hydrochloric acid, Appl. Surf. Sci. 239 (2005) 154–164.

[216] J. Friedrich, Mechanisms of plasma polymerization - reviewed from a chemical point of view, Plasma Process. Polym. 8 (2011) 783–802.

[217] B. Finke, F. Luethen, K. Schroeder, P.D. Mueller, C. Bergemann, M. Frant, A. Ohl, B.J. Nebe, The effect of positively charged plasma polymerization on initial osteoblastic focal adhesion on titanium surfaces, Biomaterials 28 (2007) 4521–4534.

[218] X. Liu, Q. Feng, A. Bachhuka, K. Vasilev, Surface modification by allylamine plasma polymerization promotes osteogenic differentiation of human adipose-derived stem cells, ACS Appl. Mater. Interfaces 6 (2014) 9733–9741.

[219] P. Qi, Y. Yang, S. Zhao, J. Wang, X. Li, Q. Tu, Z. Yang, N. Huang, Improvement of corrosion resistance and biocompatibility of biodegradable metallic vascular stent via plasma allylamine polymerized coating, Mater. Des. 96 (2016) 341–349.

[220] D. Yu, H. Qiu, X. Mou, X. Dou, N. Zhou, Q. Guo, N. Lyu, L. Lu, Z. Yang, N. Huang, One-pot but two-step vapor-based amine- and fluorine-bearing dual-layer coating for improving anticorrosion and biocompatibility of magnesium alloy, ACS Biomater. Sci. Eng. 5 (2019) 4331–4340.

[221] G. Lecayon, Y. Bouizem, C. Gressus, C. Reynaud, C. Juret, Grafting and growing mechanisms of polymerised organic films onto metallic surfaces, Chem. Phys. Lett. 91 (1982) 506–510.

[222] D. Belanger, J. Pinson, Electrografting: a powerful method for surface modification, Chem. Soc. Rev. 40 (2011) 3995–4048.

[223] M. Ascencio, M. Pekguleryuz, S. Omanovic, Corrosion behaviour of polypyrrole-coated WE43 Mg alloy in a modified simulated body fluid solution, Corrosion Sci. 133 (2018) 261–275.

[224] M.C. Turhan, M. Weiser, M.S. Killian, B. Leitner, S. Virtanen, Electrochemical polymerization and characterization of polypyrrole on Mg–Al alloy (AZ91D), Synth. Met. 161 (2011) 360–364.

[225] Y.X. Yang, Z. Fang, Y.H. Liu, Y.C. Hou, L.G. Wang, Y.F. Zhou, S.J. Zhu, R.C. Zeng, Y.F. Zheng, S.K. Guan, Biodegradation, hemocompatibility and covalent bonding mechanism of electrografting polyethylacrylate coating on Mg alloy for cardiovascular stent, J. Mater. Sci. Technol. 46 (2020) 114–126.

[226] C.Y. Li, L. Gao, X.L. Fan, R.C. Zeng, D.C. Chen, K.Q. Zhi, In vitro degradation and cytocompatibility of a low temperature in-situ grown self-healing Mg-Al LDH coating on MAO-coated magnesium alloy AZ31, Bioact. Mater. 5 (2020) 364–376.

[227] Y. Chen, J. Dou, Z. Pang, Z. Zheng, H. Yu, C. Chen, Ag-containing antibacterial self-healing micro-arc oxidation coatings on Mg–Zn–Sr alloys, Surf. Eng. (2020) 1–16.

[228] A. Besinis, T. De Peralta, R.D. Handy, The antibacterial effects of silver, titanium dioxide and silica dioxide nanoparticles compared to the dental disinfectant chlorhexidine on Streptococcus mutans using a suite of bioassays, Nanotoxicology 8 (2014) 1–16.

[229] J.R. Koduru, S.K. Kailasa, J.R. Bhamore, K.H. Kim, T. Dutta, K. Vellingiri, Phytochemical-assisted synthetic approaches for silver nanoparticles antimicrobial applications: a review, Adv. Colloid Interface Sci. 256 (2018) 326–339.

[230] X. Lin, L. Tan, P. Wan, X. Yu, K. Yang, Z. Hu, Y. Li, W. Li, Characterization of micro-arc oxidation coating post-treated by hydrofluoric acid on biodegradable ZK60 magnesium alloy, Surf. Coating. Technol. 232 (2013) 899–905.

[231] W. Xu, K. Sato, Y. Koga, M. Sasaki, T. Niidome, Corrosion resistance of HF-treated Mg alloy stent following balloon expansion and its improvement through biodegradable polymer coating, J. Coating Technol. Res. 17 (2020) 1023–1032.

[232] P. Wang, J. Liu, X. Luo, P. Xiong, S. Gao, J. Yan, Y. Li, Y. Cheng, T. Xi, A tannic acid-modified fluoride pre-treated Mg-Zn-Y-Nd alloy with antioxidant and platelet-repellent functionalities for vascular stent application, J. Mater. Chem. B 7 (2019) 7314–7325.

[233] X. Li, P. Gao, J. Tan, K. Xiong, M.F. Maitz, C. Pan, H. Wu, Y. Chen, Z. Yang, N. Huang, Assembly of metal-phenolic/catecholamine networks for synergistically anti-inflammatory, antimicrobial, and anticoagulant coatings, ACS Appl. Mater. Interfaces 10 (2018) 40844–40853.

[234] I. Perelshtein, E. Ruderman, A. Francesko, M.M. Fernandes, T. Tzanov, A. Gedanken, Tannic acid NPs - synthesis and immobilization onto a solid surface in a one-step process and their antibacterial and anti-inflammatory properties, Ultrason. Sonochem. 21 (2014) 1916–1920.

[235] J. Luo, J. Lai, N. Zhang, Y. Liu, R. Liu, X. Liu, Tannic acid induced self-assembly of three-dimensional graphene with good adsorption and antibacterial properties, ACS Sustain. Chem. Eng. 4 (2016) 1404–1413.

[236] C. Yu, L.Y. Cui, Y.F. Zhou, Z.Z. Han, X.-B. Chen, R.C. Zeng, Y.H. Zou, S.Q. Li, F. Zhang, E.H. Han, S.K. Guan, Self-degradation of micro-arc oxidation/chitosan composite coating on Mg-4Li-1Ca alloy, Surf. Coating. Technol. 344 (2018) 1–11.

[237] X. He, G. Zhang, Y. Pei, H. Zhang, Layered hydroxide/polydopamine/hyaluronic acid functionalized magnesium alloys for enhanced anticorrosion, biocompatibility and antithrombogenicity in vascular stents, J. Biomater. Appl. 34 (2020) 1131–1141.

[238] L.H. Lin, H.P. Lee, M.L. Yeh, Characterization of a sandwich PLGA-gallic acid-PLGA coating on Mg alloy ZK60 for bioresorbable coronary artery stents, Materials 13 (2020) 5538.

[239] B. Badhani, N. Sharma, R. Kakkar, Gallic acid: a versatile antioxidant with promising therapeutic and industrial applications, RSC Adv. 5 (2015) 27540–27557.

[240] K.S. Lim, J.-K. Park, M.H. Jeong, I.H. Bae, D.S. Park, J.W. Shim, J.H. Kim, H. K. Kim, S.S. Kim, D.S. Sim, Y.J. Hong, J.H. Kim, Y. Ahn, Anti-inflammatory effect of gallic acid-eluting stent in a porcine coronary restenosis model, Acta Cardiol. Sin. 34 (2018) 224–232.

[241] H. Li, F. Peng, D. Wang, Y. Qiao, D. Xu, X. Liu, Layered double hydroxide/poly-dopamine composite coating with surface heparinization on Mg alloys: improved anticorrosion, endothelialization and hemocompatibility, Biomater. Sci. 6 (2018) 1846–1858.

[242] Y. Wu, L. Chang, J. Li, L. Wang, S. Guan, Conjugating heparin, Arg-Glu-Asp-Val peptide, and anti-CD34 to the silanic Mg-Zn-Y-Nd alloy for better endothelialization, J. Biomater. Appl. 35 (2020) 158–168.

[243] W. Ma, L. Liu, X. luo, C. Han, P. Yang, Y. Zhao, N. Huang, Effects of biomimetic micropattern on titanium deposited with PDA/Cu and nitric oxide release on behaviors of ECs, J. Mater. Res. 34 (2019) 2037–2046.

[244] J. Zhao, Y. Feng, Surface engineering of cardiovascular devices for improved hemocompatibility and rapid endothelialization, Adv. Healthcare Mater. 9 (2020), e2000920.

[245] J. Chen, Q. Li, J. Xu, L. Zhang, M.F. Maitz, J. Li, Thromboresistant and rapid-endothelialization effects of dopamine and staphylococcal protein A mediated anti-CD34 coating on 316L stainless steel for cardiovascular devices, J. Mater. Chem. B 3 (2015) 2615–2623.

[246] P. Wang, P. Xiong, J. Liu, S. Gao, T. Xi, Y. Cheng, A silk-based coating containing GREDVY peptide and heparin on Mg-Zn-Y-Nd alloy: improved corrosion resistance, hemocompatibility and endothelialization, J. Mater. Chem. B 6 (2018) 966–978.

[247] Y. Shi, L. Zhang, J. Chen, J. Zhang, F. Yuan, L. Shen, C. Chen, J. Pei, Z. Li, J. Tan, G. Yuan, In vitro and in vivo degradation of rapamycin-eluting Mg-Nd-Zn-Zr alloy stents in porcine coronary arteries, Mater. Sci. Eng. C 80 (2017) 1–6.

[248] M. Deng, L. Wang, D. Höche, S.V. Lamaka, C. Wang, D. Snihirova, Y. Jin, Y. Zhang, M.L. Zheludkevich, Approaching "stainless magnesium" by Ca micro-alloying, Mater. Horiz. 8 (2021) 589–596.

[249] T.B. Matias, V. Roche, R.P. Nogueira, G.H. Asato, C.S. Kiminami, C. Bolfarini, W. J. Botta, A.M. Jorge, Mg-Zn-Ca amorphous alloys for application as temporary implant: effect of Zn content on the mechanical and corrosion properties, Mater. Des. 110 (2016) 188–195.

[250] B. Zberg, P.J. Uggowitzer, J.F. Loffler, MgZnCa glasses without clinically observable hydrogen evolution for biodegradable implants, Nat. Mater. 8 (2009) 887–891.

[251] X. Gu, Y. Zheng, S. Zhong, T. Xi, J. Wang, W. Wang, Corrosion of, and cellular responses to Mg-Zn-Ca bulk metallic glasses, Biomaterials 31 (2010) 1093–1103.

[252] A.C. Hanzi, P. Gunde, M. Schinhammer, P.J. Uggowitzer, On the biodegradation performance of an Mg-Y-RE alloy with various surface conditions in simulated body fluid, Acta Biomater. 5 (2009) 162–171.

[253] D. Del Bufalo, L. Ciuffreda, D. Trisciuoglio, M. Desideri, F. Cognetti, G. Zupi, M. Milella, Antiangiogenic potential of the Mammalian target of rapamycin inhibitor temsirolimus, Canc. Res. 66 (2006) 5549–5554.